論文 / 著書情報
Article / Book Information

題目(和文)	UFC-PC複合構造物へのUFC適用に関する研究
Title(English)	The Utilization of UFC for UFC-PC Hybrid Structures
著者(和文)	WirojjanapiromPuvanai
Author(English)	Puvanai Wirojjanapirom
出典(和文)	学位:博士（学術）, 学位授与機関:東京工業大学, 報告番号:甲第9670号, 授与年月日:2014年9月25日, 学位の種別:課程博士, 審査員:二羽　淳一郎,北詰　昌樹,岩波　光保,竹村　次朗,佐々木　栄一
Citation(English)	Degree:, Conferring organization: Tokyo Institute of Technology, Report number:甲第9670号, Conferred date:2014/9/25, Degree Type:Course doctor, Examiner:,,,,
学位種別(和文)	博士論文
Type(English)	Doctoral Thesis

THE UTILIZATION OF UFC FOR UFC-PC HYBRID STRUCTURES

by

Puvanai Wirojjanapirom

Supervisor:

Professor Junichiro Niwa

A Dissertation Submitted in Partial Fulfillment of the Requirements for the Degree of Doctor of Philosophy

Department of Civil Engineering

Tokyo Institute of Technology

Tokyo, Japan

August 2014

ABSTRACT

Ultra high strength fiber reinforced concrete (UFC) has rapidly been developed over the past decade. Due to its outstanding mechanical and durability properties, UFC has been successfully implemented in various kinds of applications throughout the world and especially in Japan. UFC provides the ultra high strength characteristics of more than 150 MPa and 5 MPa in compression and tension, respectively. High ductility can be archived due to the existence of steel fibers. Moreover, the excellent durability properties such as resistance to chloride ion attack and abrasion mean lower maintenance cost and longer service life. The utilization of UFC in practical construction is considered one of the approaches to build high performance and sustainable infrastructure.

The hybrid structures consisting of steel and prestressed concrete (PC) are widely used in Japan, such as in extradosed and cable-stayed bridges, due to their structural and economical benefit for all the design and construction processes. The steel-PC bridge consists of segmental concrete at both ends and main steel girder at the middle part of span. Because of high strength material, cross section of web member can be reduced. Besides, the decrement of self weight and longer span length can be achieved due to the steel girder employed at the middle part. However, durability problems such as the corrosion of steel girder are major concerns. By comparing the weight of prestressed UFC with H-steel beams at the same design bending moment of 150 kN-m, the self weight of both UFC and steel beams were found to be the same at 50 kg/m. Therefore, in order to eliminate the drawback while maintaining the benefits of steel girder, the so-called “UFC-PC hybrid structure”, which replaces steel girder with UFC segmental girders, is proposed in this study.

The main objective of this study is to experimentally investigate the applications of UFC for the development of UFC-PC structures. Firstly, the experimental study on shear behavior of RC beams using UFC as the permanent formwork for the PC segments was conducted. UFC U-shaped permanent formwork with the shear keys and screws and bolts construction system was introduced. Loading experiments of a total of nine specimens, varied in interface and presence of screws and bolt system, thickness of permanent formwork, presence of stirrups and shear span to effective depth ratio (*a/d*), were carried out. The shear resistance mechanisms were investigated. The results indicated that by using the UFC permanent formwork, the shear capacity of RC beams significantly increased. Moreover, the compatibility between RC and UFC permanent formwork was formed by using the shear keys

and screws and bolts system. The diagonal crack model together with tensile stress obtained from the tension softening curve were used to investigate the contribution on shear carried by UFC permanent formwork. The calculation results showed good agreement with the experimental results.

Second, the connection method, which is one of the most important factors in developing the UFC-PC hybrid structure, was studied. The perfobond strip (PBL) with cast-in-place UFC joint connection was proposed and its shear performance was examined. Push-out test of twelve specimens with simulated the construction process of the connection was conducted. Thickness of PBL, diameter of PBL, diameter of transverse rebar, prestressing stress on the connection part and the ratio of spacing to diameter of PBL were selected as the parameters in the experiment. The results indicated that PBL with cast-in-place UFC was capable of transferring the shear forces between two segments. Each contribution to the shear capacity was clarified. As a result, shear capacity equation of PBL with cast-in-place UFC connection was developed based on the shear resistance mechanism. The proposed calculation method can provide a reasonable agreement with the experimental results. In addition, the effect of bending moment on shear behavior of PBL with cast-in-place UFC was discussed. The results showed that the shear capacity gradually decreased as the increase of bending moment occurred at the location of the connection.

ACKNOWLEDGEMENTS

I would like to express my great and sincere gratitude to, first and foremost, my academic advisor Professor Junichiro Niwa for his kind and superb guidance, enthusiastic encouragement, insightful comments, and invaluable support not only for this study but also for my life in Japan. Without his patience and expert advice, the completion of this thesis would not have been possible. Sincere words of appreciation also go to the members of the examination committee -- Professor Masaki Kitazume, Professor Mitsuyasu Iwanami, Associate Professor Jiro Takemura, and Associate Professor Eiichi Sasaki -- for their valuable suggestions and helpful comments that enhanced the quality of this study.

I am grateful to Assistant Professor Koji Matsumoto for his kind and very perceptive comments and suggestions, and irreplaceable support all thorough this study. I wish to pass my gratitude to Dr. Katsuya Kono and Dr. Tetsuo Kawaguchi of Taiheiyo Cement Corporation for their constructive criticism derived from their rich experiences and invaluable supports. I am also thankful to Mr. Hikaru Okuma and Mr. Takeshi Kitamura of Taisei Corporation for their critical comments which help improve of this study. Sincere appreciation also goes to Dr. Ken Watanabe of Railway Technical Research Institute for his precise suggestion during the beginning of my study. Special thanks are to Ms. Osami Kumagai and Ms. Noriko Nakajima for their kind-hearted supports in administrative affairs. I am also indebted to the Taisei Technology Center, Taisei Corporation for the invaluable internship program which broadened my experience and attitude.

Moreover, I would like to express my appreciation to all Concrete Lab members; Niwa Lab, Otsuki Lab and Iwanami Laboratory, especially, my Thai seniors and juniors, for their kind support, encouragement and friendship throughout my academic and personal life in Japan. I am obliged to the Ministry of Education, Culture, Sports, Science and Technology (MEXT) for the opportunity and financial support through their scholarship. I would like to thank also the Center of Urban Earthquake Engineering (CUEE) for partially supporting the research fund.

For the home away from home in Japan, I heartily thank my Thai, Japanese and international friends in Tokyo institute of Technology and all over Japan.

Last and forever, I would like to express my heartfelt gratitude to my beloved parents and family for their endless love, support and sacrifices, and for always being right beside me through every up and down.

TABLE OF CONTENTS

CHAPTER 1

Introduction

1.1 Background

For the last decade, hybrid structural system integrating steel and prestressed concrete (PC) so called "Steel-PC hybrid structure" is remarkably developed and widely implemented to long-span bridges in Japan such as extradosed and cable-stayed bridges (Mutsuyoshi et al., 2010 and Yoshioka, 2005). The steel-PC hybrid bridges compose of steel girder at the middle part of span and segmental concrete at both side ends. Due to the high strength of materials, the cross sectional area of the web members can be reduced. As a result, the total weight of structure can be also reduced. Moreover, longer span can be constructed due to the steel girder employed at middle span. However, the durability is one of the main concerns of this type of structure; the middle steel girder part may face the problem of corrosion (Kayser and Nowak, 1989). To overcome this problem, Ultra High Strength Fiber Reinforced Concrete (UFC) is proposed to use instead of the steel girder for middle part of span in this study so called "UFC-PC hybrid structure".

UFC is one of the advanced cementitous compostite materials which has been aggressively developed over the decade and rapidly implemented throught out the world especially in Japan. Through the "Ultra high" strength properties, UFC provides with characteristic values in excess of 150 MPa in compressive strength and 5 MPa in the tensile strength together with very high bending toughness and ductility due to the presence of micro steel fibers. The excellent on durability properties are also reported such as resistance to chloride attack, carbonation, abrasion and freeze-thaw action which lead to the decrement of maintenance cost and service life improvement. Moreover, members can be cast with various of shapes due to high flowability.

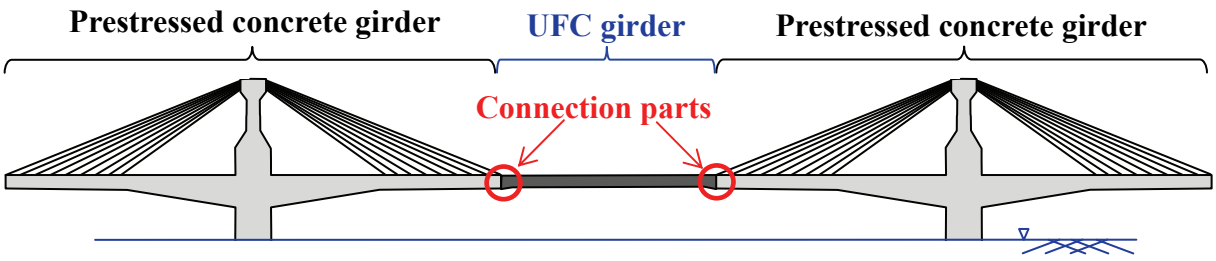

Figure 1-1 Typical view of the UFC-PC hybrid bridge

Comparing the weight of prestressed UFC beam with normal RC beam and I-shaped steel beam according to the same design bending moment equal to 150 kN-m, the result shows that the weights of steel and prestressed UFC beams have the same weight at 50 kg/m which is only 1/4 of a normal RC beam. As a result, the member depth is also reduced by half compared with normal RC beams (Musha, 2009).

Follow the above point of view, by replacing the steel girder with the UFC girder, the benefits of steel can be remained while taking the advantages of UFC. Therefore, in this study the development of UFC-PC hybrid structure is proposed. **Figure 1-1** demonstrates the typical view of UFC-PC hybrid bridge. The UFC-PC hybrid bridge consists of UFC girder at the middle part of span where the shape of UFC can be whether T-shaped or box girders and prestressed segmental concrete at the both side ends. **Figure 1-2** demonstrates the construction process of UFC-PC hybrid bridge. First is to perform the construction of PC segmental girder. After that, UFC girder is erected into the middle of span. Finally, the construction of joint connection parts which used to connect between PC and UFC girder is done. This development is focused on the new alternative structural system that proffers an improvement in durability and minimizes the required volume of material also, in which fully use of particular part of UFC can be achieved.

In this study, the use of UFC as the permanent formwork for the prestressed concrete segmental girder is developed. Moreover, one of the most essential in development of UFC-PC hybrid structure is to clarify and determine the proper joint connection which can secure the efficiently transferring force between UFC and PC girder. Unfortunately, the available study on the performance of UFC-PC hybrid structure cannot be found. In addition, the research on the connection technologies between UFC and PC girders is scarce.

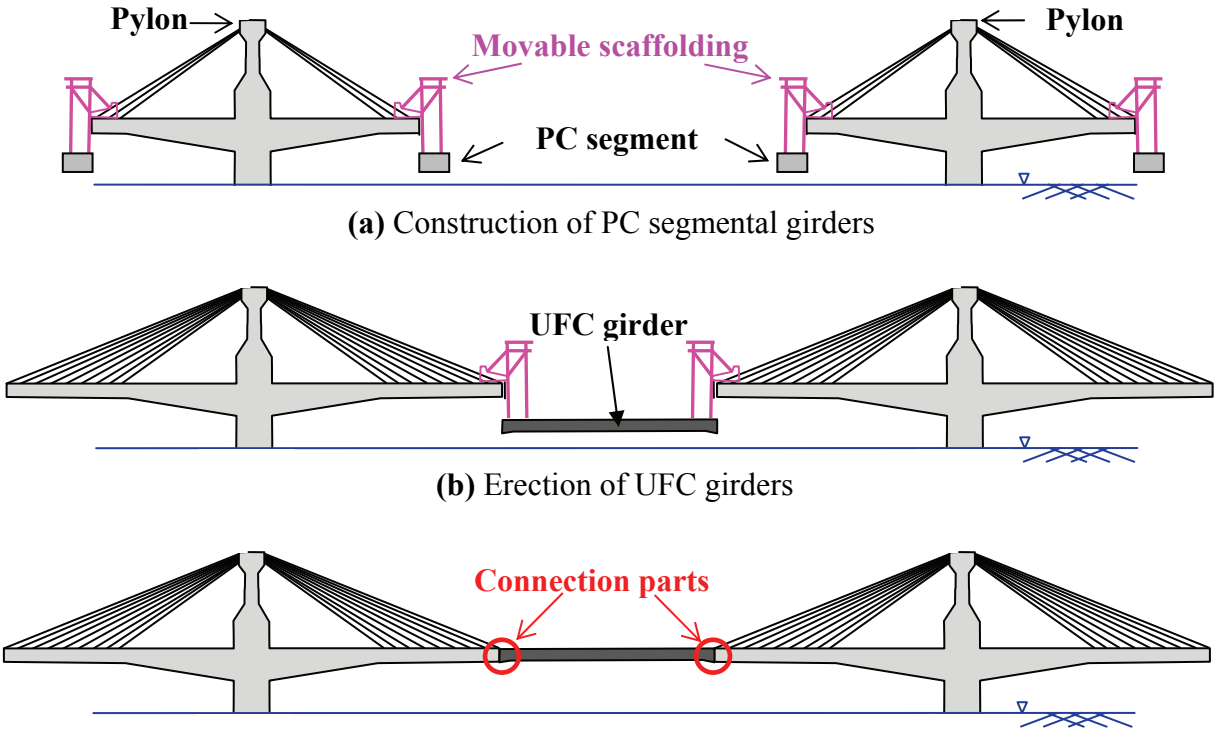

(a) Construction of PC segmental girders

(b) Erection of UFC girders

(c) Construction of connection parts

Figure 1-2 Construction process of the UFC-PC hybrid bridge

1.2 Objective and Scope of the Study

The major objective of this study is to develop the UFC-PC hybrid structures. Therefore, in order to develop the UFC-PC hybrid girders, the study on the utilization of UFC for each part of structure is focused, which includes the two main following objectives;

1. To investigate the shear behaviors of RC beams using UFC U-shaped permanent formwork

2. To investigate the shear behavior of proposed PBL with cast-in-place UFC joint connection for UFC-PC hybrid girders

In the first objective, the use of UFC as the permanent formwork is introduced to use for the precast segmental concrete part. The experiments of nine RC beams using UFC U-shaped permanent formwork were conducted. Various parameters affecting the shear behavior which are interface between UFC and inside RC and presence of screws and bolts, thickness

of UFC permanent formwork, presence of stirrups and shear span to effective depth ratio (*a/d*) were considered. The shear carried by UFC permanent formwork was investigated based on stress obtained from the tension softening curve. The weights of RC beams using UFC permanent formwork were compared with the normal RC beams, in order to discuss the weight reduction.

To achieve the second objective which is one of the most important requirements in developing of UFC-PC hybrid girders, the PBL with cast-in-place UFC connection is proposed and the experimental study by the push-out tests of twelve specimens was performed. The fabrication step of the connection is pointed out. Shear resisting mechanisms is discussed based on the various affecting parameters which are thickness of PBL, hole diameter of PBL, diameter of transverse rebar, prestressing stresses on the connection and the ratio of spacing to the diameter of PBL (*S/D*). Predictive equation is proposed based on the observed resisting mechanism. In addition, the effect of bending moment on the shear capacity also discussed

The findings on the utilization of UFC in this study provide the understanding and offer the basic knowledge for the development of competitive UFC-PC hybrid structural system that proffers an improvement in durability and minimize the required volume of material, in which fully use of particular part of UFC can be made.

1.3 Outline of the Dissertation

The dissertation consists of six chapters as the flowchart is shown in **Fig. 1-3**. The contents of each chapter are briefly explained as follows.

Chapter 1 introduces the general background of UFC-PC hybrid structure, together with objective of this study. The explanation of the outline of the dissertation is also briefly summarized in this chapter.

Chapter 2 reviews the basic knowledge and the use of UFC, along with the hybrid structural system technologies. Mechanical properties and structure with practical use of UFC are introduced. Previous researches on performance of composite and hybrid structure using UFC are also reviewed.

In **Chapter 3**, the use of UFC as the permanent formwork for reinforced concrete (RC) beams is introduced. The experimental study on shear behavior of RC beams using UFC U-shaped permanent formwork is presented. The outline of the experiment is explained as the specimen details, materials, experimental parameters, fabrication of specimen, loading method and measurement items are described in details. Shear behaviors of RC beams using UFC permanent formwork and reference specimen are compared in terms of shear capacities, crack patterns and load-displacement relationship and shear resistance mechanisms are also discussed based on the effect of each experimental parameters. In addition, weight reduction of beams is also examined. The shear carried by UFC permanent formwork of both specimens failed in diagonal tension and shear compression is also investigated.

Chapter 4 focuses on joint connection for the UFC-PC hybrid girders. The Perfobond strip (PBL) filled with cast-in-place UFC joint connection is proposed as the connection method for UFC-PC hybrid girders. The construction process of the connection is explained. The results push-out tests of PBL with cast-in-place UFC connection specimens are discussed in order to investigate the shear behavior of PBL with cast-in-place UFC connection. Shear resisting mechanism with various affecting parameters is examined. Predictive equation is mechanically modelled based on the shear resistance mechanism of the connection.

In **Chapter 5**, the effect of bending moment on the shear capacity of the PBL with cast-in-place UFC connection is examined. The results from four-point bending tests of three UFC-PC hybrid girder specimens are presented. The experimental program is explained. Shear behaviors of PBL with cast-in-place UFC from bending test in this chapter and push-out test from chapter 4 are compared in term of shear capacities, force-displacement relationship and failure patterns.

Finally, the conclusions of this study and the recommendations for the further study are presented in **Chapter 6**.

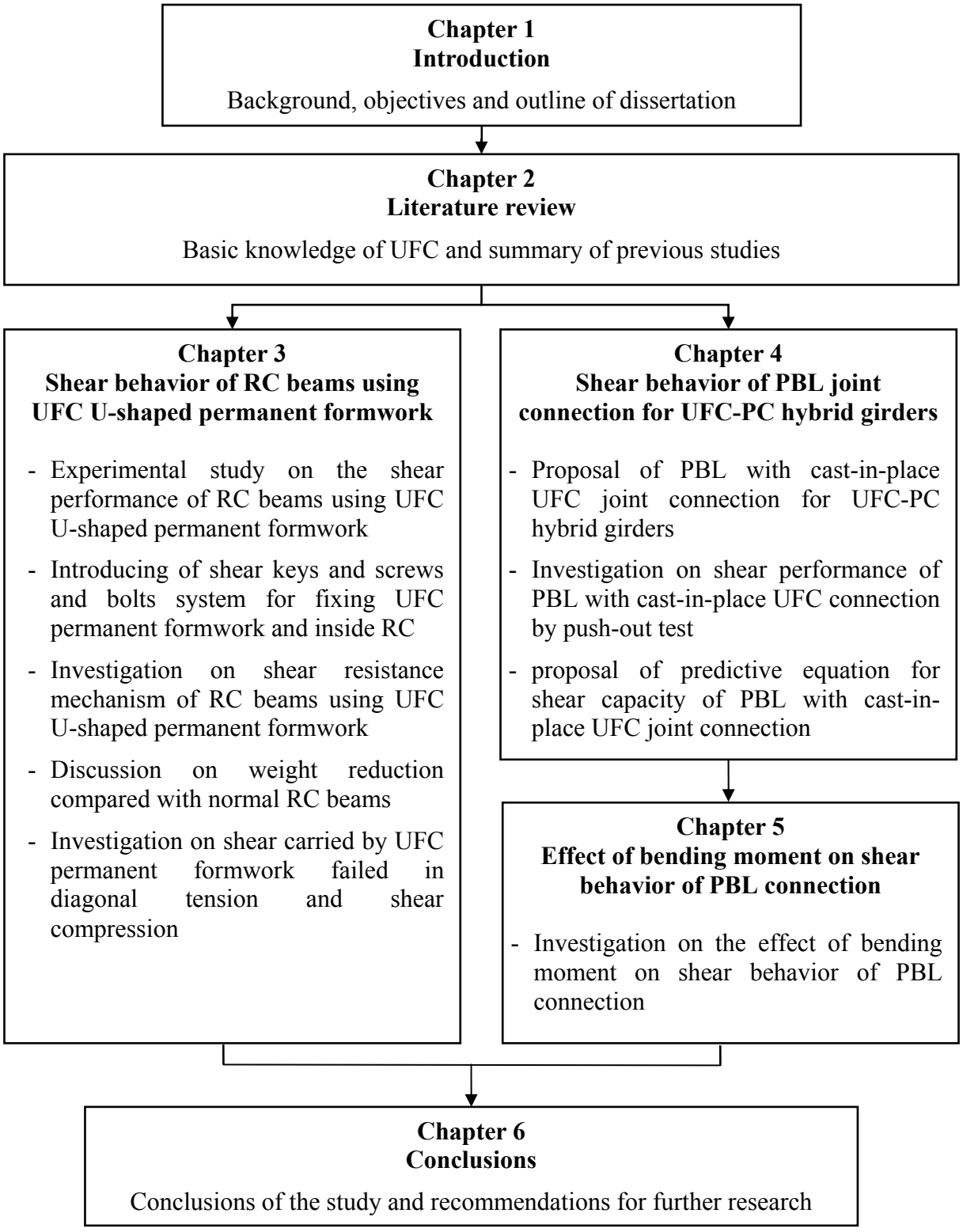

Figure 1-3 Outline of the dissertation

CHAPTER 2

Literature review

2.1 Introduction

In this chapter, the definition and basic knowledge of Ultra High Strength Fiber Reinforced Concrete (UFC) and hybrid structure are introduced. The existing composite and hybrid prestressed concrete and UFC structures are presented. Moreover, previous investigations on mechanical performance of UFC composite structures are reviewed.

2.2 Ultra High Strength Fiber Reinforced Concrete (UFC)

Ultra high Strength Fiber Reinforced Concrete (UFC) as also known as Ultra High Performance Fiber Reinforced Concrete (UHPFRC) in Europe region (AFGC, 2013) is an advanced cementitious composite material which has been rapidly developed in recent years. Due to its high performance, UFC has been implemented in several applications especially in the bridge construction in Japan and throughout the world (Hajar et al., 2004, Musha et al., 2013(a)). UFC was developed based on the original technology of RPC (Reactive Powder Concretes) in France in 1994 (Richard and Cheyrezy, 1995). The technology of UFC is adopted and utilized in Japan as the design and construction of Sakata-Mirai Bridge is the initiated example (JSCE, 2006).

2.2.1 General mechanical properties of UFC

UFC can be made by mixing premixed powder, water, superplasticizer and steel fibers. Premixed powder is consisted of cement, silica sand and silica fume in the optimum proportion. The close-packed particle structures can be achieved by controlling the size of particles in the premixed powder.

Table 2-1 summarizes the mechanical properties of UFC and normal concrete. **Figure 2-1** shows materials for UFC. Through the proper “Ultra high” strength parameters, this

Table 2-1 Mechanical properties of UFC (Murata, 2007)

Characteristics	UFC	High strength concrete (28 days curing)	Normal concrete (28 days curing)
Density (t/m^3)	2.5	2.4	2.3
Compressive strength (MPa)	150-200	60	30
Flexural strength (MPa)	45	9	5
Tensile strength (MPa)	9	4	3
Young's modulus (GPa)	50	35	25
Abrasion resistance *1 (mm)	1	8	2.3
Freeze-thaw resistance *2 (%)	100	95	-

*1 by Abrasion resistance test (ASTM-C779), *2 by Freeze-thaw test (JIS A 6204)

Figure 2-1 Materials for UFC

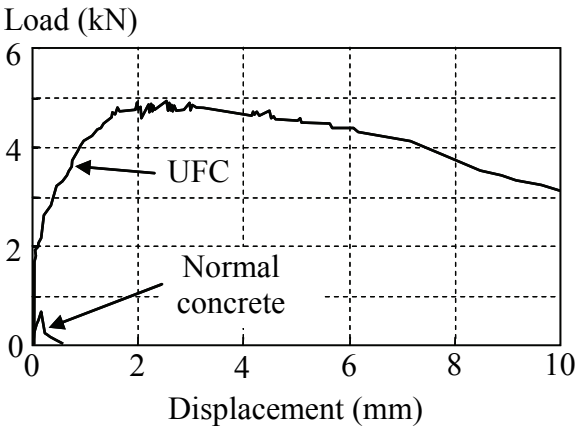

Figure 2-2 Load-displacement curves of notch beams tests (Murata, 2007)

material provides with characteristic values in excess of 150 MPa in the compressive strength and 5 MPa in the tensile strength which is several times higher than normal concrete. Due to the existence of steel fibers, the high bending toughness and ductility can be achieved. **Figure 2-2** shows the load-displacement relationship of notched beams under three point bending test of UFC and normal concrete.

Furthermore, with close-packed micro-structures as shown in **Fig. 2-3**, UFC has excellent durability properties such as resistance to chloride ion attacks and abrasion which lead to maintenance cost reduction and service life improvement. In addition, due to high workability, members can be formed with various shapes.

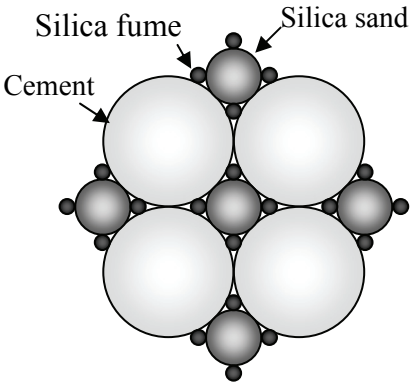

Figure 2-3 Close-packed structures (Murata, 2007)

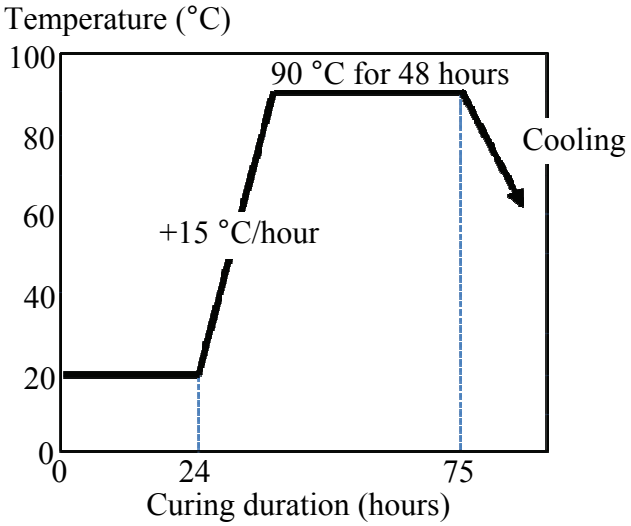

Figure 2-5 Heat curing pattern of UFC

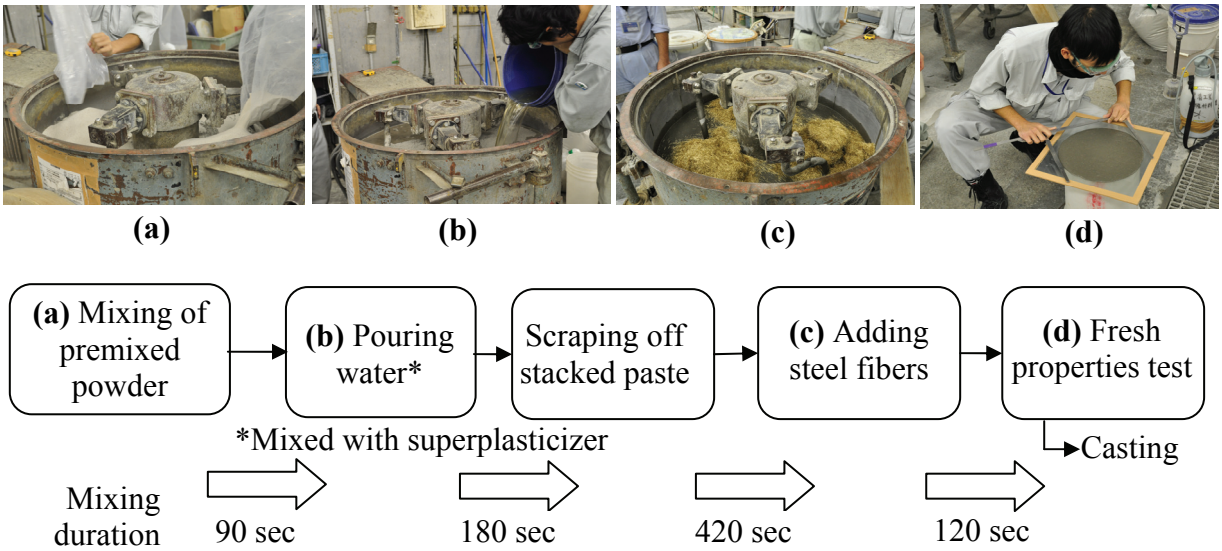

Figure 2-4 Mixing process of UFC

2.2.2 Production of UFC

Figure 2-4 explains the mixing process of UFC. The longer mixing duration is required in UFC comparing with normal concrete due to the high amount of powder and very low water to cement ratio. The high workability of UFC is measured following JIS R5201 standard. In general, the flow value of UFC is around 250-270 mm (corresponding to 600-650 mm in slump flow of normal concrete) and the segregation cannot be observed due to the high viscosity of UFC. In order to attain a high density and decrease the effect of shrinkage and

creep, the heat curing process is performed. **Figure 2-5** illustrates the heat curing pattern of UFC. The compressive strength of 200 MPa can be achieved after the heat curing process.

2.3 Existing Structures using UFC

Since the introduction of Sherbrook footbridge, Quebec, Canada in 1997 as the world's first major structure using UFC (Blais and Couture, 1999), and in 2002, Sakata-Mirai bridge in Yamagata prefecture had been introduced as the first bridge made by UFC in Japan (Tanaka et al., 2002), many advanced application in bridges have been reported and the proven of the efficiency of designing the slender structure with high durability performance (Hosotani et al., 2008, Benjamin, 2013, Resplendino and Toutlemonde, 2013, Musha et al., 2013(b)). Over the past decades, the technologies in design and contruction using UFC have advanced and definitively boarded wide over the world especially in Japan. Emphasizing of some essential demonstration of UFC structure is explained hereby. UFC slab for the Runway D extension project is considered as the world's largest utilization of UFC (Musha et al., 2013(a)). 6,900 precast UFC slabs with total volume of 22,000 m^3 were installed in 192,000 m^2 area of runway over the sea. By using UFC slab, the high durability of structure against the aggressive environment of Tokyo bay can be secured. Moreover, the dead load can be reduced by 56% comparing with normal concrete slab, resulting in the improvement of seismic

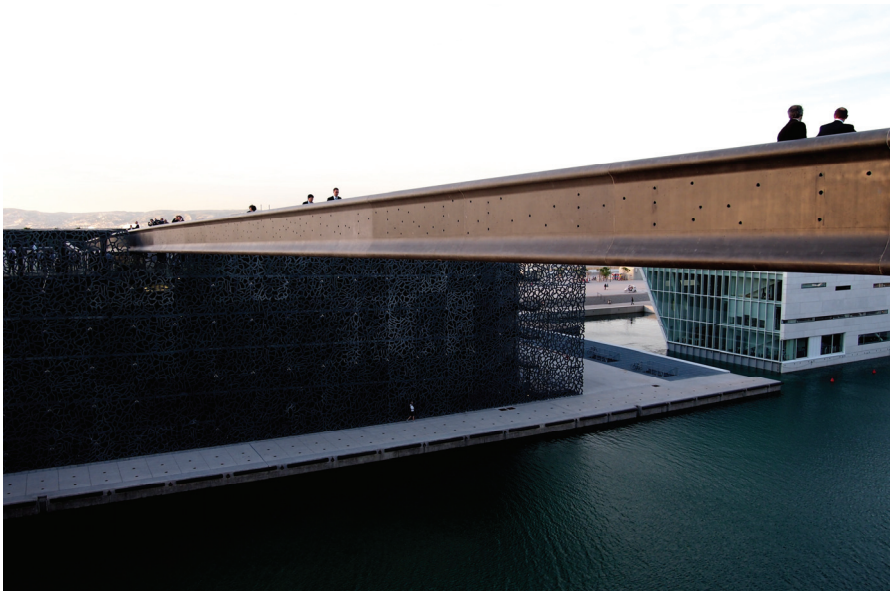

Figure 2-6 MuCEM footbridge

performance. The Kayogawa railway bridge, the first railway bridge constructed by UFC is one of the applications in order to overcome the unreachable condition of ordinary concrete. The lower slab thickness of bridges can be reduced from 390 in normal concrete to 250 mm in UFC. Recently, MuCEM footbridge is illustrated the achievement which the very long span length of 76.52 m can be constructed with maintain the slender cross section (Mazzacane et al., 2013).

2.4 Existing Steel-Prestressed Concrete Hybrid Bridges

The hybrid structure integrating prestressed concrete (PC) and steel are widely used to long-span bridges in Japan such as the extradosed and cable-strayed bridges due to the economical and structural advantages all thought the design and construction process. A steel-PC hybrid bridge consists of steel girder at the middle span and segmental prestressed concrete at the both side ends. **Figure 2-7** shows the typical view of Steel-PC hybrid bridge. Shinkawa bridges which located in Takamatsu, Kagawa prefecture is the example of Steel-PC hybrid bridges (Kurita and Ohyama, 2003). Kiso-Ibi kawa bridges are also of the example in Japan (Ikeda et al., 2002) . The extradosed system is also provided in this bridge in order to reduce the height of pylon and construct the longer span length of bridge (Ikeda et al., 2002). In such a case, the weight of structure can be more reduced by using the corrugated steel web PC box girder instead of ordinary PC box girder, as the Yahagigawa bridges located in Aichi prefecture is one of the example (Yoshioka, 2005). **Figure 2-8** shows the side view of corrugated steel web PC box girder bridge.

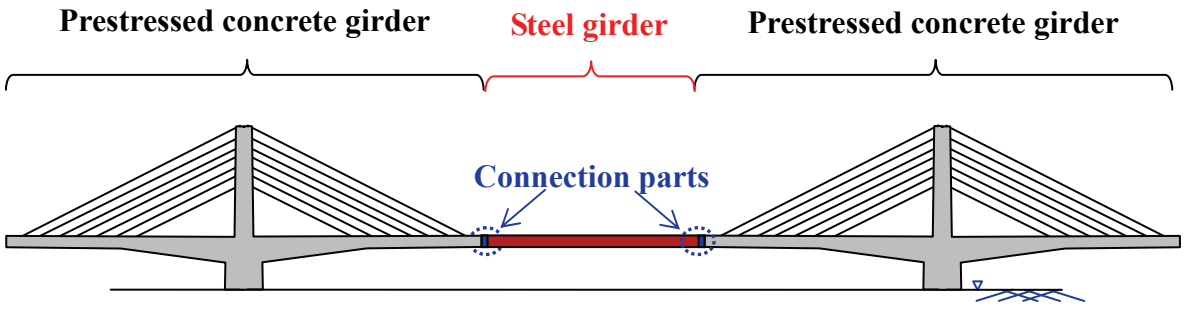

Figure 2-7 Typical view of the steel-PC hybrid bridge

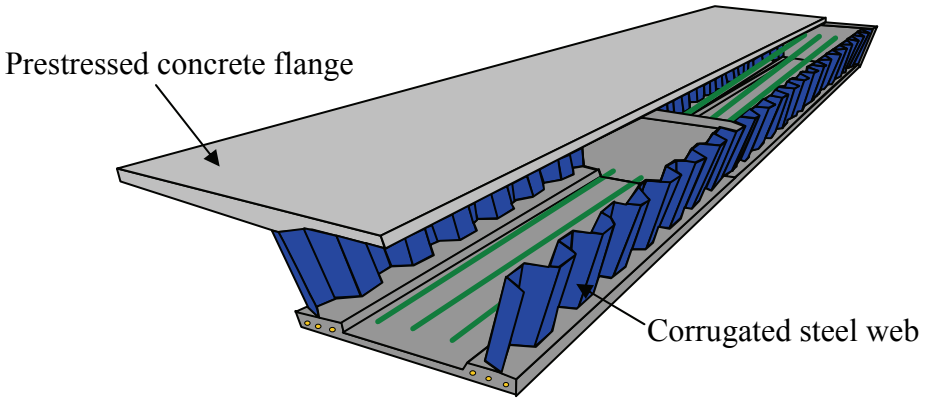

Figure 2-8 Typical view of corrugated steel web PC box girder bridge

2.5 Previous Study on Composite Structures using UFC

2.5.1 UFC permanent formwork

Until now, many studies for developing UFC permanent formwork have been carried out. In combination with the normal concrete, the implementation of UFC as thin layer structure is one of the promising applications. Considerable researches have been conducted on concrete structures with using UFC permanent formwork can be summarized as follow.

Shirai et al. (2008) studied on the durability of UFC permanent formwork and its application which applied for strengthening of Tedorigawa bridge pier in Ishikawa prefecture, Japan. Various experiments such as chloride ion penetration test, impact wear resistance and abrasion resistance were conducted. It is reported that UFC permanent formwork significantly increased durability against chloride ion attack, abrasion and impact wear for bridge pier.

Abe et al. (2009) introduced a composite slab system which consists of concrete slab cast onto a UFC permanent formwork. The punching shear failure mechanism was investigated, a RC slab and UFC permanent formwork composite structure failed in punching shear and the UFC permanent formwork separated from the composite surface at the same time.

Hong and Kang (2013) performed the experimental study on the flexural behavior of RC and UFC composite beams in order to investigate the structural performance of RC and UFC composite slab system. The 30 mm thickness of UFC permanent formwork which the

main parameter was the presences of longitudinal steel inside UFC permanent formwork were prepared. Moreover, the effect of with and without providing heat treatment was presented. The results indicated that by providing longitudinal steel inside UFC permanent formwork, the flexural capacity increased drastically. However, the heat treatment of UFC deteriorates the efficiency of composite bond as resulting in the brittle bond failure of composite beams.

2.5.2 Composite structures using UFC

Murata et al. (2007) proposed to replace the steel web with UFC web for the corrugated steel PC box girder. The test of simply supported composite PC beams using the UFC warren truss for the web was performed in order to investigate the mechanical properties. The results indicated that comparing composite PC beams with I-shaped PC beams having the same resistance capacity, the weight of a beam with prestressed UFC truss can be extremely reduced.

Shibata et al. (2009) studied the shear strengthening effect of UFC panels on RC beams. UFC panels were attached by epoxy resin and anchor bolts. The various shaped and attached location of UFC panels were investigated. Test results showed that by attaching UFC panels on the bottom or both sides of RC beams, the shear carrying capacity increased drastically. The researchers also discussed that the bond characteristics between concrete and UFC panels would be very important in order to improve the load carrying capacity.

Makita and Bruhwiler (2013) studied the fatigue behavior of composite RC structure with adding the thin (30 to 50 mm) UFC layer on the surface. It was reported that the high fatigue resistance was achieved by adding the the thin UFC layer on the surface. The practical application of layered thin UFC for strengthening of bridges's slab was also presented.

2.6 Connection System for UFC-PC Hybrid Structures

One of the most important items in order to examine the hybrid girder with different materials is to ensure the continuous behavior of two girders. At present, many connection methods are practically used for steel girder with concrete slab such as stud shear connector, angel steel joint (Kurita and Ohyama, 2003) and perfobond strip (PBL) (JSCE, 2009). The some of the combination of those connections are also existed. However, researches reported on the connection method between UFC and PC girders are slight.

Tanaka et al. (2006) reported the use of perfobond strip (PBL) applied for UFC girder with normal concrete slab. Various experiment programs were performed to confirm the shear performance of the PBL joint. The results demonstrated that shear transferring capacity and transferring rigidity between the UFC web and slab were efficient than stud shear connector. In addition, the practical application of PBL for construction of Akakura Onsen Yukemuri footbridge and Horikoshi highway bridge were also demonstrated.

Perry and Royce (2007) presented the cast-in-place UFC together with dowel steel bar for the connection of precast concrete deck in bridge construction. The increase of bond capacity and decrease the congested steel can be achieved.

CHAPTER 3

Shear behavior of RC beams using UFC U-shaped permanent formwork

3.1 Introduction

In this chapter, the application of UFC as structurally integrated permanent formwork for concrete structures is focused in order to implement for the prestressed concrete segmental part in UFC-PC hybrid girders. The shear behavior of RC beams using UFC permanent formwork is presented as for the fundamental study of the performance of composite system.

The definition for permanent formwork described from CIRIA C558 (Wringley, 2001) is the structural elements that is used to contain the cast-in-place concrete and mold it according to the required dimensions and will remain in place for the whole life of the structure. By using permanent formwork systems, the outstanding properties of UFC and concrete can be maximized while facilitating the construction process. A permanent formwork is first fabricated, and then the process involves only the casting of fresh concrete into the permanent formwork. Therefore, such a site's needed skill work can be neglected, erection time can be speed up and etc. Moreover, wastes from construction can also reduced in comparison of using wooden formwork.

The UFC permanent formwork is practically used in Japan for strengthening durability of concrete structure. However, the available studies on the mechanical performance of RC beams using a UFC permanent formwork is insufficient and the interfacial bonding between concrete and UFC has not been considered. To overcome this problems, the UFC U-shaped permanent formwork with interface shear keys and screws and bolts system has been examined. The explanation of the UFC permanent formwork concept is firstly presented in this chapter as shown above. Shear behavior of RC beams using a UFC permanent formwork with considering the effect of internal surface and presence of screws and bolts has been examined. Moreover, discussion about weight reduction compared with normal RC beams is presented. Finally, a calculation method for evaluating the shear carried by UFC permanent formwork is proposed.

Table 3-1 List of the experimental cases

No.	Name	*t* (mm)	Internal surface	Screw and bolt	Stirrup ratio (%)	*a/d*	Series
1	Ref	-	-	-	0	3.27	I, II
2	UFC20-K	20	Shear keys	-	0	3.27	I
3	UFC20-SB	20	Smooth	Provided	0	3.27	
4	UFC20-S	20	Smooth	-	0	3.27	
5	UFC20-KB	20	Shear keys	Provided	0	3.27	I, II, III, IV
6	UFC30-KB	30	Shear keys	Provided	0	3.27	II
7	UFC20-KB-ad1	20	Shear keys	Provided	0	1.00	III
8	UFC20-KB-ad21	20	Shear keys	Provided	0	2.16	III
9	UFC20-KB-r	20	Shear keys	Provided	0.28	3.27	IV

t: the thickness of UFC permanent formwork (mm), *a/d*: shear span to effective depth ratio

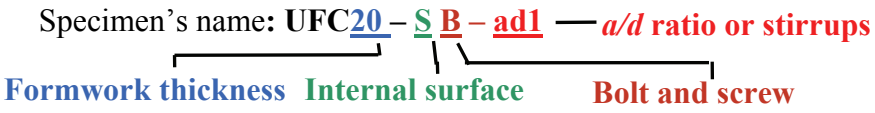

3.2 Experimental Program

3.2.1 Experimental cases

Totally nine specimens were prepared in order to investigate the shear behavior of RC beams with U-shaped UFC permanent formwork. Four-point bending tests were conducted. **Table 3-1** summarizes the test variation and the designated specimen name. **Figure 3-1** shows the details of specimens; dimension, arrangement of reinforcing bar and cross section of all specimens. The effective depth, width, height and tension reinforcement ratio are d=220 mm, b=250 mm, h=300 mm and p_w=1.41%, respectively. The failure side of shear span is controlled by differently provide a number of stirrups in each span. The experimental parameters which influencing the shear mechanism were selected and can be classified into four series as the details are described as follow;

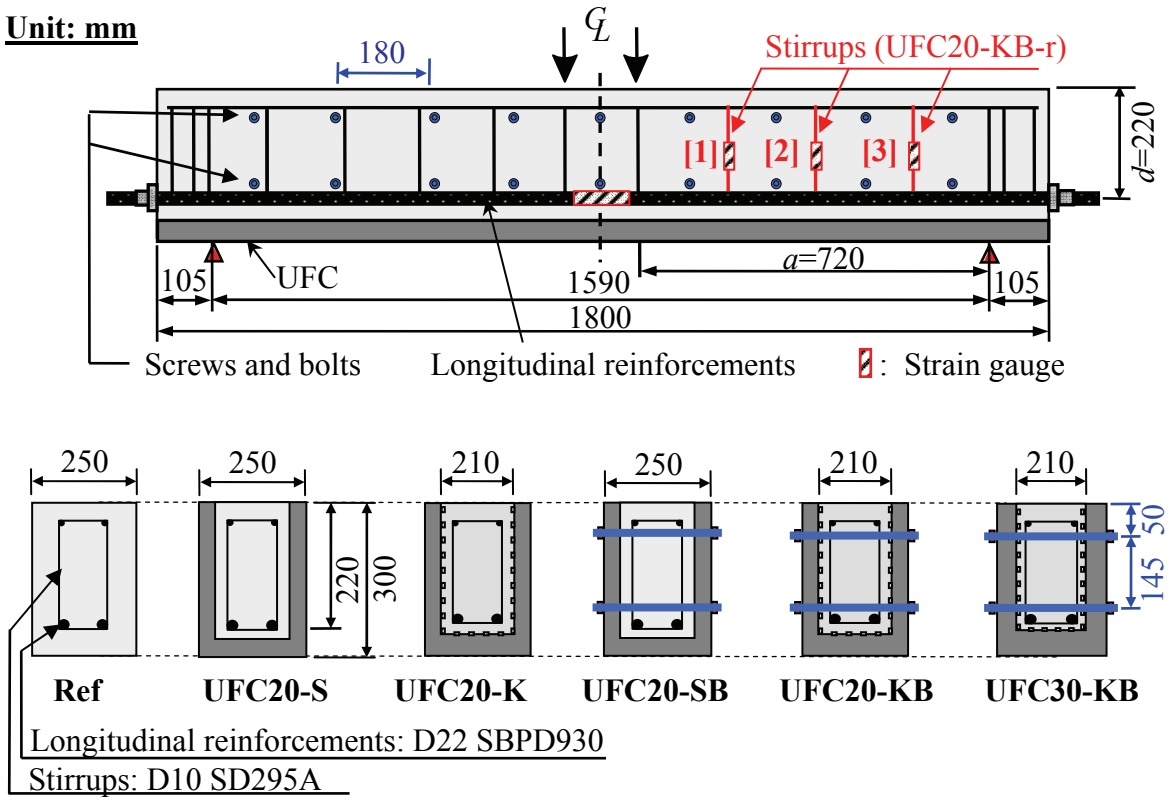

Figure 3-1 Detail of specimens

In Series-I, the shear keys and screws and bolts are introduced in order to fix the inside RC and UFC permanent formwork. Therefore, the effect of shear keys at the internal surface between UFC formwork and inside RC together with the presence of screws and bolts were considered. The name of specimens as shown in **Table 3-1** corresponds to the internal surface condition and presence of screws and bolts. The detail of UFC permanent formwork and the shear keys internal surface are shown in **Fig. 3-2**. It should be noted that shear key at interface used in this study is commercially used in Japan. The reference specimen which is the UFC U-shaped permanent formwork was not provided was also prepared named as Ref. For UFC20-S specimen, only smooth surface on the internal surface was provided. In UFC20-K specimen, shear keys at the internal surface between UFC formwork and inside RC were provided. UFC20-SB is the specimen which smooth surface at the internal surface and screws and bolts were provided. On the other hand, both shear keys on the internal surface and screws and bolts were provided for UFC20-KB specimen.

The effect of thickness of UFC permanent formwork was investigated in Series-II. The total cross section of the specimen was the same but the thickness of UFC permanent formwork increased to 30 mm in UFC30-KB in both sides and bottom part.

In Series-III, there are three specimens with different shear span length in order to examine the effect of shear span to effective depth ratio (*a/d*). Effective depth of the beams was the same, but the shear span was varied. UFC20-KB specimen with *a/d* was 3.27 is the original specimen. The *a/d* of UFC20-KB-ad1 and UFC20-KB-ad21 were 1.00 and 2.16, respectively. **Figure 3-3** presents the details of specimens in Series-III.

In Series-IV, the stirrups were provided in UFC20-KB-r with 0.28% of the stirrup ratio and spacing of 240 mm. The dimension of specimen was the same as that in Series-I and shear keys and screws and bolts were provided.

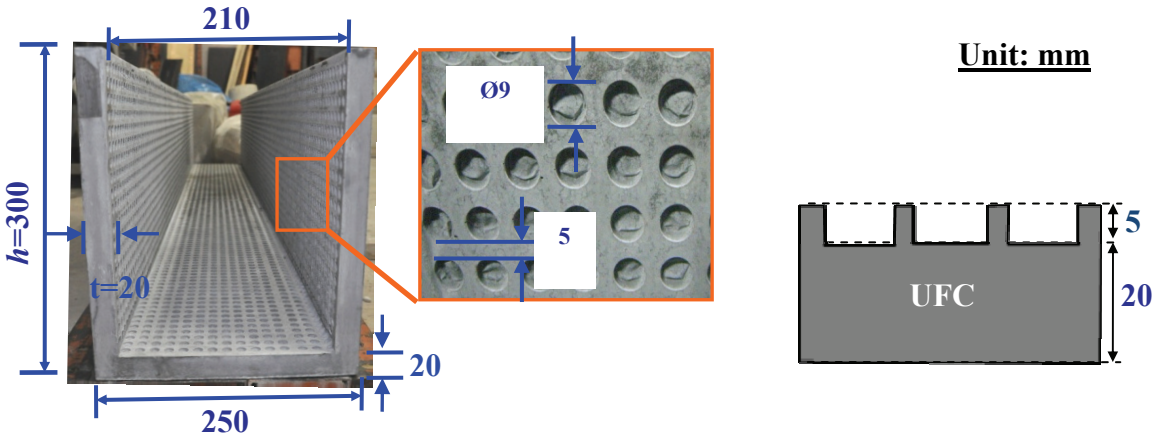

Figure 3-2 Detail of UFC formwork and shear keys

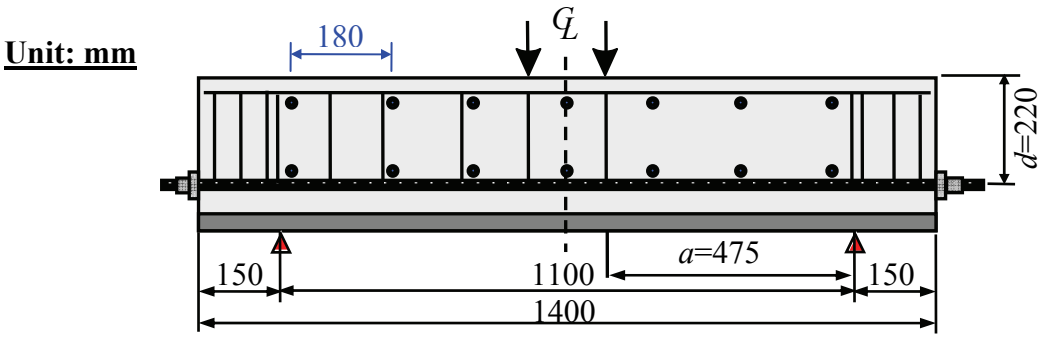

a) UFC20-KB-ad21 (*a/d*=2.16)

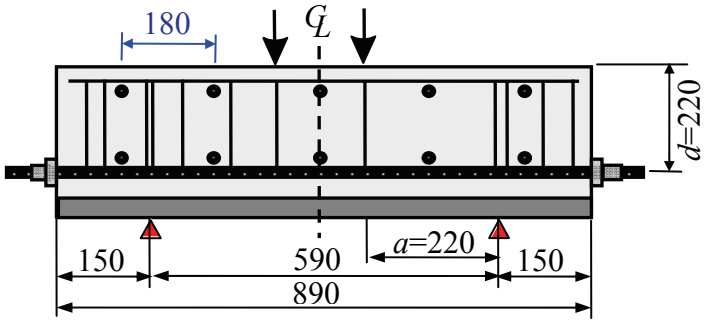

b) UFC20-KB-ad1 (*a/d*=1.0)

Figure 3-3 Detail of specimens in Series-III

Table 3-2 Mix proportion of concrete

G_{max}	Water Cement Ratio	Fine Aggregate Ratio	Unit weight (kg/m^3)						
(mm)	(%)	(%)	*W*	*C*	*L*	*S*	*G*	*SP*	*V*
13	57	45	165	292	249	718	857	*C*×1.5%	*C*×0.15%

where, G_{max} : maximum size of coarse aggregate
W : water
C : high early strength cement, density = 3.14 g/cm^3
L : Lime stone powder
S : fine aggregate, density = 2.64 g/cm^3, F.M. = 2.75
G : coarse aggregate, density = 2.61 g/cm^3, F.M. = 6.37
SP : Superplasticizer
V : Viscosity improver

Table 3-3 Mix proportion of UFC

Flow (mm)	Unit quantity (kg/m^3)			Admixture (kg/m^3)
	Water	Premix binder	Steel fiber	
260±20	180	2254	157	24

3.2.2 Materials

Self-compacting concrete, UFC, steel reinforcements and screws and bolts were used in the experiment. The detailed description of the each material is provided as follow.

a) Concrete

Table 3-2 summarizes the details of mix proportion. The self-compacting concrete was used in this experiment because the complex shaped of shear keys at the internal surface of UFC U-shaped permanent formwork. The materials used in the concrete mixes were high-early strength cement, lime stone powder, fine aggregates, coarse aggregates, viscosity improver and superplasticizer, which was high-performance air entrained (AE) water reducing agent. The maximum aggregate size was 13 mm. The designed compressive strength of concrete was 35 MPa at 7-day age.

Table 3-4 Characteristics of steel fiber

Type	Nominal Diameter (mm)	Fiber Length (mm)	Aspect Ratio	Density (g/cm^3)	Nominal Tensile Strength (MPa)	Elastic Modulas (GPa)
Steel fiber	0.2	15	75	7.86	2500	210

Table 3-5 Details of steel reinforcements

Reinforcement	Type	Diameter (mm)	Grade	Yield strength (MPa)
Longitudinal reinforcements	D22	21.4	SPBD930	1022
Stirrups	D10	9.53	SD295A	339
Compression reinforcement	D10	9.53	SD295A	336

Table 3-6 Details of screws and bolts

	Diameter (mm)	Grade	Yield strength (N/mm^2)	Tensile strength (MPa)
Screw	10	SUS304	240	568
Bolt	10	SUS304	240	568

b) UFC

UFC can be produced by mixing pre-mix powder silica sand with water and high performance polycarboxylic superplasticizer and steel short fiber in the designed proportion. **Table 3-3** shows the mix proportion of UFC. The steel fiber with 0.2 mm diameter x 15 mm length was used and the volume of steel short fiber was 2%. The characteristics of steel fiber are shown in **Table 3-4**.

c) Steel reinforcements

The detailed properties of the steel reinforcements used in this study are listed in **Table 3-5**. A deformed steel reinforcement with nominal diameter equal to 21.4 mm was used for the longitudinal reinforcement. The specifications for the longitudinal reinforcements are according to JIS G 3109. The deformed steel reinforcement of 9.53 mm in nominal diameter was arranged as compression reinforcement. The yield strength was 336 MPa.

d) Screws and bolts

The stainless steel screws and bolts with 10 mm diameter follow SUS304 specification grade were used in the experiment. The yield strength and the tensile strength were 240 and 568 MPa, respectively as shown in **Table 3-6**.

e) UFC permanent formwork

The UFC U-shaped permanent formwork was fabricated in advance. The mold for casting the UFC U-shaped permanent formwork was made from the plywood which is designed for concrete work. The plywood was cut and form as a pattern of shear keys. The flowability performance of UFC is achieved to exhibit a flow value (JIS-R-5202.11) with around 260 mm for the material temperature of 20-25ºC even for including the steel fiber by 2% in volume. Therefore, it turns to be able to cast into the mold with only 20 mm thickness. After 24 hours, the UFC permanent formwork was removed of the mold. Then, it undergoes the stream curing at 90ºC for 48 hours. In each casting batch of UFC, three cylinders of Ø50x100 mm and three cylinders with Ø100x200 mm were prepared and put in the same condition as specimen in order to measure the compressive strength and tensile strength of UFC, respectively.

3.2.3 Fabrication of specimens

The fabrication step of specimen is presented in this section. The specimen consisted of two parts. One was a UFC U-shaped permanent formwork which has been fabricated in advance. The other was reinforced concrete which was then cast into the formwork in order to make a integrated component. **Figure 3-4** illustrates the fabrication step of UFC20-SB specimen. First, UFC formwork which has been already fabricated was prepared in the position. Then, the internal surface of UFC permanent formwork was cleaned by using air spray. After that, reinforcing bars were arranged and put in a UFC permanent formwork. In the case of specimen with screws and bolts, screws and bolts were provided according to the location of the screws and bolts shown in **Fig. 3-1**. Then, the concrete was cast into the UFC permanent formwork. After the casting, the specimens were covered with moist cloths and plastic sheets. The specimens were cured under covered with moist cloths and plastic sheet for 7 days and three specimen of Ø100x200 mm and three cylinders with Ø150x300 mm were prepared for compressive and tensile strength test, respectively.

Cleaning of permanent formwork

Installing reinforcement bars

Installing the screws and bolts

Specimen with ready for casting

Mixing of concrete

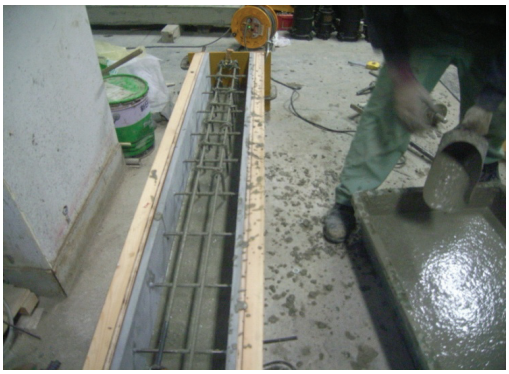

Casting of concrete

Moist-curing

Figure 3-4 Fabrication steps of the specimen (UFC20-SB)

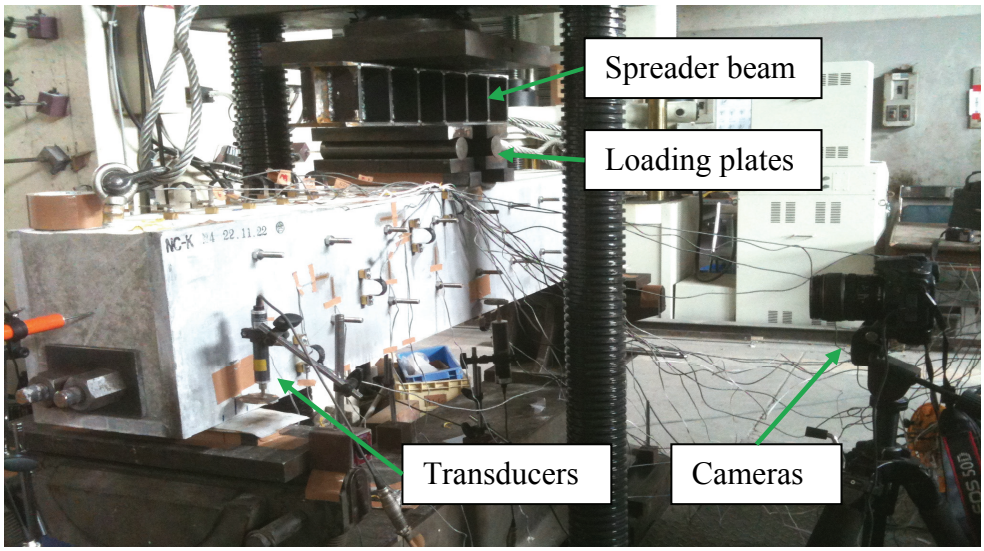

Figure 3-5 Loading test condition and setup

3.2.4 Loading method

Figure 3-5 presents the environment of specimen under the loading test. The specimens were subjected to a four-point bending test. The load was applied to both the UFC and RC at the same time. The specimens were placed on the roller supports in order to satisfy the simple supporting condition. The horizontal friction was prevented by inserted Teflon sheets and grease between the specimen and supports. The steel plates with 50 mm width, steel rollers and load distribution beam were placed on the top surface of the specimen at the location of loading points. The loading rate was about 0.2 kN per second.

3.2.5 Measurement Items

Figure 3-6 illustrates the general measuring items and loading condition during the loading test. The applied load was monitored and mid-span deflection was measured by using transducers. Strain gauges were used for measuring the strain of tension steel bars at mid-span and concrete on the top fiber at mid-span. At the top surface of UFC permanent formwork and RC parts, the strain gauges were attached to check the compatibility between UFC and concrete in the longitudinal direction of the beam as shown in **Fig. 3-6**. Moreover, the separation widths between inside concrete and UFC permanent formwork were also measured by using π-gauges along longitudinal direction of the specimen with interval of 90 mm. In addition, on the side surface of UFC permanent formwork of the test span, the diagonal crack opening widths along the diagonal line between the loading point and supporting point were measured by using four π-gauges as the position is presented in **Fig. 3-7**.

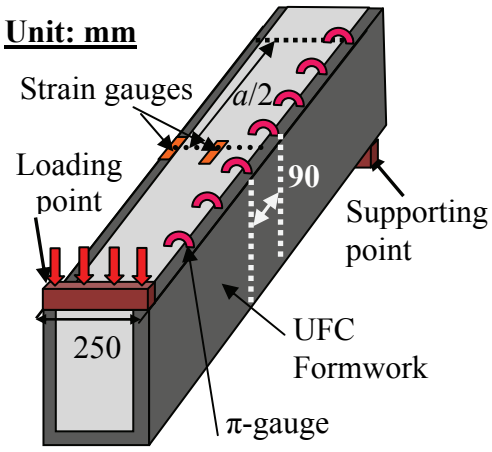

Figure 3-6 Measurement items and loading condition

π: π-gauge with 100 mm length

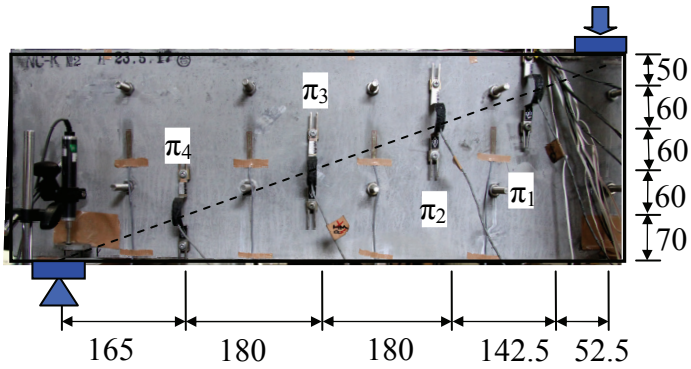

Figure 3-7 π-gauges along the diagonal crack line

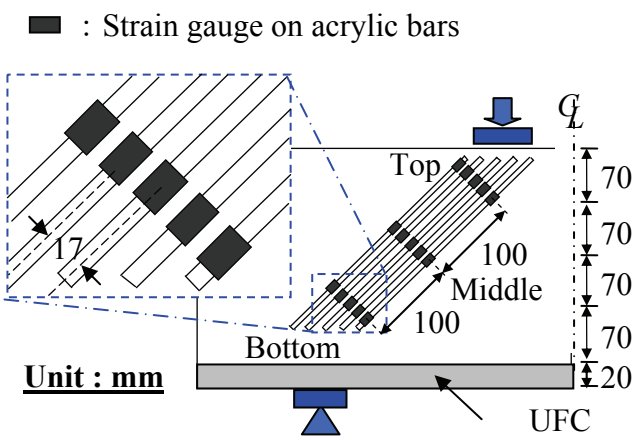

Figure 3-8 Location of acrylic bars

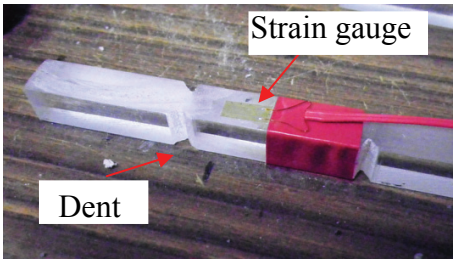

Figure 3-10 Details of acrylic bars

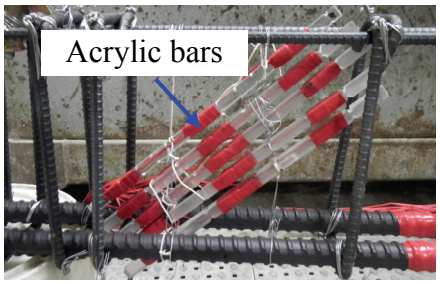

Figure 3-9 Arrangement of acrylic bars

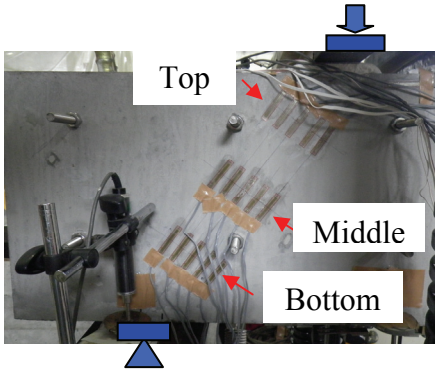

Figure 3-11 Arrangement of strain gauges on UFC permanent formwork

In case of UFC20-KB-ad1 specimen, strains of inside concrete and side surface of UFC permanent formwork were measured by using the acrylic bars and strain gauges, respectively. **Figure 3-8** shows the location of acrylic bars inside concrete. Three strain gauges were attached on each acrylic bar and set at the center of the cross section width of compressive strut from along the loading point to the supporting point in order to measure the compressive strain near the loading point, center of the compressive strut and the supporting point as the details and arrangement of acrylic bars is shown in **Fig. 3-9**. Five acrylic bars were set at 17

Table 3-7 Mechanical properties of concrete and UFC, and the testing result in Series-I

Name	Mechanical properties of concrete		Mechanical properties of UFC		Results of loading test			
	f'_c (MPa)	f_t (MPa)	f'_{c_UFC} (MPa)	f_{t_UFC} (MPa)	P_{cr} (kN)	P_{max} (kN)	V_u (kN)	R
Ref	32.8	2.1	-	-	45.0	138.0	69.0	1.0
UFC20-S	43.5	2.5	194.7	10.1	105.1	319.6	159.8	2.32
UFC20-K	36.6	2.7	191.5	13.9	90.6	334.6	167.3	2.42
UFC20-SB	33.5	2.5	192.6	11.4	95.3	355.8	177.9	2.58
UFC20-KB	40.4	2.1	184.2	11.9	82.1	384.0	192.0	2.78

f'_c: compressive strength of concrete, f_t : tensile strength of concrete, f'_{c_UFC} : compressive strength of UFC, f_{t_UFC} : tensile strength of UFC, P_{cr}: Flexural cracking load, P_{max}: Peak load, V_u : Shear Capacity, R : Ratio of shear capacity

mm intervals. According to the method by Nakamura and Higai (1999), acrylic bar was fixed by making the dent form as details is shown in **Fig. 3-10**. Concrete strain gauges were also attached at the same position of those on acrylic bars as shown in **Fig. 3-11**.

3.3 Experimental Results and Discussions

3.3.1 Shear capacities in Series-I

Table 3-7 summarizes the mechanical properties of concrete and UFC, and the testing results in Series-I. The ratio of shear capacity (R) is a ratio of shear capacity in each specimen divided by that of the Ref specimen which can be calculated by using Eq. (3-1).

$$R = \frac{V_u}{V_{\mathrm{Re}f}} \tag{3-1}$$

where, V_u is shear capacity of each specimen, V_{Ref} is shear capacity of Ref specimen

From **Table 3-7**, in order of the ratio of shear capacity, the specimens can be arranged as UFC20-S, UFC20-K, UFC20-SB and UFC20-KB with 2.32, 2.42, 2.58 and 2.78, respectively. This result indicates that the shear capacity significantly increase by using the U-shaped UFC formwork on the cross section of a RC beam. Even if only smooth surface was provided and without presence of screws and bolts in UFC20-S specimen, the drastically

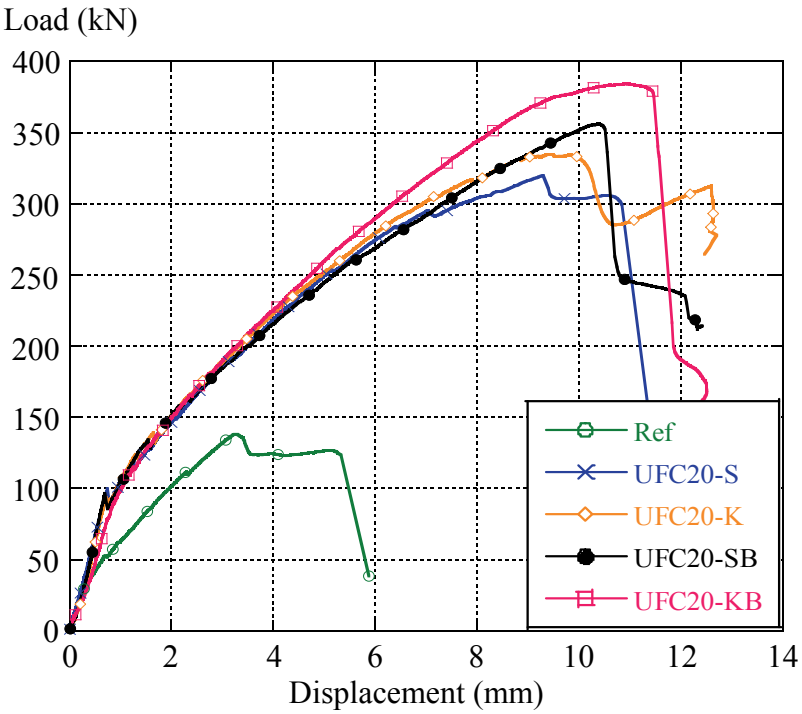

Figure 3-12 Load-displacement relationships in Series-I

increase of shear capacity with more than twice comparing with normal RC beam was observed. Moreover, the shear capacity of the beam with providing screws and bolts was much larger than that with only providing shear keys. Furthermore, the shear capacity of the beam with shear keys and providing screws and bolts was the largest. It should be noted that the variation of compressive strength of concrete was very slight.

3.3.2 Load-displacement relationships and crack patterns in Series-I

The relationships between the load and the mid-span displacement of all specimens in Series-I are shown in **Fig. 3-12**. The mid-span displacement was obtained by subtracting the displacements at the supporting points from the mid-span displacement. **Figure 3-13** shows the crack patterns observed after the loading tests. In case of UFC20-S, UFC20-K, UFC20-SB and UFC20-KB specimens, the crack patterns of both UFC and inside RC part are illustrated. The critical cracks are represented by the bold lines in **Fig. 3-13**. The crack and failure pattern in each specimen is discussed below.

a) Ref

The flexural crack was observed at 45.0 kN. The diagonal crack initiated at the middle of test span and load suddenly dropped at the peak load (138.0 kN) as shown in **Fig. 3-13(a)**.

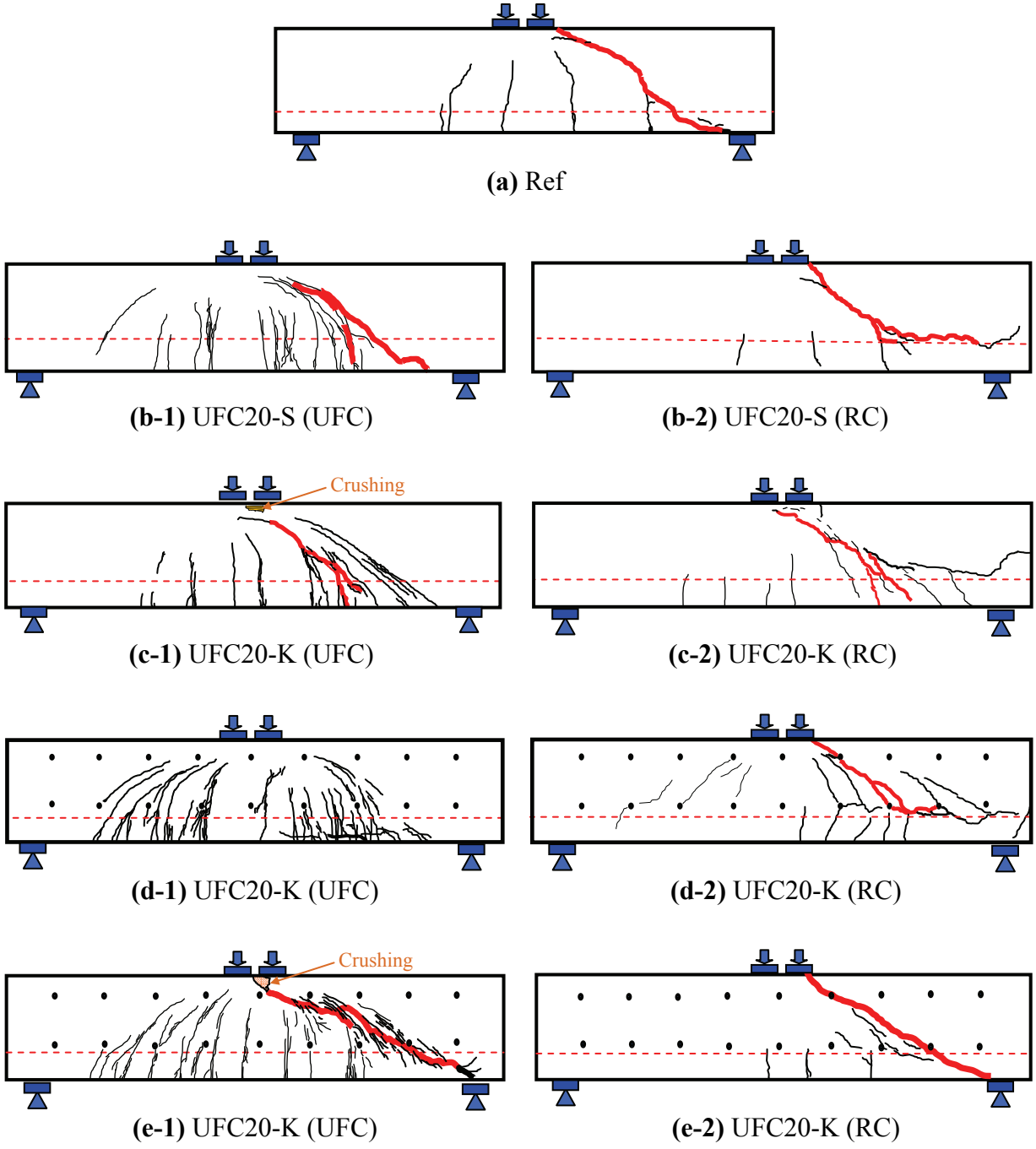

Figure 3-13 Crack patterns in Series-I

b) UFC20-S

When the load reached 105.1 kN, the flexural cracks on UFC permanent formwork on the UFC permanent formwork was observed. Then, the inclined crack on UFC permanent formwork initiated. And then, slipping between RC and UFC permanent formwork occurred at the peak load. After the testing, UFC formwork was removed and a diagonal crack of inside RC part was observed as shown in **Figs. 3-13(b-1)** and **(b-2)**.

c) UFC20-K

The flexural cracks on UFC permanent formwork initiated when the load was 90.6 kN. When the load reached to the peak, the inclined crack located from the support to loading point propagated as shown in **Figs. 3-13(c-1)** and **(c-2)**. Moreover, the crushing under the loading point on UFC permanent formwork was observed. The separation crack between UFC permanent formwork and internal RC was observed after the loading test.

d) UFC20-SB

From the beginning, the specimen behaved linearly until the first flexural crack at 95 kN. After that, the flexural and flexural shear cracks appeared in a sequence form the mid-span to mid of the shear span. When the load reached to the peak, a number of cracks occurred as shown in **Fig. 3-13(d-1)**. **Figure 3-13(d-2)** shows the diagonal crack of internal RC part. The critical crack penetrated from a bolt to a bolt and looked very different from those in UFC.

e) UFC20-KB

The flexural crack on UFC appeared around mid of span at the load of 82 kN. At 215 kN, the main diagonal crack on the UFC permanent formwork was observed. At the peak load, the critical diagonal crack was propagated and widened, and the crushing of UFC under the loading point occurred as shown in **Fig. 3-13(e-1)**. After the loading test, UFC permanent formwork was removed. It is shown that the diagonal crack of internal RC part occurred at the same location of that in the UFC permanent formwork as shown in **Fig. 3-13(e-2)**.

3.3.3 Shear resistance mechanisms in Series-I

The shear resistance mechanisms of UFC20-S, UFC20-K, UFC20-SB and UFC20-KB were investigated. The effect of shear keys at the internal surface and the effect of screws and bolts on the shear resistance mechanisms is pointed out. The shear resistance mechanisms in all specimens are explained below.

a) UFC20-S

Figure 3-14 shows the relationships between the load and average separation width between internal RC and UFC permanent formwork on the top surface of all specimens except for Ref as the location of π-gauges are shown in **Fig. 3-6**. The relationships between the load

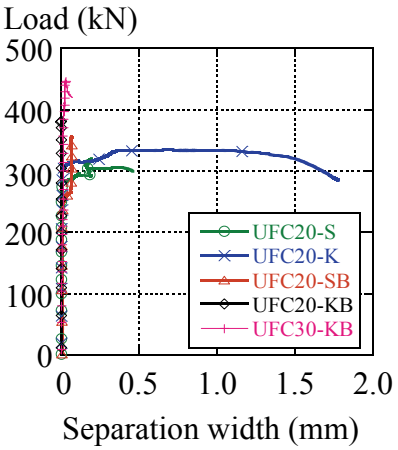

Figure 3-14 Load-separation width in Series-I and II

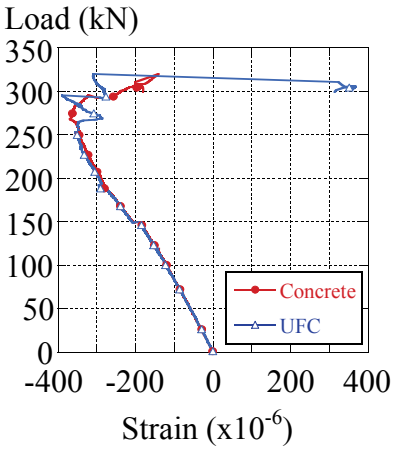

Figure 3-15 Load-strains at the upper surface (UFC20-S)

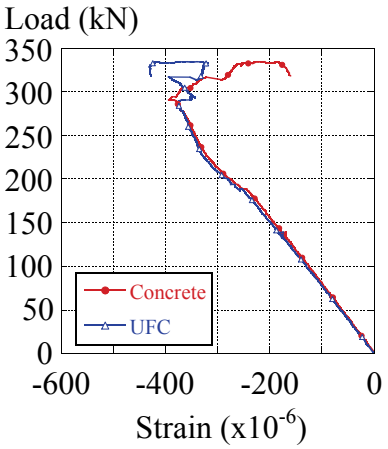

Figure 3-16 Load-strains at the upper surface (UFC20-K)

and strain at the top surface of RC and UFC formwork at the mid of shear span of UFC20-S specimen (see **Fig. 3-6**) is illustrated in **Fig. 3-15**. Positive value represents the tensile strain, conversely, negative shows the compressive strain. The widening of diagonal crack was prevented due to the bonding between UFC and RC. However, at 90 percent of the peak load ($0.9P_{max}$) or 287.5 kN, UFC formwork could not resist the opening of diagonal crack. Hence, the slipping between RC and UFC permanent formwork occurred and the UFC formwork and RC part showed different behavior after $0.9P_{max}$ as shown in **Fig. 3-15**.

b) UFC20-K

The opening of the diagonal crack of the RC part was prevented through the side shear keys between UFC and concrete surface. At $0.9P_{max}$, the opening width between RC and UFC formwork increased drastically due to the lateral force from the interlocking action as shown in **Fig. 3-14**. It is reflected that the UFC permanent formwork and RC part showed different behavior after $0.9P_{max}$ as illustrated in **Fig. 3-16**.

c) UFC20-SB

In UFC20-SB where smooth surface and screws and bolts are provided, the diagonal crack in RC part attempted to widen as the load increased, but it was resisted by forces which were generated at the top and bottom of bolts. Consequently, since the forces were concentrated around the bolts, the diagonal crack was propagated to connect from a bolt to a bolt as shown in **Fig. 3-13(d-1)**. At $0.7P_{max}$, the opening width between RC and UFC

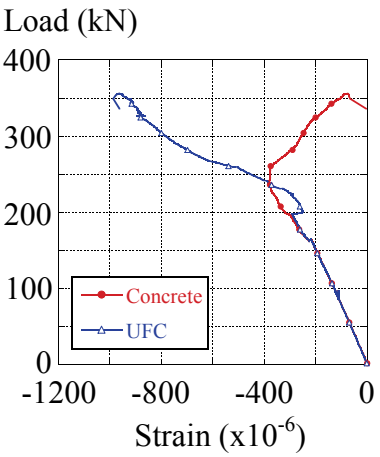

Figure 3-17 Load-strain at the upper surface (UFC20-SB)

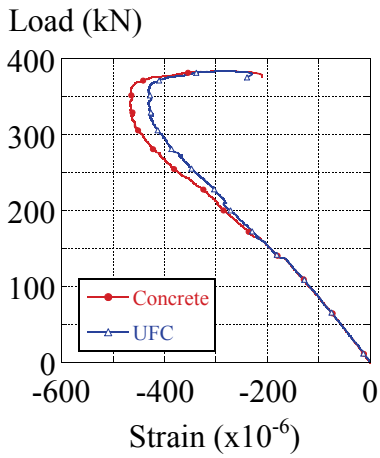

Figure 3-18 Load-strain at the upper surface (UFC20-KB)

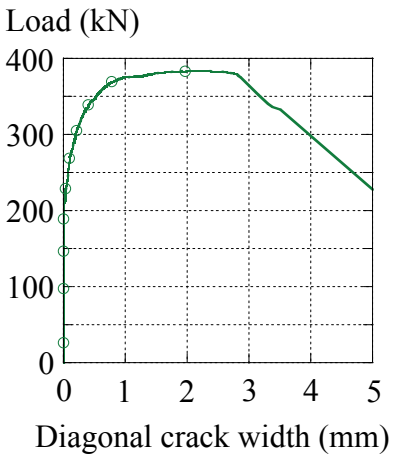

Figure 3-19 Load-diagonal crack width (UFC20-KB)

formwork was slightly increased (**Fig. 3-14**). After that, the difference of strain behavior between UFC permanent formwork and RC part was observed as shown in **Fig. 3-17**.

d) UFC20-KB

Figure 3-18 presents the strains at the top surface of RC part and UFC permanent formwork. The similar behavior between UFC permanent formwork and RC was observed. In other words, the beam had compatibility until the test finished. It should be noted that the separation width between RC and UFC permanent formwork was very small as shown in **Fig. 3-14**. The diagonal crack in RC part was resisted by synergetic effect of forces which were generated at the top and bottom of screws and bolts and the shear key at the interface as the load increased. After that, the main diagonal crack on UFC permanent formwork occurred at 0.7 P_{max}, while the opening width of diagonal crack was increasing as the average crack width from four measured crack widths along the diagonal crack is shown in **Fig. 3-19**. Then, the load dropped and failure occurred.

In comparison, the diagonal crack was resisted to widen by shear keys at the internal surface in the beam with only providing shear keys. On the other hand, for the beam with providing screws and bolts, the diagonal crack was resisted and transferred effectively by screws and bolts. Therefore, as the combination of both screws and bolts and shear keys, the synergetic action occurred. Consequencely, the compatibility system and efficiency bonding between UFC permanent formwork and inside RC part of the beam were secured and the shear resistance mechanism became effective. From the above reason, the UFC permanent formwork with shear keys internal surface and screws and bolts system were used in the latter series.

3.3.4 Effect of the thickness of permanent formwork

In Series-II, The effect of thickness of UFC permanent formwork is discussed based on the experimental results of Ref, UFC20-KB and UFC30-KB specimens.

Table 3-8 shows the mechanical properties of concrete and UFC, and the testing result in Series-II. **Figure 3-20** presents the load-displacement relationships of all speciemens in Series-II. The specimens can be arranged as UFC20-KB and UFC30-KB in order of enhancement ratio of shear capacity (R). Also, **Fig. 3-21** illustrates that as replacement percentages of UFC formwork per total cross section area of beams increased by 0, 22.9 and 33.6 %, the shear capacity increased with the actual shear capacity of each case was 69, 192.0 and 223.5 kN, respectively. It is indicated that the shear capacity of RC beams with using U-shaped UFC permanent formwork increased drastically with increase in thickness of UFC

Table 3-8 Mechanical properties of concrete and UFC, and the testing result in Series-II

Name	Mechanical properties of concrete		Mechanical properties of UFC		Results of loading test			
	f'_c (MPa)	f_t (MPa)	f'_{c_UFC} (MPa)	f_{t_UFC} (MPa)	P_{cr} (kN)	P_{max} (kN)	V_u (kN)	R
Ref	32.8	2.1	-	-	45.0	138.0	69.0	1.0
UFC20-KB	40.4	2.1	184.2	11.9	82.1	384.0	192.0	2.78
UFC30-KB	36.2	2.2	181.8	12.0	92.0	447.0	223.5	3.24

f'_c: compressive strength of concrete, f_t : tensile strength of concrete, f'_{c_UFC} : compressive strength of UFC, f_{t_UFC} : tensile strength of UFC, P_{cr}: Flexural cracking load, P_{max}: Peak load, V_u : Shear Capacity, R : Ratio of shear capacity

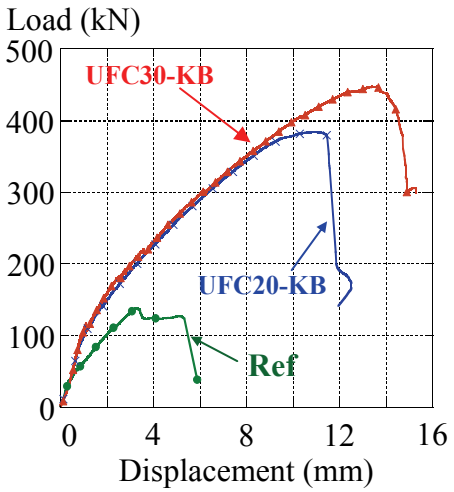

Figure 3-20 Load-displacement relationship in Series-II

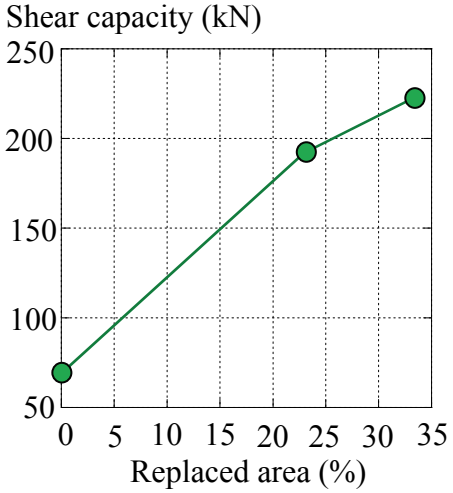

Figure 3-21 Shear capacity and replaced area of UFC relationship

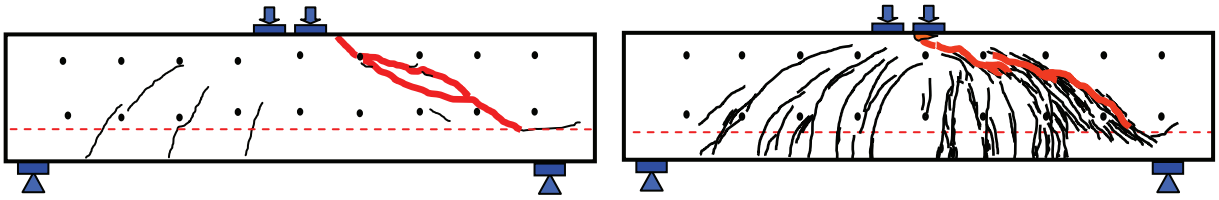

(a) RC **(b)** UFC

Figure 3-22 Crack patterns of UFC30-KB

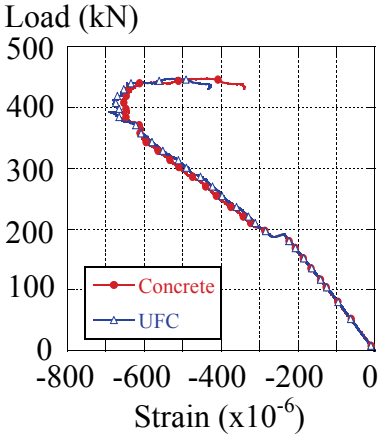

Figure 3-23 Load-strain at the upper surface (UFC30-KB)

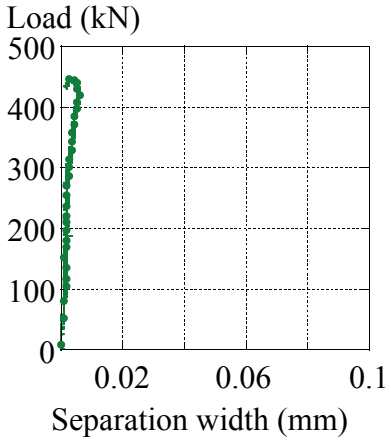

Figure 3-24 Load-separation width (UF30-KB)

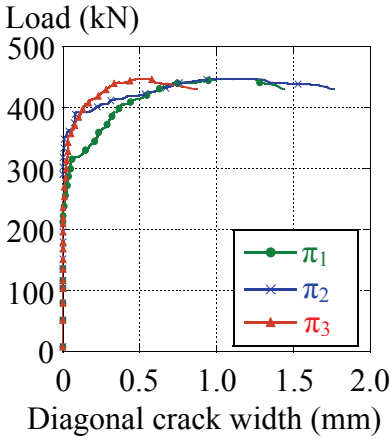

Figure 3-25 Load-diagonal crack width (UFC30-KB)

permanent formwork and it was proportional. This is because the separation opening width between RC and UFC permanent formwork slightly increased compared to UFC20-KB specimen as shown in **Fig. 3-14**. Then, the shear transfer from the internal surface decreased. Therefore, the shear capacity slightly decreased.

Figure 3-22 shows the crack patterns of UFC30-KB. In UFC30-KB, the failure pattern was the same as that observed in UFC20-KB specimen. **Figure 3-23** presents the load-strain relationship at the upper surface. The shear resisting mechanism of UFC30-KB was also the same as observed in UFC20-KB specimen as already explained. Moreover, separation width between RC and UFC permanent formwork was very small as shown in **Fig. 3-24**. Hence, even if the thickness of formwork increased, shear keys and screws and bolts system could contribute the compatibility and sufficient bonding between UFC permanent formwork and RC part. **Figure 3-25** shows the load-diagonal crack width relationship of UFC30-KB.

Table 3-9 Mechanical properties of concrete and UFC, and the testing results of Series-III

Name	Mechanical Properties of concrete		Mechanical Properties of UFC		Results of loading test			
	f'_c (MPa)	f_t (MPa)	f'_{c_UFC} (MPa)	f_{t_UFC} (MPa)	P_{cr} (kN)	P_{max} (kN)	V_u (kN)	Failure mode
UFC20-KB	40.4	2.1	184.2	11.9	82.1	384.0	192.0	DT
UFC20-KB-ad21	33.1	2.2	182.7	12.6	142.8	496.2	248.1	SC
UFC20-KB-ad1	30.6	2.3	177.8	10.8	334.2	1058.6	529.3	SC

f'_c: Compressive strength of concrete, f_t : Tensile strength of concrete, f'_{c_UFC} : Compressive strength of UFC, f_{t_UFC} : Tensile strength of UFC, P_{cr}: Flexural cracking load, P_{max}: Peak load, V_u : Shear Capacity, DT: Diagonal tension failure, SC: Shear compression failure

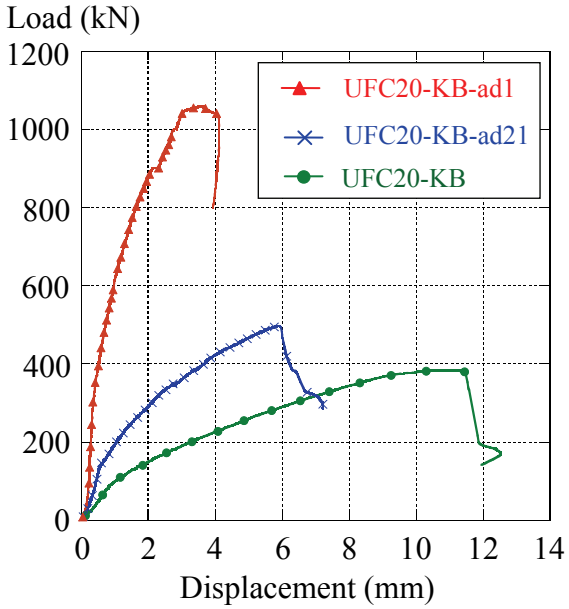

Figure 3-26 Load-deplacement relationships in Series-III

3.3.5 Effect of shear span to effective depth ratio

a) Load-displacement relationships and crack patterns in Series-III

Table 3-9 summarizes the experimental results in Series-III. The relationships between the load and the mid-span displacement are illustrated in **Fig. 3-26**. **Fig. 3-27** shows the crack patterns of UFC20-KB-ad21, UFC20-KB-ad1 and UFC20-KB which the first two specimens failed in shear compression failure mode and UFC20-KB failed in diagonal tension.

In UFC20-KB-ad21 specimen, the diagonal crack on the UFC formwork occurred at 347.3 kN, however, the load was still increasing. The crushing of UFC under the loading point

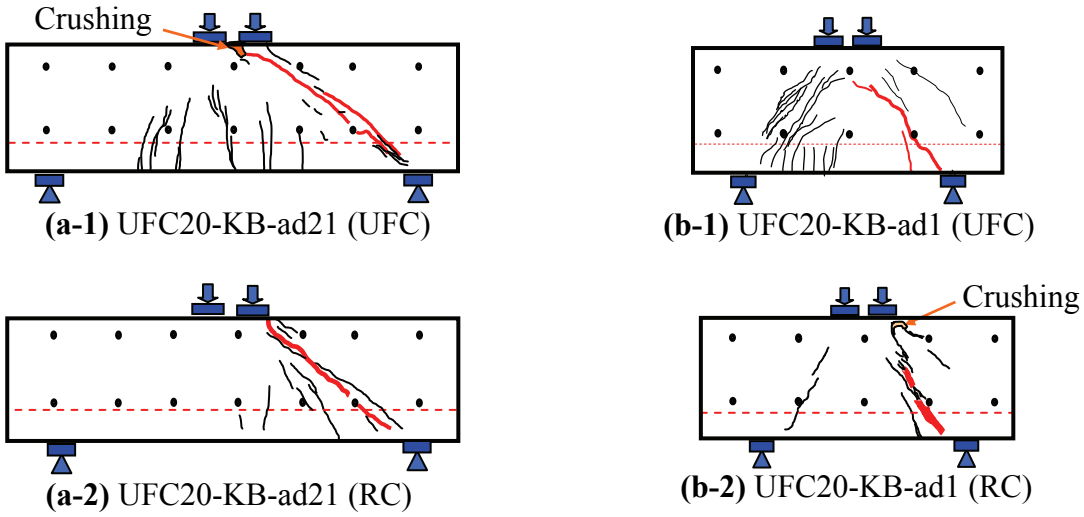

Figure 3-27 Crack patterns (Series-III)

occurred at the peak load as crack pattern of UFC permanent formwork is shown in **Fig. 3-27(a-1)**. **Figure 3-27(a-2)** shows the diagonal crack of inside RC part.

In case of UFC20-KB-ad1 specimen, at 334.2 kN, the flexural crack on the UFC permanent formwork was initiated. Then, a number of cracks propagated in the direction from the support to the loading point with increasing in load as shown in **Fig. 3-27(b-1)**. After the loading test, the separation failure of RC and UFC permanent formwork and the crushing of inside RC part under the loading point were observed as shown in **Fig. 27(b-2)**.

b) Shear resisting mechanism of UFC20-KB-ad21

UFC20-KB-ad21 specimen failed with the shear compression failure. Even if a diagonal crack on UFC permanent formwork occurred, the diagonal tension failure did not occur since UFC permanent formwork prevented widening of diagonal crack inside RC part. Hence, the compressive stress acted above the diagonal crack. Consequently, the strains at the top fiber of both UFC permanent formwork and concrete were changed into the reverse direction as shown in **Fig. 3-28**. Therefore, the tension stress occurred at the upper edge of both UFC and RC. Finally, the load reached to the peak because of the crushing of UFC near the loading point as shown in **Fig. 3-27(a-1)**.

As the discussion above, it is found that the failure mode changed from the diagonal tension failure to the shear compression failure when the *a/d* ratio changed from 3.27 to 2.16 because of the compression stress acted above the diagonal crack and crushing of the UFC occurred near the loading point.

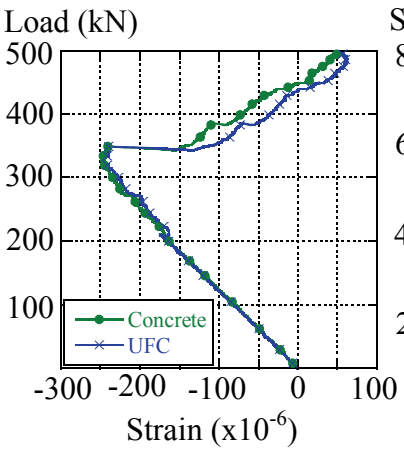

Figure 3-28 Load-strain at the upper surface (UFC20-KB-ad21)

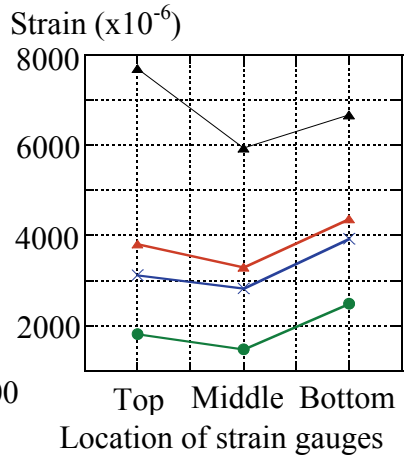

Figure 3-29 Maximum compressive strain of concrete

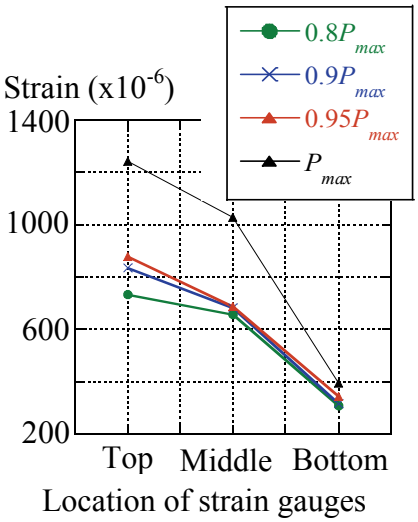

Figure 3-30 Maximum compressive strain of UFC

c) Compressive strain of concrete in the strut formation of UFC20-KB-ad1

UFC20-KB-ad1 also failed in shear compression failure mode same as in UFC20-KB-ad21. Therefore, the failure mechanism of UFC20-KB-ad1 was examined by using the strains measured in the compressive strut of both concrete and UFC. The locations of strain gauges are shown in **Figs. 3-8** and **3-11**.

The development of the maximum compressive strain of concrete near the loading point (Top), center of the strut (Middle) and near the supporting point (Bottom) of concrete and UFC are shown in **Figs. 3-29** and **3-30**, respectively. In both concrete and UFC, compressive strains increased drastically near the peak load because the compression struts were formed in both concrete and UFC formwork. As a result, the compressive strains reached ultimate strain and reflected that crushing of concrete occurred as shown in **Fig. 3-27(b-2)**. It should be noted that the distribution of compressive strain of both concrete and UFC seems to be different. This is because the compatibility between RC and UFC permanent formwork cannot be secured and the separation crack between UFC permanent formwork and inside RC was also observed.

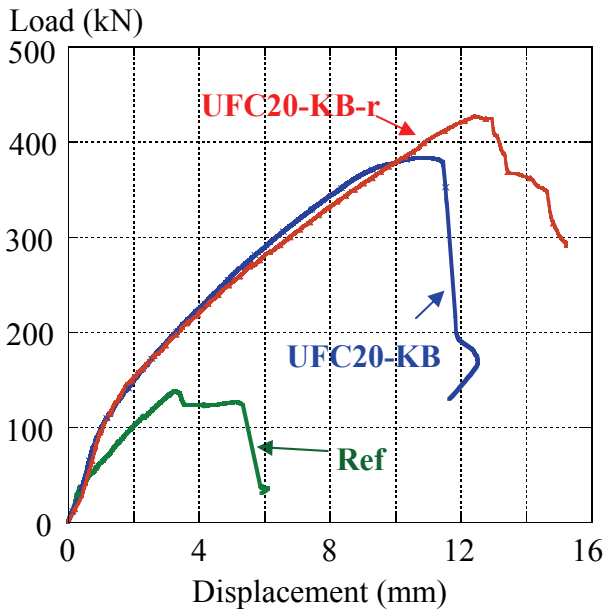

Figure 3-31 Load-displacement relationship in Series-III

Table 3-10 Mechanical properties of concrete and UFC, and the testing result in Series-IV

Name	Mechanical properties of concrete		Mechanical properties of UFC		Results of loading test			
	f'_c (MPa)	f_t (MPa)	f'_{c_UFC} (MPa)	f_{t_UFC} (MPa)	P_{cr} (kN)	P_{max} (kN)	V_u (kN)	R
Ref	32.8	2.1	-	-	45.0	138.0	69.0	1.0
UFC20-KB	40.4	2.1	184.2	11.9	82.1	384.0	192.0	2.78
UFC30-KB	36.4	2.7	170.5	12.4	92.6	427.6	213.8	3.10

f'_c: compressive strength of concrete, f_t : tensile strength of concrete, f'_{c_UFC} : compressive strength of UFC, f_{t_UFC} : tensile strength of UFC, P_{cr}: Flexural cracking load, P_{max}: Peak load, V_u : Shear capacity, R : Ratio of shear capacity

3.3.6 Effect of presence of stirrups

In Series-IV, the influence of the presence of stirrups was investigated based on the experimental result of UFC20-KB and UFC20-KB-r. **Figure 3-31** shows the load-displacement relationships of UFC20-KB and UFC20-KB-r specimen. In order of enhancement ratio of shear capacity (R), the specimens can be arranged as UFC20-KB and UFC20-KB-r with 2.78 and 3.10, respectively as shown in **Table 3-10**. The failure pattern of UFC20-KB-r was similar to UFC20-KB and UFC30-KB as explained before. The crack patterns of UFC20-KB-r are shown in **Fig. 3-32(a)** and **(b)**.

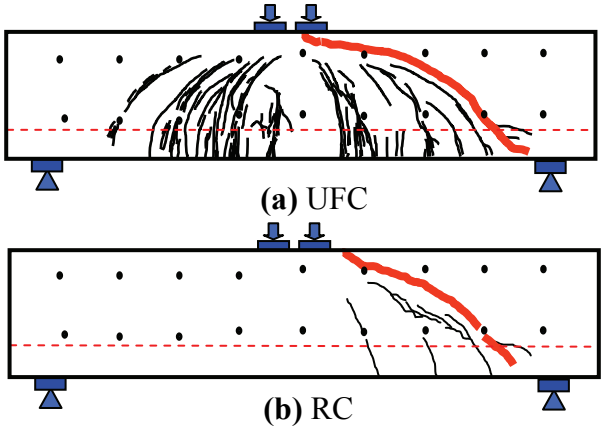

Figure 3-32 Crack patterns of UFC20-KB-r

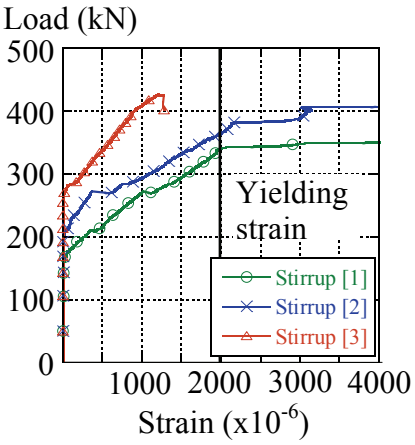

Figure 3-33 Load-stirrup strain relationships

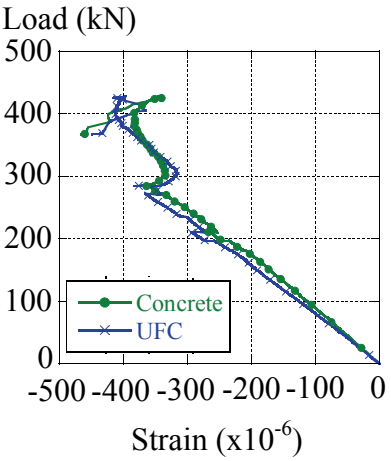

Figure 3-34 Load-strain at the upper surface (UFC20-KB-r)

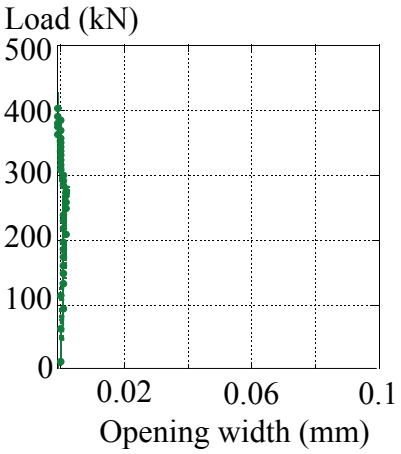

Figure 3-35 Load-opening width between RC and UFC (UF20-KB-r)

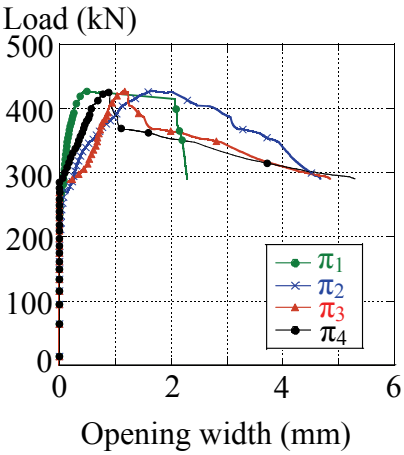

Figure 3-36 Load-diagonal crack width (UFC20-KB-r)

Figure 3-33 shows the relationship between the load and stirrup strains. Stirrup [1], [2] and [3] are corresponding to those in **Fig. 3-1**. Strains of stirrup [1] and [2] reached the yielding strain before the peak load. It indicated that the opening of diagonal crack in concrete was resisted by UFC formwork and stirrups, and both still carried the load until the peak load. Hence, since the stirrups were provided in RC part, the shear capacity of the beams was increased.

In comparison, the shear resisting mechanism of UFC20-KB-r was the same as that of UFC20-KB and UFC30-KB as mentioned above. As the similar strain behavior is shown in **Fig. 3-34** and the separation crack width is shown in **Fig. 3-35**, in case of stirrups were provided, compatibility and efficient bonding of RC and UFC formwork by using shear keys and bolts can be secured. **Figure 3-36** shows diagonal crack widths of UFC20-KB-r.

3.4 Weight Reduction Compared with Ordinary RC Beams

3.4.1 Design of normal RC beams

In order to discuss about the degree of weight reduction of the RC beams using UFC permanent formwork, ordinary RC beams with the same load carrying capacity as specimens in series I and II were designed. The characteristics of designed RC beams are the same as in the RC beams with U-shaped UFC permanent formwork as shown in **Fig. 3-1** and described in **Table 3-11**. The shear carrying capacity of ordinary RC beams can be obtained from Eq. (3-2) (Niwa, 1987).

$$V_c = 0.2(f'_c)^{1/3}(100p_w)^{1/3}(\frac{1000}{d})^{1/4}(0.75+\frac{1.4}{a/d})b_w d \quad (3\text{-}2)$$

where, V_c is shear capacity of ordinary RC beam without stirrups (N), f'_c is the compressive strength of concrete (MPa), p_w is longitudinal reinforcement ratio, b_w is web thickness (mm), d is the effective depth (mm)

By set the value of shear capacity of ordinary RC beam (V_c) corresponding to the half of the load carrying capacity of RC beam using U-shaped UFC permanent formwork from the experiments, the width of beams (b_w), can be calculated. Therefore, the width of cross section and weight of RC beams with the same load carrying capacity as composites beams were determined. From the densities of RC and UFC are 2.5 t/m^3, the weights of the normal RC and RC beam using U-shaped UFC permanent formwork were compared. The rate of weight reduction is calculated from Eq. (3-3).

$$R_W = \frac{(W_{RC} - W_{UFC})}{W_{RC}} \times 100 \quad (3\text{-}3)$$

where, R_w is the rate of weight reduction (%), W_{RC} is weight of ordinary RC beam (kg), W_{UFC} is weight of RC beam using U-shaped UFC permanent formwork obtained from the experiment (kg)

Table 3-11 Characteristics of ordinary RC beams and its material properties

Compressive strength of concrete, f'_c (MPa)	35
Shear span, a (mm)	3.27
Effective depth, d (mm)	220
Cross sectional area of longitudinal reinforcement, A_s (mm^2)	774.2

Table 3-12 Comparison of the weight using experimental results

Name	V_c (kN)	b_w (kN)	W_{RC} (kg)	W_{UFC} (kg)	R_w (%)
UFC20-S	159.8	784.19	935.15	298.1	68
UFC20-K	167.3	915.6	1091.8	298.1	73
UFC20-SB	177.9	1049.4	1251.4	298.1	76
UFC20-KB	192.0	1071.7	1277.9	298.1	77
UFC30-KB	223.5	1420.5	1693.9	298.1	82

W_{RC} = Total weight of normal RC beams, W_{UFC} = Total weight of composite beams

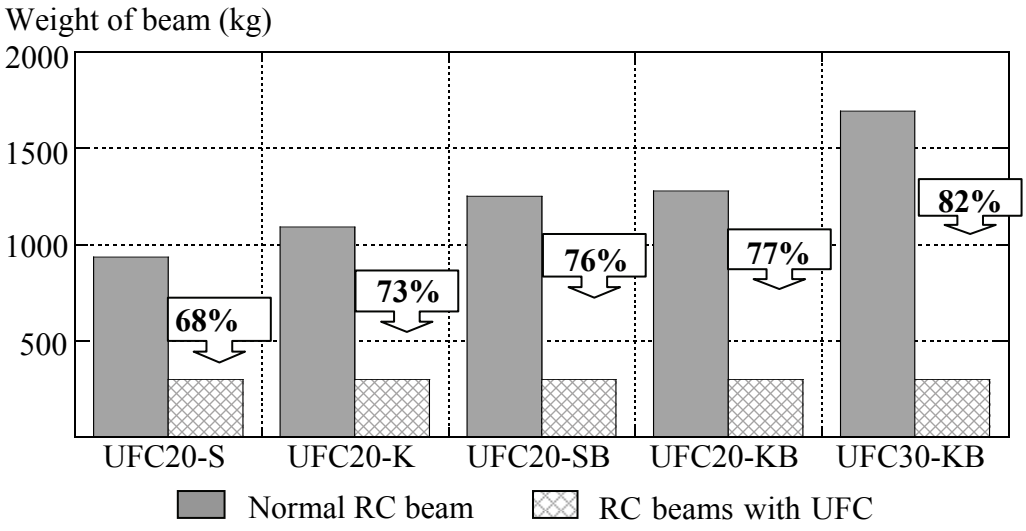

Figure 3-37 Weight reduction rates

3.4.2 Comparison of weight

Table 3-12 and **Fig. 3-37** show the calculation results of weight reduction by using UFC permanent formwork. The weight of the members can be reduced with 68.1, 72.7, 76.2, 76.7 and 82.4 % in UFC20-S, UFC20-K, UFC20-SB, UFC20-KB and UFC30-KB, respectively. From this result, it clearly indicates that the RC beams using U-shaped UFC permanent formworks can make a significant contribution on the weight reduction of the members.

3.5 Investigation on Shear Carried by U-Shaped UFC Permanent Formwork

In this section, the shear carried by UFC permanent formwork is presented. First, the shear carried by UFC permanent formwork of the specimens failed in diagonal tension is discussed. In second half, the shear carried by UFC permanent formwork of UFC20-KB-ad1 which failed in the shear compression failure is examined.

3.5.1 Shear carried by UFC U-shaped permanent formwork failed in diagonal tension

The shear carried by UFC permanent formwork of UFC20-KB, UFC30-KB and UFC20-KB-r which failed in diagonal tension was investigated. The shear capacity of RC beams using UFC U-shaped permanent formwork was assumed to be the summation of shear carried by concrete, stirrups and UFC permanent formwork. The calculation method for UFC permanent formwork is discussed below.

a) Shear carried by UFC permanent formwork observed from the experiment

From the experimental result, the shear carried by UFC permanent formwork was obtained by subtracting the shear carried by concrete and stirrups from the total shear capacity observed from the loading test with as can be obtained by Eq. (3-4)

$$V_{UFC} = V_u - V_c - V_s \tag{3-4}$$

where, V_{UFC} is the shear carried by UFC formwork, V_u is the total shear capacity, V_c is the shear carried by concrete, V_s is the shear carried by stirrups

In this study, the shear carried by concrete was calculated by Eq. (3-2) which considering only inside RC part. The thickness of permanent formwork was excluded from the width of beams (b_w).

The shear carried by stirrups was obtained from the measured strain of steel by strain gauges as can be calculated by Eq. (3-5).

$$V_s = \begin{cases} A_s E_s \varepsilon_s (\varepsilon_s < \varepsilon_y) \\ A_s f_{wy} (\varepsilon_s \geq \varepsilon_y) \end{cases} \tag{3-5}$$

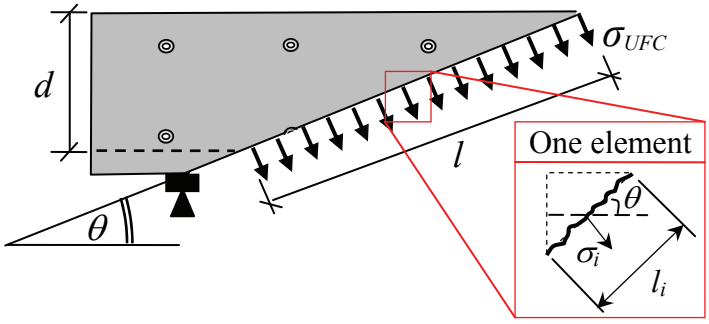

Figure 3-38 Shear carrying model for UFC permanent formwork

where, A_s is the total cross section area of stirrup, E_s is the elastic modulus of stirrup, ε_s is the average stirrup strain, ε_y is the yielding strain of stirrup, f_{wy} is the yielding strength of stirrup

b) Shear carried by UFC permanent formwork obtained in the calculation

The shear carried by UFC permanent formwork was calculated based on a simplified shear carrying model. A linear crack with maintaining the angle of diagonal crack is assumed in order to compute the shear carried by UFC permanent formwork, as shown in **Fig. 3-38**. The crack length of UFC permanent formwork and the angle of diagonal crack are represented by l and θ, respectively. Therefore, the crack length of UFC permanent formwork is given by,

$$l = \frac{d}{\sin\theta} \tag{3-5}$$

where, l is the crack length (mm), θ is the angle of the diagonal crack (°)

The tensile stress of UFC permanent formwork is assumed to be applied in the perpendicular direction to the linear crack line. Consequently, the shear carried by UFC permanent formwork is vertical component of the summation of tensile stress along the diagonal crack line. The pictures of the side surface of UFC permanent formwork taken at the peak load were used to measure the angles of diagonal cracks. Therefore, the shear carried by UFC permanent formwork based on this model is given by Eq. (3-6).

$$V_{UFC} = \frac{2 \cdot t \cdot \sigma_{UFC} \cdot d}{\tan\theta} \tag{3-6}$$

where, t is the thickness of UFC permanent formwork (mm), and d is effective depth (mm)

Table 3-13 Shear carried by UFC permanent formwork

Specimens	t (mm)	θ (°)	f_{t_UFC} (MPa)	$\bar{\sigma}$ (MPa)	$V_{UFC\text{-}exp}$ (kN)	$V_{UFC\text{-}cal1}$ (kN)	$V_{UFC\text{-}cal2}$ (kN)	$V_{UFC\text{-}exp}$ /$V_{UFC\text{-}cal1}$	$V_{UFC\text{-}ex}$ /$V_{UFC\text{-}cal2}$
UFC20-KB	20	22.1	11.9	3.8	127.3	297.0	118.8	0.43	1.07
UFC30-KB	30	21.0	12.0	5.0	160.9	375.0	156.3	0.43	1.03
UFC20-KB-r	20	25.3	12.4	4.0	102.7	319.6	103.0	0.32	1.00

t: thickness of UFC permanent formwork, θ: angle of diagonal crack measured from the experiment, f_{t_UFC}: tensile strength of UFC, $\bar{\sigma}$:the average of tensile stress obtained from tension softening curve, $V_{UFC\text{-}exp}$: experimental value of shear carried by UFC permanent formwork, $V_{UFC\text{-}cal1}$: calculated value of shear carried by UFC permanent formwork by using tensile strength, $V_{UFC\text{-}cal2}$: calculated value of shear carried by UFC permanent formwork by using tensile stress obtained from tension softening curve

If the tensile stress (σ_{UFC}) is assumed to be the tensile strength of UFC (f_{t_UFC}) at the peak load, the shear carried by UFC permanent formwork is given as,

$$V_{UFC} = \frac{2 \cdot t \cdot f_{t\_UFC} \cdot d}{\tan\theta} \tag{3-7}$$

where, f_{t_UFC} is the tensile strength of UFC (MPa)

c) Result of the calculation

Table 3-13 lists the experimentally investigated and computationally calculated shear carried by UFC permanent formwork of UFC20-KB, UFC30-KB and UFC20-KB-r specimens by using Eqs. (3-4) and (3-7), respectively. The shear carried by UFC permanent formwork obtained from the experiment became smaller than that calculated by Eq. (3-7) in all three specimens. This is explained as the tensile strength was used for the stress of UFC permanent formwork ($\sigma_{UFC} = f_{t\_UFC}$). However, from the experimental observation, it is found that the crack width corresponding to the tensile strength value were definitely smaller than the critical crack width in the UFC permanent formwork, for example, in the case of UFC20-KB-r as shown in **Figs. 3-39 (a)** and **(b)**. Therefore, the tensile stress (σ_{UFC}) was modified and examined according to the tension softening curve of UFC measured by Kakei et al. (2003). The procedures of obtaining tensile stress from the tension softening curve are shown in **Fig. 3-39**. The diagonal crack width measured by using four π-gauges along the diagonal crack as

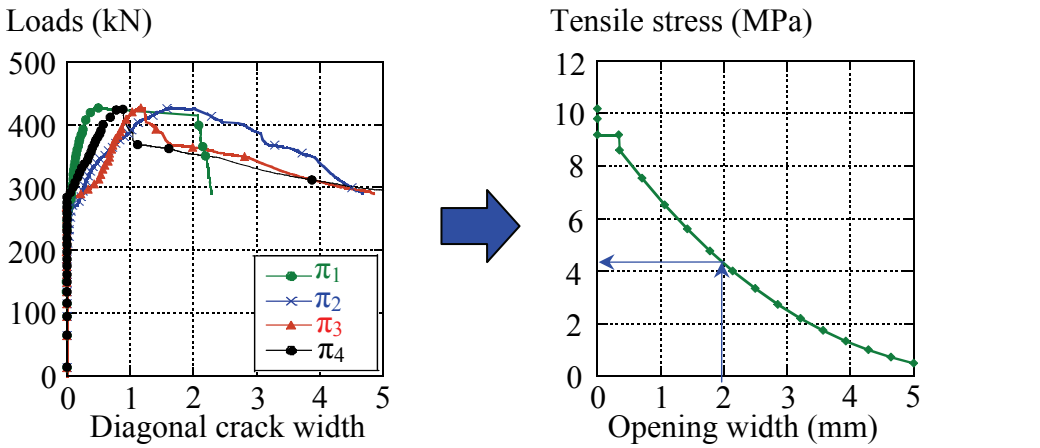

(a) Load-diagonal crack width (UFC20-KB-r)

(b) Tension softening relationship of UFC (Kakei, 2003)

Figure 3-39 Investigation procedures of tensile stress.

the locations of π-gauges are shown in **Fig. 3-7**. Consequently, the tensile stresses were modeled as four elements corresponding to the interval of π-gauge (**Fig. 3-7**). After that, the diagonal crack width along the diagonal crack line was transformed to the tensile stress by using the tension softening curve as shown in **Fig. 3-39(b)**. The average tensile stress is given by the following equation.

$$\bar{\sigma} = \frac{\sum_{i=1}^{4} \sigma_i l_i}{\sum_{i=1}^{4} l_i} \tag{3-8}$$

where, $\bar{\sigma}$ is the average of tensile stress (MPa), σ_i is the tensile stress obtained from tension softening curve of each element (MPa) , l_i is diagonal crack length of each element (mm)

After the average of tensile stress was obtained, the average value of tensile stress was substituted into Eq. (3-6) and the shear carried by UFC permanent formwork can be computed. The computationally value of shear carried by UFC permanent formwork obtained by using tensile stress obtained from the tension softening curve and its ratio compared with experimentally observed are summarized in **Table 3-13**. In all three specimens, the good agreement between calculation values and the experimental values are shown. Therefore, the proposed model with using the tensile stress obtained from the tension softening curve of UFC was able to give a reasonable result. This is also inferred to the diagonal crack on both

UFC formwork and RC part was located almost the same position is one of the obvious reason, and also the diagonal crack width of UFC was measured. From the result of average tensile stress, it is also indicated that the thickness of UFC permanent formwork affects the shear carried by UFC permanent formwork. In the case of specimens with stirrups, On the other hand, the diagonal crack width on UFC permanent formwork did not reduce compared to the specimens without stirrup. Therefore, it can be said that the effect of presence of stirrups on shear carried by UFC permanent formwork is not significant. Moreover, it should be noted that the results have not been discussed up to the design level yet. Further experiment should be done. The rational reduction factor of the tensile strength which is the empirical value of tensile strength based on the results from the tension softening curve which can be used for design should be introduced.

3.5.2 Shear carried by UFC U-shaped permanent formwork failed in shear compression

As aforementioned, UFC20-KB-ad1 specimen failed in the shear compression failure mode. The shear carried by UFC permanent formwork failed in the shear compression failure mode is discussed.

a) Width of the compressive strut and the compressive stress distribution

The compressive stress distribution of inside concrete and surface of UFC permanent formwork were investigated. The compressive stress acting on the concrete was calculated based on the result of the strain gauges attached on acrylic bars, and the compressive stress of UFC was calculated by using the strain measured by strain gauges at the location are shown in **Fig. 3-8** and **3-11**. **Figure 3-40** illustrates the definition of the width of the compressive strut. At $0.95P_{max}$, both minimum strain points and the maximum strain point were connected by straight lines as shown in **Fig. 3-40**. The distance between the points where the strains equal to 0 is assumed to be the width of compression strut. By assuming that the strains of acrylic bars and concrete were the same and the stress state was assumed as uni-axial compression and the strain that measured on UFC was considered also in the same way, the measured strains of both concrete and UFC were transformed to the stress by using the stress-strain relationship. In case of concrete, the compressive stress was calculated by using the stress-strain model proposed by Thorenfeldt et al. (1987) as shown in **Fig. 3-41(a)** and can be obtained as follow.

$$\sigma_c^{'} = \left\{ \frac{n\left(\varepsilon_c^{'} / \varepsilon_p^{'}\right)}{n-1+\left(\varepsilon_c^{'} / \varepsilon_p^{'}\right)^{nk}} \right\} f_c^{'} \tag{3-9}$$

$$n = 0.8 + \frac{f_c^{'}}{17} \tag{3-10}$$

$$k = \begin{cases} 1 & (0 \le \varepsilon_c^{'} \le \varepsilon_p^{'}) \\ 0.67 + \dfrac{f_c^{'}}{62} & (\varepsilon_c^{'} > \varepsilon_p^{'}) \end{cases} \tag{3-11}$$

$$\varepsilon_p^{'} = \frac{n}{n-1} \cdot \frac{f_c^{'}}{1000 E_c} \tag{3-12}$$

where, $\sigma_c^{'}$ is the compressive stress of concrete (MPa), $\varepsilon_p^{'}$ is the strain of concrete at the maximum stress, $\varepsilon_c^{'}$ is the compressive strain of concrete, E_c is the modulus of elasticity of concrete (GPa)

In case of UFC, the stress-strain model of UFC based on the experimental results proposed by Kakei et al. (2003) shown in **Fig. 3-41(b)** was used to calculate the compression stress.

The compressive stress distributions of concrete and UFC permanent formwork are shown in **Figs. 3-42(a)** and **(b)**, respectively. In concrete, the strut width at the middle was

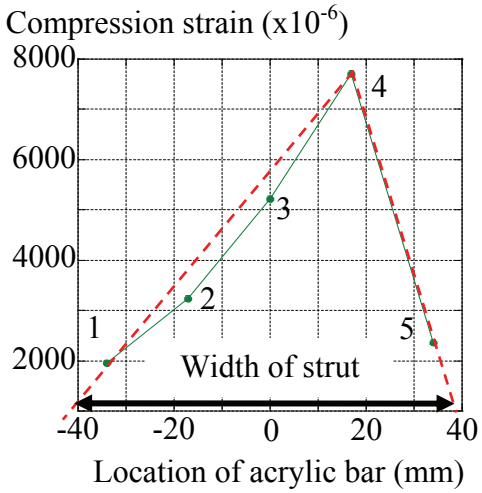

Figure 3-40 Definition of the compressive strut

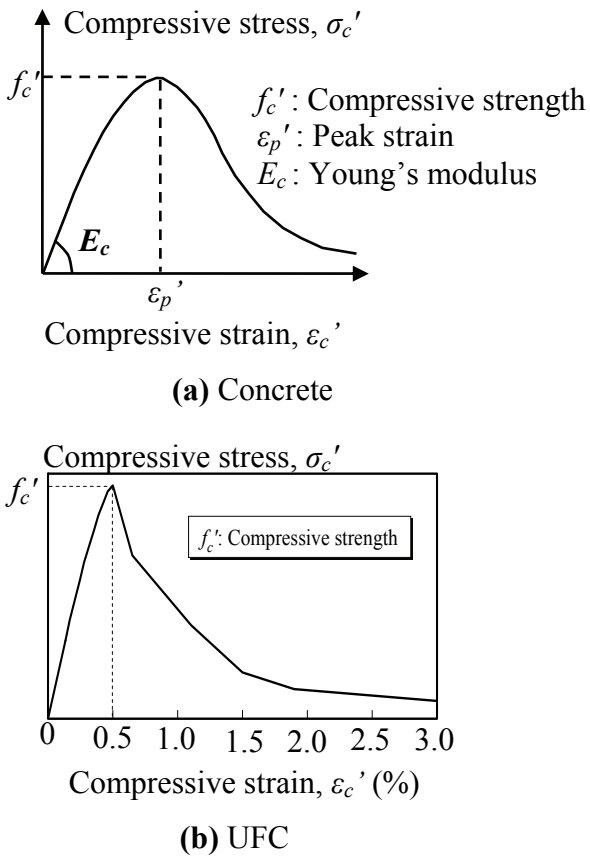

Figure 3-41 Stress-strain relationship for concrete and UFC in compression

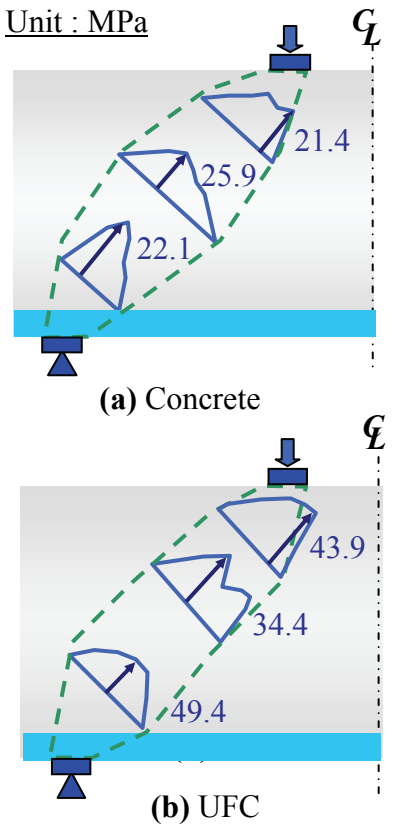

Figure 3-42 Compressive stress distributions

wider than that at near the loading point and near the support. This can be inferred that the stress concentrations were observed at both near the loading and supporting points. On the other hand, in case of UFC, the significant difference on the strut width of all locations on UFC permanent formwork was not observed. This is due to the constraint effect of UFC permanent formwork that confined the inside RC part with screws and bolts.

b) Calculation of the compressive force

The compressive force acting on the concrete strut and UFC strut can be calculated as the vertical component of the stress distributions of both concrete and UFC by using Eqs. (3-13) and (3-14).

$$F_{st} = D \times b_i \tag{3-13}$$

$$F' = F_{st} \times \sin\alpha \tag{3-14}$$

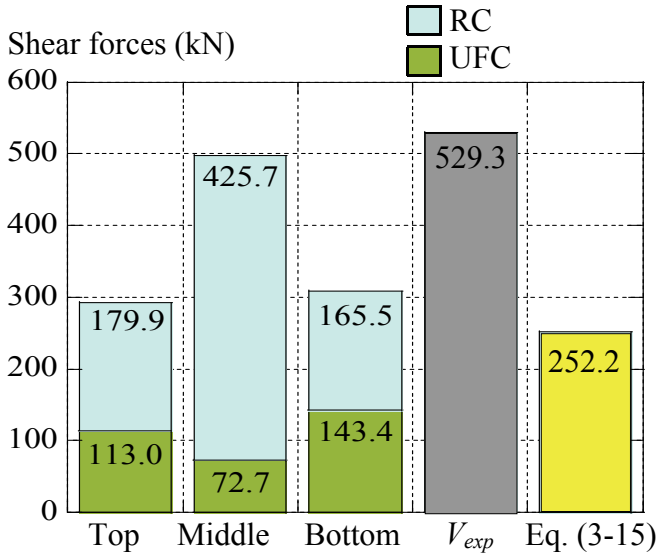

Figure 3-43 Comparison of calculation and experimental value of shear resisting force

where, F_{st} is the compressive force acting on the concrete or UFC strut, D is the force per unit width under the compressive stress distribution curve, b_i is the width of cross section of concrete or both of UFC formwork thickness, F' is the vertical component of F_{st}, α is the angle of the strut with respect to the longitudinal axis of beams

The comparison of the summation of calculated value F' from RC and UFC with the experimental shear capacity V_{exp} is shown in **Fig. 3-43**. In addition, in order to examine the increase of shear capacity, the shear capacity of normal RC deep beams which having the same cross section as UFC20-KB-ad1 specimen (250 mm width) was calculated. The shear carrying capacity of normal RC deep beams can be obtained from Eq. (3-15) (Niwa, 1983).

$$V_{c\_deep} = \frac{0.244 f_c'^{2/3} b_w d(1+3.33r/d)(1+\sqrt{p_w})}{1+(a/d)^2} \quad (3\text{-}15)$$

where, V_{c_deep} is shear carrying capacity of normal RC deep beams (N), r is width of loading and supporting plates (mm)

From **Fig. 3-43**, it is clearly found that by using the UFC U-shaped permanent formwork, the shear capacity increased more than twice in case of the RC deep beam failed in shear compression. The summation of vertical component of compressive forces at the middle

provided the good agreement with V_{exp}. However, the summation of vertical component of compressive forces at the top and bottom location underestimated the experimental result. This is because the uni-axial stress-strain model (Thorenfeldt's model) was used for the calculation. However, the compression strut of inside concrete was constrained by the UFC formwork with screws and bolts.

3.6 Summary of Chapter 3

The application of UFC as the U-shaped permanent formwork was presented in this chapter. The shear keys and screws and bolts system was also introduced. The shear behavior of RC beams using U-shaped UFC permanent formwork was discussed based on the experimental results of nine specimens. The influences of four experimental parameters which were internal surface and presence of screws and bolts, thickness of UFC permanent formwork, shear span to effective depth ratio and the presence of stirrups on shear resisting mechanisms were examined. Shear carried by UFC permanent formwork were also reported. The results can be summarized as follow.

1) By using a U-shaped UFC permanent formwork, the shear carrying capacity of RC beams increased drastically. The shear carrying capacity varied depending on the internal surface between UFC formwork and RC inside and the presence of screws and bolts. This is because a UFC formwork carried shear force and resisted the opening of diagonal crack in RC part.

2) Shear resisting mechanism of RC beams using a UFC U-shaped permanent formwork with shear keys and bolts was investigated. By using shear keys and screwed bolts system, the sufficient compatibility behavior between UFC and RC can be formed. Since a UFC permanent formwork prevented widening of diagonal crack inside RC by shear keys and screws and bolts, the shear capacity drastically increased.

3) With increasing in the thickness of UFC permanent formwork, the shear capacity of RC beams with using a UFC permanent formwork increased. However, it was proportional to the thickness of a UFC permanent formwork.

4) By providing the stirrups, the shear capacity of RC beams with using a UFC permanent formwork increased. This is because both UFC permanent formwork and stirrups

prevented widening of the diagonal crack. However, the effect of stirrups on the shear carried by a UFC permanent formwork was very slight.

5) Failure mode of RC beams using a UFC U-shaped permanent formwork changed depending on the shear span to effective depth ratio. Compression strut was formed in a UFC formwork in the case of *a/d* equal to 2.16 and 1.0.

6) By comparing RC beams whose cross section was replaced by a UFC U-shaped permanent formwork to normal RC beams having the same shear capacity, the weight of the member can be extremely reduced by 68% to 82%. Especially, the specimens with providing shear keys and screws and bolts showed the highest in the weight reduction rate.

7) The shear carried by a UFC permanent formwork in RC beams failed in the diagonal tension mode was investigated by assuming and using the tensile stress obtained from the tension softening curve. The computational values showed the good agreement with the experimental values.

8) The calculation of compression forces of a UFC permanent formwork and RC part in the specimen with *a/d* equal to 1.0 by using uni-axial stress-strain model did not show the good agreement near the screwed bolts. It indicated that the constraint effect of screwed bolts should be considered to evaluate the shear compressive capacity.

CHAPTER 4

Shear behavior of PBL joint connection for UFC-PC hybrid girders

4.1 Introduction

In hybrid structure problems when two difference materials are connected together along the span of structure, the forces are transferred from one to another which resulting the connection part as the critical point. The assurance of continuously and efficiently transferring force between two materials is crucial. As mentioned in Chapter 2, the available studies on the connection technology for UFC structures structure is insufficient, moreover, the connection system for UFC and PC girder could not be found. Therefore, the objective of this chapter is to propose connection part for UFC-PC hybrid girders and investigate its shear behavior. As shear failure of connection is the most severe and needed to be prevented. Therefore, shear resistance was firstly considered in this study.

The connection consisted of Perfobond strips (or Perfobond Leisten, PBL) filled with cast-in-place UFC is proposed as the one of solution technologies. By using the PBL together with cast-in-place UFC, the high shear resistance capacity is expected. This chapter is therefore presented the experimental study using push-out test of PBL joint connection specimen. The element specimen simulated the construction process was prepared. Various experimental parameters affecting the shear behavior were carefully selected. The shear behavior of PBL with cast-in-place UFC was discussed based on the result of shear capacities, load and displacement relationship, crack patterns and shear resisting mechanism. Subsequently, the effect of thickness of PBL, hole diameter of PBL, transverse rebar, prestressing level and spacing between PBLs were clarified. Finally, the predictive equation for evaluating the shear capacity was also developed.

4.2 Proposed PBL Connection and Materials Used

The PBL with cast-in-place UFC joint connection is proposed in this study. The PBLs and cast-in-place UFC were used in the connection part. Moreover, self-compacting concrete,

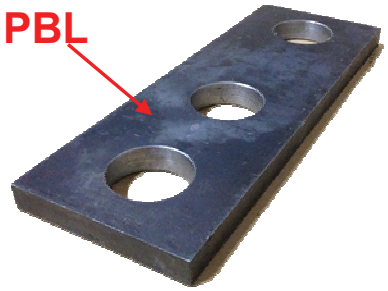

Figure 4-1 Example of PBL used in this study

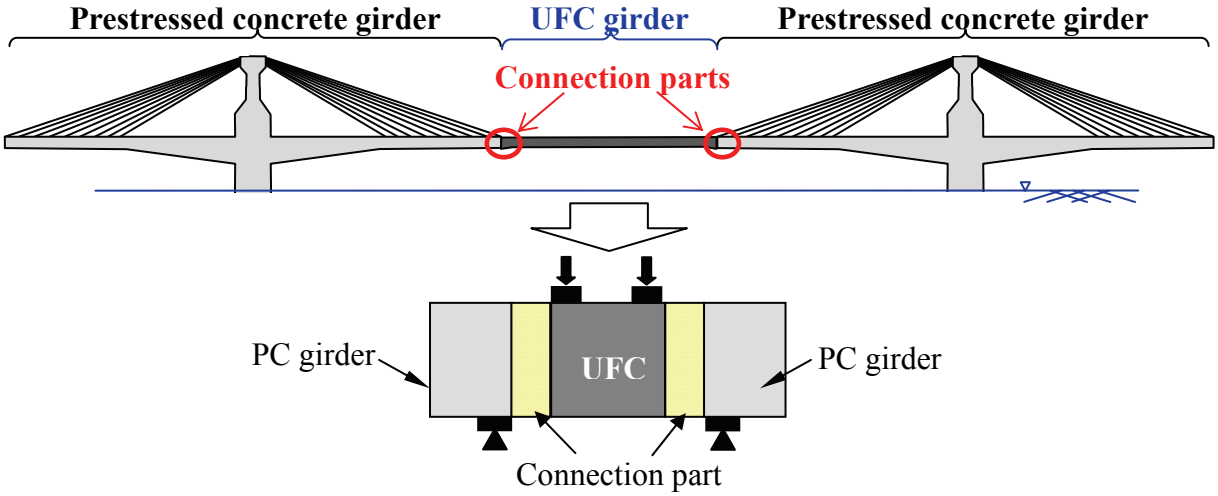

Figure 4-2 Schematic outline of proposed structure

steel reinforcement, UFC and prestressing bars were used in the specimen. The detailed description of the each material is explained as follow.

4.2.1 Proposed connection

The connection consisted of Perfobond strip (PBL) filled with cast-in-place UFC is proposed. PBL is a steel flat plate containing a number of holes as shown in **Fig. 4-1**. The PBL was originally developed in Germany by Leonhardt (1987). It is widely used as the connector for steel girder with RC deck slab composite bridges due to many advantages such as high shear resisting capacity and stiffness. Easy installation is also achieved according to the flat shaped of the PBL rib. As a result, used together with filled cast-in-place UFC, the connection can eliminate the imperfection of segmental girder erection and also the need for

fabricate a segment by the match cast method can be eliminated. The specimens consisted of middle UFC part and concrete parts at the both side which were connected by the proposed connection. **Figure 4-2** shows a schematic outline of the proposed structure considering the connection part.

4.2.2 PBL

One of the PBL used in this study is shown in **Fig. 4-1**. The dimension, thickness and hole diameter of PBL were varied depending on the specimen. The nominal yield strength was 325 MPa and tensile strength was 422 MPa according to SS400 steel grade.

4.2.3 UFC

UFC is a material produced by mixing pre-mix powder of cement, silica fume, silica fine powder and silica sand in the optimum proportion with water and high performance polycarboxylic superplasticizer and steel short fiber. The volume fraction of steel short fiber (0.2 mm diameter x 15 mm length) used in this research was 2%. **Table 4-1** shows the mix proportion of UFC.

The UFC segment was fabricated in advance before the connection with RC segment. After casting, the segment underwent the steam curing following the JSCE recommendation (2004). The designed compressive strength of UFC segment was 180 MPa. In case of cast-in-place UFC, the designed compressive strength was 100 MPa with normal curing for 7 days.

4.2.4 Concrete

Table 4-2 summarizes the details of mix proportion which self-compacting concrete was used in this experiment. The materials which are high-early strength cement, fine aggregates, coarse aggregates, viscosity improver and superplasticizer which was high-performance air entrained (AE) water reducing agent were used in the concrete mixes. The designed compressive strength of 7-day age concrete was 70 MPa.

Table 4-1 Mix proportion of UFC

Flow (mm)	Unit quantity(kg/m^3)			Admixture (kg/m^3)
	Water	Premix binder	Steel fiber	
260±20	180	2254	157	22

Table 4-2 Mix proportion of concrete

G_{max}	Water Cement Ratio	Fine Aggregate Ratio	Unit weight (kg/m^3)					
(mm)	(%)	(%)	*W*	*C*	*S*	*G*	*SP*	*V*
15	30	45	165	550	831	792	*W*×1.1%	*C*×0.15%

where, G_{max} : maximum size of coarse aggregate
W : water
C : high early strength cement, density = 3.14 g/cm^3
S : fine aggregate, density = 2.59 g/cm^3, F.M. = 2.42
G : coarse aggregate, density = 2.68 g/cm^3, F.M. = 6.82
SP : Superplasticizer
V : Viscosity improver

Table 4-3 Details of PBL, steel reinforcements and prestressing rod

	Nominal diameter (mm)	Grade	Yield strength (MPa)	Tensile strength (MPa)
PBL	-	SS400	325	422
Steel reinforcement	9.53	SD345	405	510
Prestressing rod	20.46	SBPR930	1206	1287
Transverse rebar	9.53	SD345	395	530

4.2.5 Steel reinforcement and prestressing rod

The steel reinforcements with 9.53 mm nominal diameter were used for RC part and as transverse rebar inside the hole of PBL. A prestressing rod with nominal diameter: d=20.46 mm, the yield strength: f_y=1206 MPa and the ultimate strength: f_u=1287 MPa were used for the specimen in series of prestressing force. The specifications for the rebars were according to JIS G 3109. The characteristics of the reinforcement and prestressing rod used in this study are shown in **Table 4-3**.

Table 4-4 List of the experimental cases

No.	Name	*t* (mm)	Diameter of PBL hole (mm)	Diameter of rebar (mm)	Prestressing level (MPa)	*S/D*	Series
1	PBL9	9	40	10	-	1.5	I
2	PBL16	16	40				I, II, III, IV, V
3	PBL22	22	40				I
4	PBL-D30	16	30				II
5	PBL-D50		50				II
6	PBL-r13		40	13			III
7	PBL-r16			16			III
8	PBL-P5			10	5		IV
9	PBL-P10				10		IV
10	PBL-P15				15		IV
11	PBL-1				-	-	V
12	PBL-SD25					2.5	V

t: the thickness of PBL, *D*: diameter of PBL hole, *S*: spacing between inner two PBL, *S/D*: shear span to effective depth ratio

4.3 Experimental Program

4.3.1 Experimental parameters and specimens

The push-out tests of twelve specimens were carried out in order to investigate the shear behavior of PBL with cast-in-place UFC connection. The summary of test variables and details of specimens are provided in **Table 4-4** and **Fig. 4-3**. **Figure 4-3** displays the detailed dimension, locations of PBLs and arrangement of steel reinforcement inside RC part of all specimens. The specimens consisted of three parts in order to simulate the connection part between UFC and PC girders by using proposed PBL with cast-in-place UFC connection. The UFC precast segment was located at the middle part and two RC parts were located at both sides of a specimen. All parts were connected together with two joints between RC and UFC parts. Transverse rebars were inserted into the hole of PBL. Then, cast-in-place UFC was cast

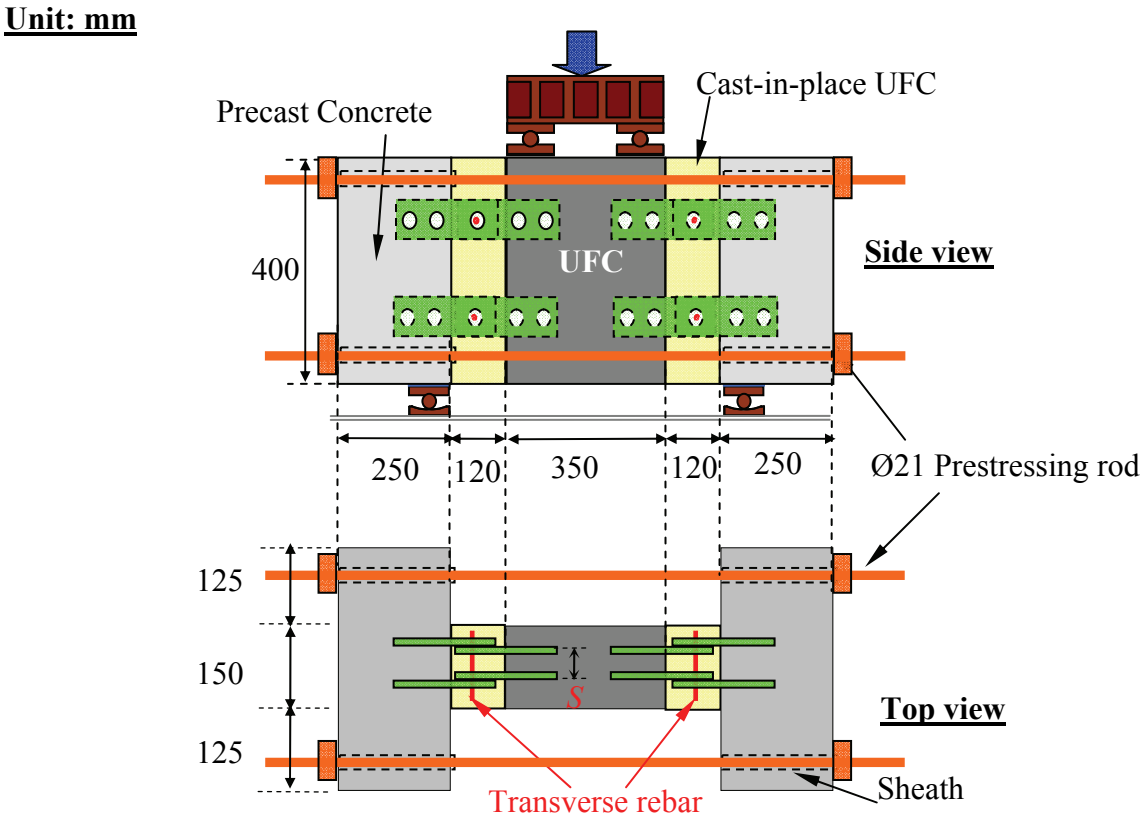

Figure 4-3 Detail of specimens

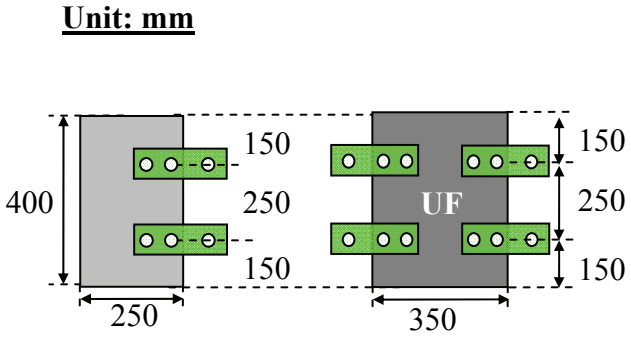

Figure 4-4 Detail of RC and UFC segments (side view)

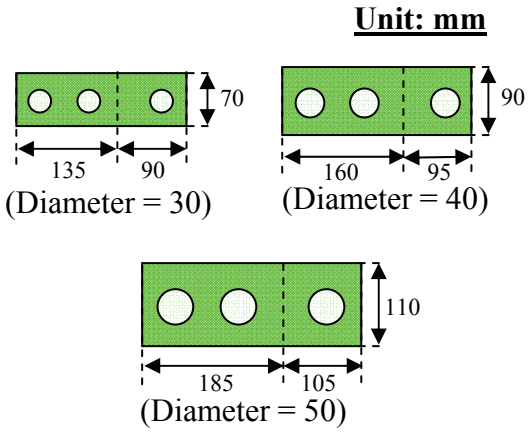

Figure 4-5 Dimension of PBLs used in this study

in the connection part of all specimens. The whole PBLs were embedded in all parts as the configuration is shown in **Fig. 4-4**. The detail dimension of PBLs used in the experiment is shown in **Fig. 4-5**. The height and length of specimen are about 10 time smaller comparing with real connection of Kiso-gawa bridge (Nakasu et al., 2000)

Five series of experimental parameters were selected in order to investigate the influence of each parameter on the shear resistance mechanism. Consequently, the predictive equation was mechanically modelled based on the contribution of each shear resistance. The experimental cases can be classified into five series. The effect of thickness of PBL was examined in Series-I. The influence of diameter of hole in PBL was studied in Series-II. The effect of transverse rebar inside the hole of PBL was studied in Series-III. The prestressing force on the connection part was simulated and its influence was investigated in Series-IV. Lastly, Series-V was for the effect of spacing of PBLs. The details in each parameter are explained follow.

First, the effect of thickness of PBL was investigated in Series-I. The name of specimens listed in **Table 4-4** corresponds to them. The thickness of PBL was varied from 9, 16 and 22 mm in PBL9, PBL16 and PBL22, respectively. The same height and length of PBL were provided in all specimens.

Three specimens with different in the holes diameter of PBL were tested in order to discuss the influence of the holes diameter of PBL in Series-II. The dimension and arrangement of PBL are illustrated in **Fig. 4-5**. The hole diameter of PBL-D30, PBL 16 and PBL-D50 were 30, 40 and 50 mm, respectively. The thickness of all specimens were the same which was 16 mm. Size of PBL was different in this case according to the size of hole diameter of PBL. The results of PBL-D30 and PBL-D50 were discussed with PBL16.

In Series-III, the influence of dowel action by varying the diameter of transverse rebar inside PBL hole was examined in Series-III, the transverse rebars that were inserted in the PBL holes were varied from 10, 13 and 16 mm in the specimens PBL16, PBL-r13 and PBL-r16, respectively.

In Series-IV, the prestressing force was induced to the connection part by using the prestressing rods as the locations are shown in **Fig. 4-3**. The size of the specimen and PBL remained the same as previous specimens. The prestressing levels were determined based on the real construction of the connection for Kiso-Ibi gawa bridges (Nakasu et al., 2000) which was around 15 MPa. The prestressing level can be calculated from the forces divided with the cross section area of connection which equal to 400 mm height and 150 mm width in this study. The prestressing levels were 5, 10 and 15 MPa in PBL-P5, PBL-P10 and PBL-P15, respectively.

In Series-V, the effect of spacing of PBL was considered. In this case of the ratio of the PBL spacing between inner two PBLs to the hole diameter of PBL (*S/D*). In all specimens except PBL-SD25, the ratio of spacing to the hole diameter of PBL was 1.5 (60 mm spacing in actual). However, the spacing to diameter ratio of PBL-SD25 was 2.5 (100 mm spacing in actual). The spacing was measured as the distance between centerline of PBL embedded in UFC segments. The number of PBL was reduced from two PBLs per row to only one per row in the case of PBL-1. Therefore, there was no spacing in this case.

4.3.2 Fabrication of the specimens

The specimen consisted of three parts. One was the precast concrete segment located at both ends of the specimen. The middle part was precast UFC segment. Both precast concrete and UFC segment had been fabricated in advance. **Figure 4-6** shows the fabrication of the UFC segment and precast concrete segments. The fabrication step of UFC segment is sequenced in **Fig. 4-6(a)**, **(b)** and **(c)**. The formwork was made from the plywood which is designed for concrete work. The plywood was cut and the form as the shape of segment which the location of PBL was also made. The PBLs were embedded into the formwork as the closed up view is shown in **Fig. 4-6(b)**. Then, UFC was cast into the formwork. After 24 hours, the UFC permanent formwork was removed of the mold. Then, it undergoes the stream curing at 90ºC for 48 hours. Three cylinders of Ø50x100 mm and three cylinders with Ø100x200 mm were prepared and put in the same condition as the specimens in order to measure the compressive strength and tensile strength of UFC, respectively. The target compressive strength of the UFC segment was 180 MPa. In case of precast concrete segment, the step of fabrication was similar to UFC segment as the sequence is shown in **Figs. 4-6(d), (e)** and **(f)**. Steel reinforcement was provided in the precast concrete segment in order to prevent the failure of precast concrete part as the location is shown in **Fig. 4-6(e)**. After PBLs and steel reinforcements were arranged into the formwork, concrete was cast. Precast concrete segment was cured under covered with moisted cloths and plastic sheet for 7 days. The designed compressive strength of the precast concrete segment was 70 MPa.

After all segments were prepared, the process of connection was performed. **Figures 4-7(a1)**, **(a2)** and **(a3)** show the all completed segment which are precast concrete (Left), UFC and precast concrete (Right) segments, respectively. The PBLs were embedded in both concrete and UFC precast segments. First, the three segments were set into the designed position as shown in **Fig. 4-7(b)**. Then, transverse rebars were inserted into PBL holes

(a) Formwork for UFC segments

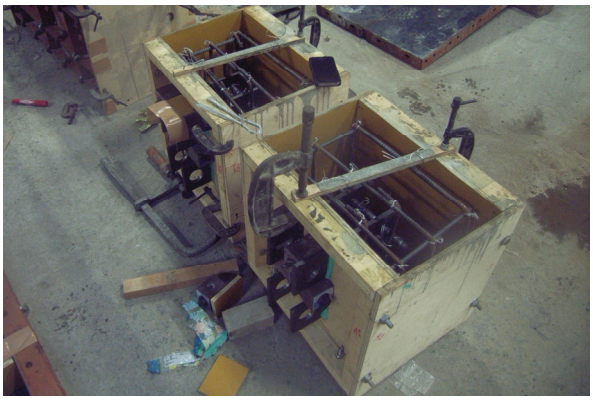

(d) Formwork for precast concrete segment

(b) Close-up of formwork for UFC segment

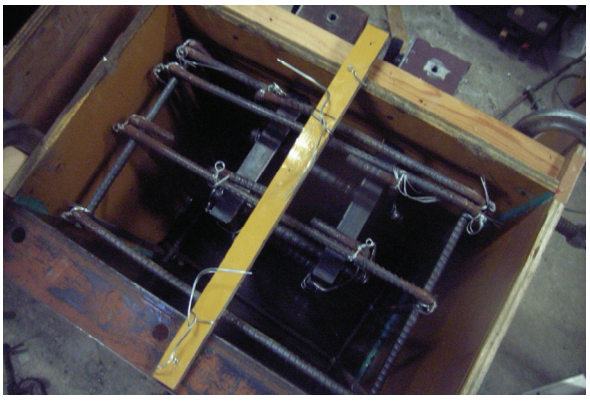

(e) Close-up of formwork for precast concrete

(c) Casting of UFC

(f) Casting of concrete

Figure 4-6 Fabrications of UFC and precast concrete segments

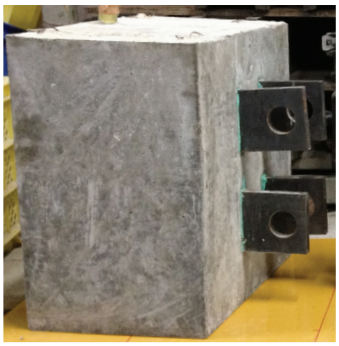

(a1) Concrete segment (Left)

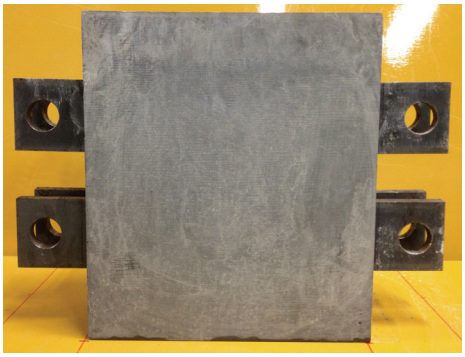

(a2) UFC segment

(a3) Concrete segment (Right)

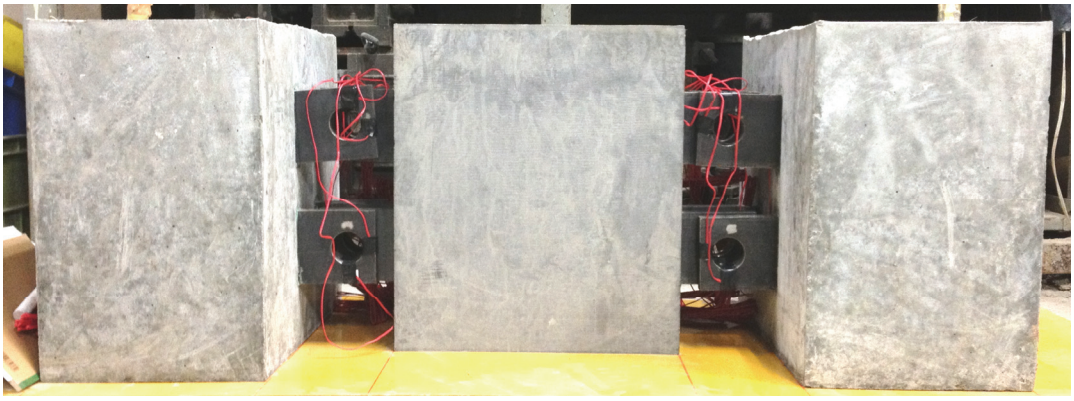

(b) Positioning of all segments

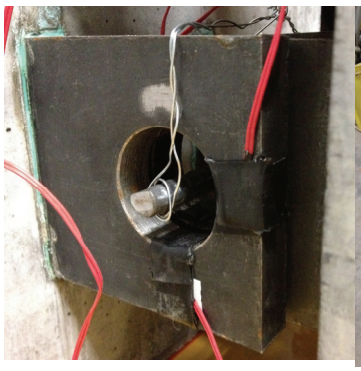

(c) Transverse rebar

(d) Formwork for cast-in-place UFC

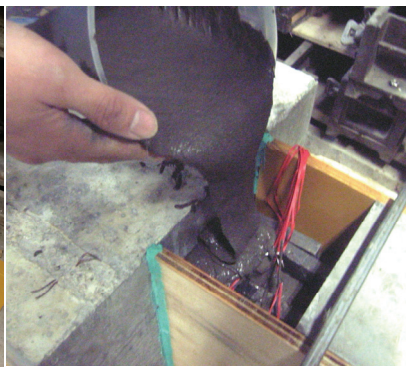

(e) Cast-in-place UFC

(f) Curing of specimen

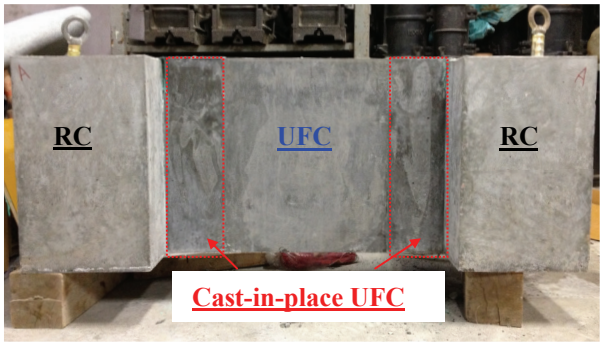

(g) Completed specimen

Figure 4-7 Fabrication of specimen

(**Fig. 4-7(c)**). **Figure 4-7(d)** shows the specimen which ready for casting. Last step, cast-in-place UFC was cast into the connection position (**Fig. 4-7(e)**). After that UFC was cured for 7 days. The target compressive strength of the cast-in-place UFC was 100 MPa. The completed specimen is shown in **Fig. 4-7(g)**.

4.3.3 Loading method

The specimens were subjected to a push-out test with the load applied at the both end of UFC segment beside the connection part as shown in **Fig. 4-8**. The supporting points which located at the end of RC segment near the connection part were placed on the roller supports. Teflon sheets and grease were inserted between the specimen and supports. At the loading points on the top surface of the specimen, steel plates with 50 mm width, steel rollers and a load distribution beam were placed. The loading rate was about 0.15-0.25 kN per second.

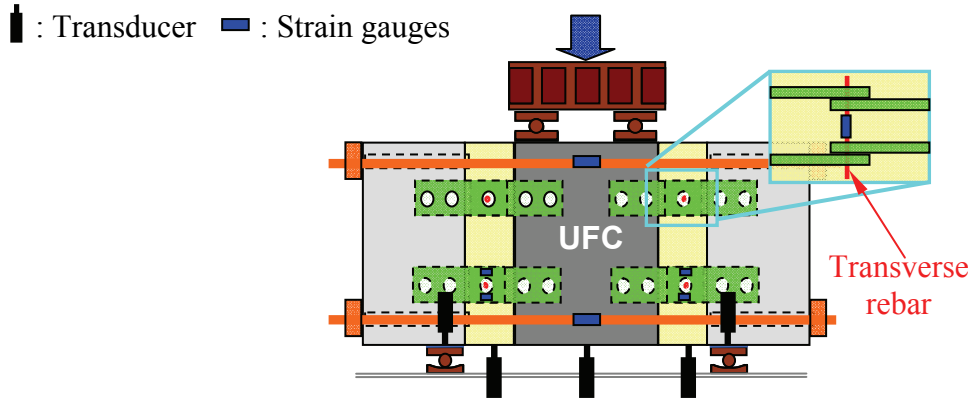

Figure 4-8 Measurement items

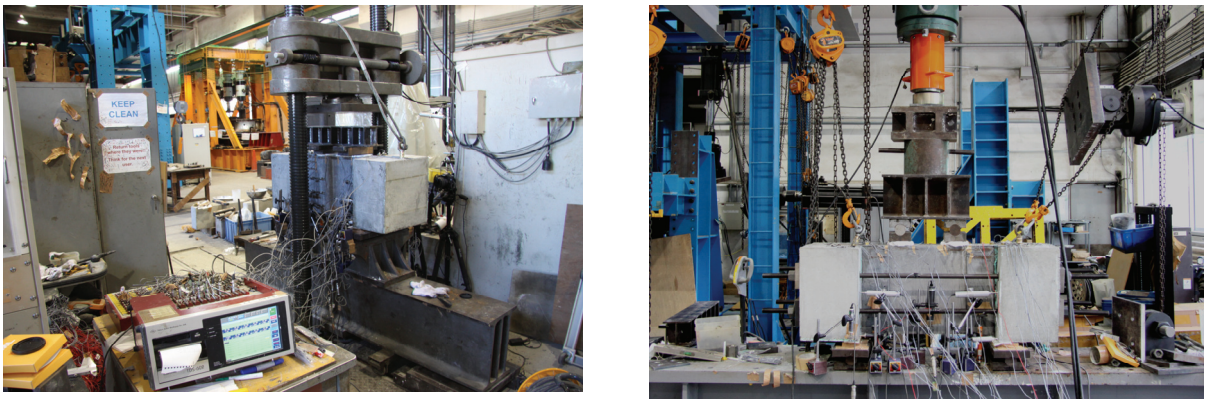

(a) PBL22 **(b)** PBL-P5

Figure 4-9 Specimen setup

4.3.4 Measurement items

The location of measurement items used in the experiment is shown in **Fig. 4-8**. During the loading test, the applied load was measured. Displacement at the middle of connection part and supporting point was measured by using transducers as shown in **Fig. 4-8**. Strain gauges were used for measuring the strain of PBL strips plate. Moreover, the strains of the transverse rebars were measured at the middle point of rebars by using strain gauges. The opening widths between RC segment and connection part were measured by using transducers with interval of 100 mm along vertical direction of the specimens. In the same way, the opening widths between connection part and UFC segment were measured by using π-gauges and transducers with interval of 100 mm along vertical direction of the specimen. In addition, in PBL-P5, PBL-P10 and PBL-P15, the strains of prestressing rod were measured at the mid-span. **Figure 4-9** illustrates the specimen setup and environment of loading tests.

Table 4-5 Mechanical properties of concrete and UFC, and the result of loading tests

Name	Mechanical properties of concrete		Mechanical properties of cast-in-place UFC		Mechanical properties of precast UFC		Results of loading test		
	f'_c (MPa)	f_t (MPa)	f'_{c_UFC} (MPa)	f_{t_UFC} (MPa)	$f'_{c\_UFC\_PC}$ (MPa)	$f_{t\_UFC\_PC}$ (MPa)	P_{max} (kN)	V_u (kN)	V_{UFC} (kN)
PBL9	78.7	3.7	102.5	10.5	185.4	13.6	765.8	382.9	374.5
PBL16	84.3	3.3	123.8	11.2			789.4	394.7	
PBL22	76.5	2.9	107.5	11.8			858.2	429.1	
PBL-D30	74.6	3.0	112.4	11.5			701.8	350.9	
PBL-D50	76.1	2.8	107.9	11.3			835.0	417.5	
PBL-r13	75.1	2.6	110.2	10.8			880.5	440.2	
PBL-r16	73.2	3.1	107.5	10.4			908.1	454.0	
PBL-P5	75.3	3.1	108.5	11.6	187.5	12.8	1440.8	720.4	
PBL-P10	74.1	3.4	107.4	10.5			1633.0	816.5	
PBL-P15	72.5	2.9	113.5	11.1			2147.0	1073.5	
PBL-1	71.6	3.1	109.4	10.4			590.8	295.4	
PBL-SD25	73.5	2.7	104.6	10.6			750.2	375.1	

f'_c: compressive strength of concrete, f_t: tensile strength of concrete, f'_{c_UFC}: compressive strength of cast-in-place UFC, f_{t_UFC}: tensile strength of cast-in-place UFC, $f'_{c\_UFC\_PC}$: compressive strength of UFC segment, $f_{t\_UFC\_PC}$: tensile strength of UFC segment, P_{max}: peak load, V_u: shear capacity of connection, V_{UFC}: shear capacity of UFC segment

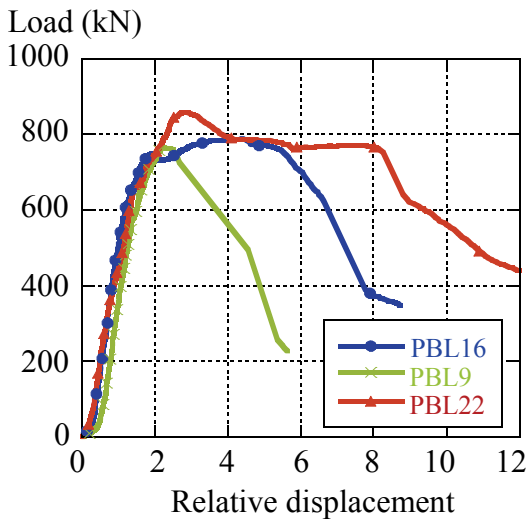

Figure 4-10 Load-relative displacement in Series-I

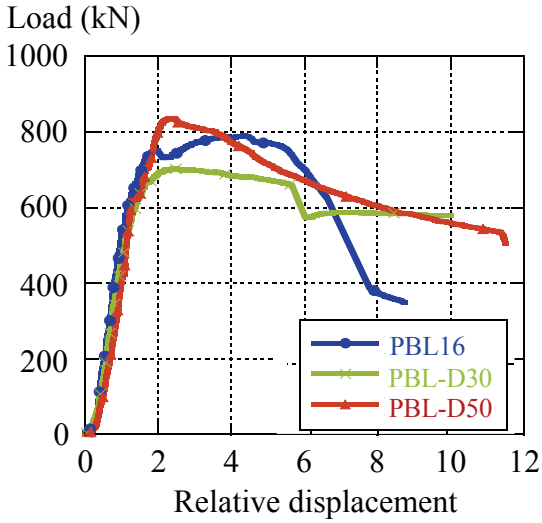

Figure 4-11 Load-relative displacement in Series-II

4.4 Experimental Results and Discussions

4.4.1 Shear capacities

Table 4-5 lists the mechanical properties of concrete, cast-in-place UFC and precast UFC, and the result of loading tests. The shear capacity of UFC segment can be calculated based on the JSCE recommendation (JSCE, 2006) by using Eqs. (4-1), (4-2) and (4-3).

$$V_{UFC} = V_{rpcd} + V_{fd} \tag{4-1}$$

$$V_{rpcd} = 0.18\sqrt{f'_{c\_UFC\_PC}}\, b_w d \tag{4-2}$$

$$V_{fd} = (f_{vd} / \tan\beta_u) b_w z \tag{4-3}$$

where, V_{UFC} is shear capacity of UFC segment (N), V_{rpcd} is shear capacity of a linear member without shear reinforcement (N), V_{fd} is shear capacity provided by fiber reinforcement (N), $f'_{c\_UFC\_PC}$ is compressive strength of UFC segment (MPa), b_w is width of web (mm), d is effective depth (mm), f_{vd} is the design average tensile strength (MPa), β_u is an angle between member axis and a diagonal crack (º), z is the distance from the location of compressive stress resultant to the centroid of tension steel which is equal to d/1.15 (mm)

From **Table 4-5**, the shear capacities of PBL with cast-in-place UFC (V_u) obtained from the experiment in Series-I and II were higher than the calculated shear capacity of UFC

segment (V_{UFC}) excepted in PBL-D30 specimen. It can be seen that by using the PBL with cast-in-place UFC connection, the sufficiently transferring forces can be secured between two girders because the connection failure can be prevented.

4.4.2 Load-displacement relationships, failure modes and crack patterns

The relationships between the load and the relative displacement of Series-I and II are plotted in **Figs. 4-10** and **4-11**, respectively. The relative displacement was obtained by subtracting the displacements at the supporting points from the displacement at the middle point of the connection part as locations are shown in **Fig. 4-8**.

Figures 4-12 and **4-13** present the observed crack patterns at the peak loads in Sereis-I and II. It is obvious that only one critical crack was remarkable in each specimen. The failure

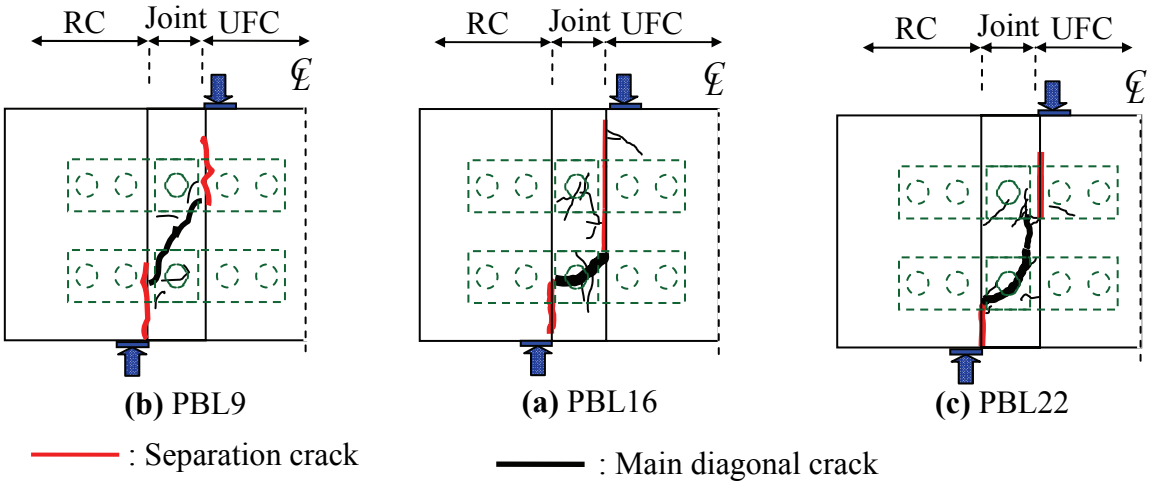

Figure 4-12 Crack patterns of Series-I

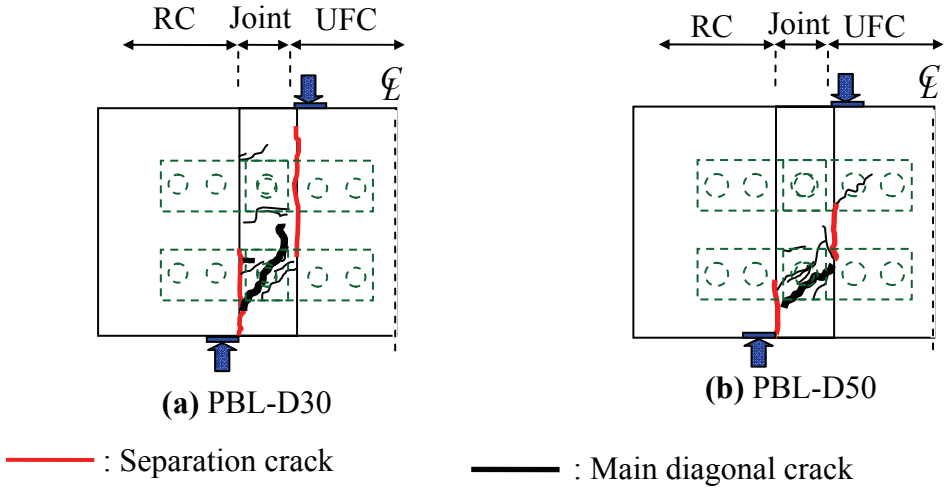

Figure 4-13 Crack patterns in Series-II

modes of all specimens with PBL connections were determined as the shear failure at the connection.

Similar behavior was found in all specimens and can be explain as follow. First, specimens exhibited linear behavior from the initial up to the first separation crack at the interface between concrete and cast-in-place UFC. After the first separation crack occurred, the load and relative displacement relation was still linear increase up to the propagation of the main diagonal crack occurred on a connection part. The main diagonal crack continuity initiated from first separation crack. Afterwards, the main crack propagated to the interface between precast RC and cast-in-place UFC. Additionally, the appearance of the diagonal crack reduced the inclination of load-displacement relationship of the specimens. After this stage, the rate of load increment became slow and the load and relative displacement behaved nonlinearly. Near the peak, the separation crack between precast and cast-in-place UFC propagated, the load reached the peak and dropped as the separation crack between precast and cast-in-place UFC propagated and widened. Similar failure pattern of shear failure was observed in all specimens.

4.4.3 Effect of the thickness of PBL

In series-I, the influence of thickness of PBL is discussed based on the experimental results of PBL9, PBL16 and PBL22 specimens which the thickness was varied as 9, 16 and 22 mm, respectively. From **Table 4-5** and **Fig. 4-14**, the specimens can be arranged as PBL9,

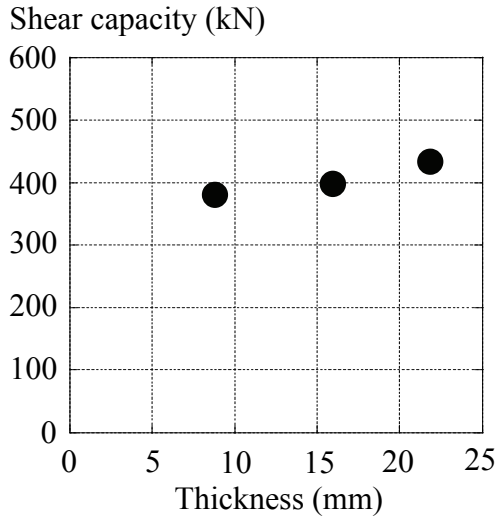

Figure 4-14 Shear capacity-thickness of PBL relationship

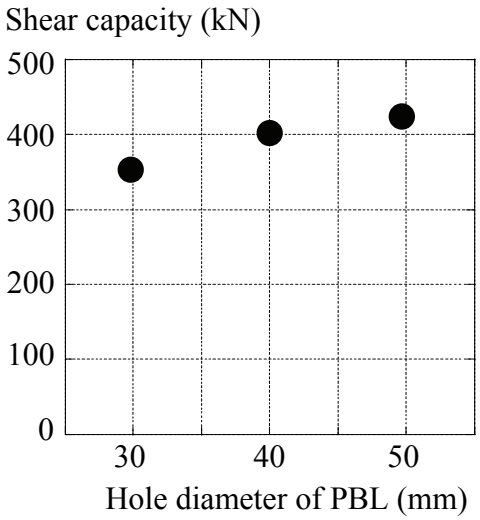

Figure 4-15 Shear capacity-hole diameter of PBL relationship

PBL16 and PBL22 in order of shear capacity of connection with 382.9, 394.7 and 429.1 kN, respectively. **Figure 4-10** shows the load and relative displacement of Series-I. It is clear that the shear capacity of PBL joint filled with cast-in-place UFC increased with the increase in thickness of PBL. Additionally, it should be noted that the crushing of cast-in-place UFC at the end of PBLs was not observed in all specimens. As seen from load-relative displacement relationship, it can be seen that there is the clear tendency of the influence of thickness of PBL on the post-peak behavior of PBL with cast-in-place UFC connection. The ductility of connection in post-peak region increases as the thickness of PBL increases as shown in **Fig. 4-10**. This is because the contacting area between the end of PBL and cast-in-place UFC increases. As the crushing was not observed in all specimens, it can be confirmed that the end-bearing resisting force was still in elastic manner.

4.4.4 Effect of the hole diameter of PBL

Three specimens (PBL-D30, PBL16 and PBL-D50) with the hole diameter of PBL varied from 30, 40 and 50 mm in Series-II are used to clarify the effect of hole diameter of PBL. **Figure 4-15** draws the relationship between shear capacities against hole diameter of PBL. **Figure 4-11** demonstrates the load-relative displacement in Series-II. From the observation, the separation cracks between concrete and cast-in-place UFC were observed at 568.4, 580.2 and 654.0 kN in PBL-D30, PBL16 and PBL-D50, respectively. Then, the main diagonal cracks initiated on the connection part and the load reached to the peak at 701.8, 789.4 and 835.0 kN, respectively. It is obvious that the shear capacity gradually increases with the increase in hole diameter of PBL because the area of cast-in-place UFC inside PBL hole increased which it is comfirmed that the shear resistance of PBL depends on the hole diameter of PBL. However, it should be pointed out that there was the dispersing behavior on the post-peak region of load-relative displacement curves where the increment tendency on ductility of the connection due to the increase in diameter of PBL hole could not be found.

4.4.5 Effect of the diameter of transverse rebar

In order to explain the effect of the diameter of transverse rebar, the results of three specimens in Series-III are discussed. In this series, diameter of transverse rebar inserted in PBL hole was varied from 10, 13 and 16 mm in PBL16, PBL-r13 and PBL-r16 specimens, respectively. **Figure 4-16** displays the relationship between the load and relative displacement

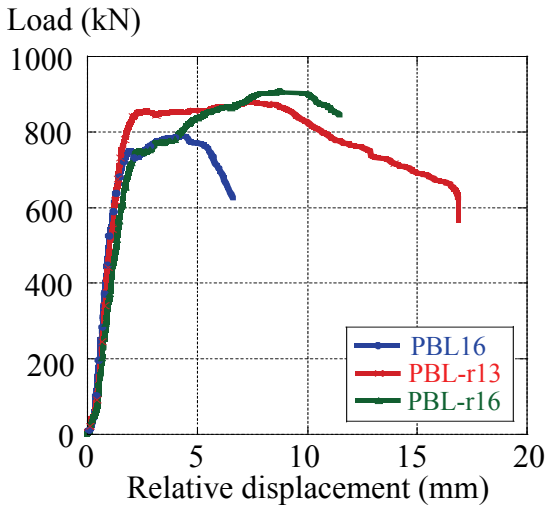

Figure 4-16 Load-relative displacement in Series-III

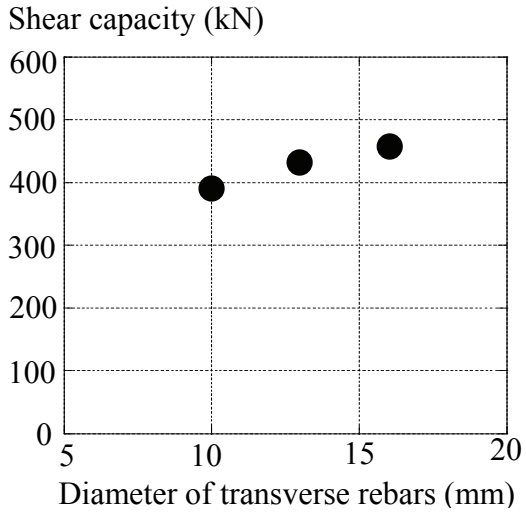

Figure 4-17 Shear capacity-diameter of transverse rebar relationship

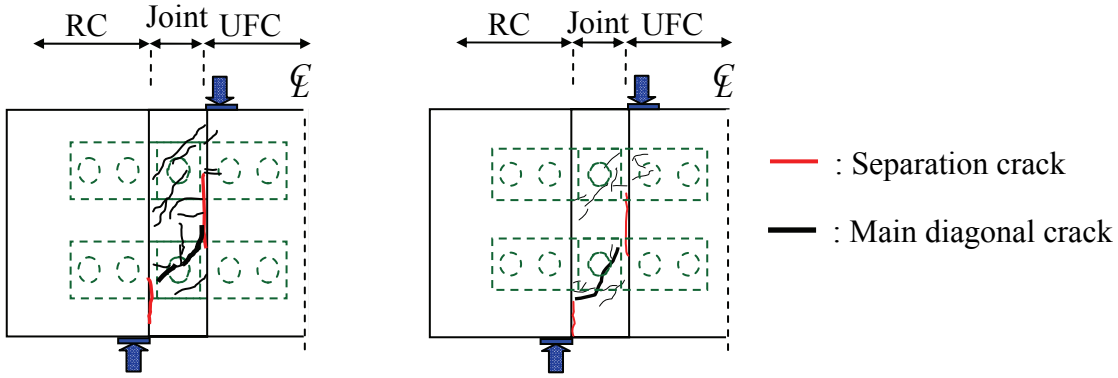

(a) PBL-r13 **(b)** PBL-r16

Figure 4-18 Crack patterns in Series-III

in Series-III. The relationship between shear capacities and diameter of transverse rebar in PBL hole is drawn in **Fig. 4-17**. The increase of shear capacity is obvious as the increase in of diameter of transverse rebar. This is because the contribution of shear resisting of rebar is increased when the diameter of rebar increases. Furthermore, as indicated in **Fig. 4-16**, the increase of relative displacement at the peak load with the increase in diameter of transverse rebar was observed. From this discussion, it can be inferred that the diameter of transverse rebar affects the ductility of PBL with cast-in-place UFC connection. In addition, it should be pointed out that no yielding of transverse rebars was observed in all specimens. It implied that the shear resistance of transverse rebar was still in elastic manner. However, even if the diameter of transverse rebar affected the relative displacement at the peak load, there was the scattering behavior on the post-peak region of load-relative displacement curves. Therefore, the tendency on ductility of the connection due to the increase in diameter of transverse rebar could not be observed.

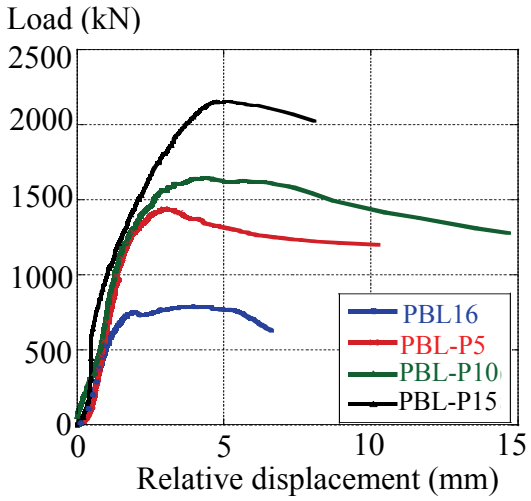

Figure 4-19 Load-relative displacement in Series-IV

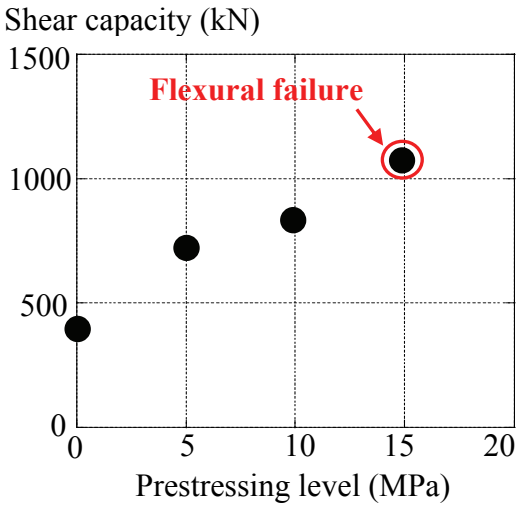

Figure 4-21 Shear capacity-prestressing stress relationship

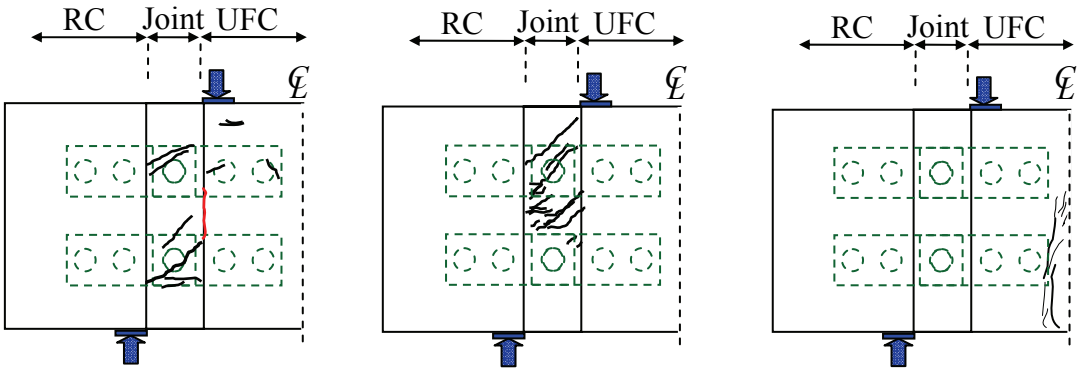

(a) PBL-P5 **(b)** PBL-P10 **(c)** PBL-P15

Figure 4-20 Crack patterns in Series-IV

4.4.6 Effect of prestressing forces

The prestressing force on the connection in segmental bridge was simulated. The prestressing rods were used to induce the confining forces on the cross section of connection area. The prestressing area in this study was 400 mm height and 150 mm width. The prestressing stress was varying from 0, 5, 10 and 15 MPa in PBL16, PBL-P5, PBL-P10 and PBL-P15, respectively.

The relationship between the load and relative displacement in Series-IV is demonstrated in **Fig. 4-19**. **Table 4-5** summarizes the experimental results in Series-IV. The crack patterns of PBL-P5, PBL-P10 and PBL-P15 with the last specimen failed in flexural failure of UFC segment are illustrated in **Fig. 4-20(a)**, **(b)** and **(c)**.

In PBL-P5 and PBL-P10, The shear capacity increased by 82.5 and 106.9% compared to PBL16 specimen with the actual load of each was 1440.8 and 1633.0 kN in PBL-P5 and PBL-P10, respectively. The specimens failed in shear at the connection part. **Fig. 4-19** shows the load-relative displacement relationships in Series-IV. PBL-P5 and PBL-P10 behaved similarly which the load linearly increased with relative displacement until the first diagonal crack on the connection part with 864.0 and 915.0 kN in PBL-P5 and PBL-P10, respectively. The separation crack between connection part and other was not observed during the test. This indicates that the prestressing force significantly influences the shear capacity of connection. The load would be drastically carried by the friction between connection part and the other. Hence, due to the confining stress on the connection, the main diagonal crack width significantly reduced. Apparently, the crack pattern of both specimens looked different from previous specimens. In which the separation width could not be observed. It is noted that load relative displacement of both specimens are slightly different from previous specimen.

In PBL-P15 specimen, the specimen failed in flexural failure of UFC segmental part. The separation crack and cracking on connection part were not observed. When the load reached 2035 kN, the flexural crack appeared at the middle part of UFC segment as shown in **Fig. 4-20(c)**. Then, the load reached to peak at 2147 kN.

The relationship between shear capacities and prestressing level is plotted in **Fig. 4-21**. It is demonstrated that with the increase in prestressing level, the shear capacity increases and the linear relationship agrees well between the test results. Nevertheless, the failure mode changes from shear failure of connection to flexural failure of UFC part when the prestressing level reaches 15 MPa. In this specimen, the shear failure load of connection was higher than the observed maximum load in the experiment. Therefore, the failure was changed to the flexural failure of UFC segment instead. This can be denoted that the PBL with cast-in-place UFC is efficient and conservative for the shear capacity of the connection between UFC and PC segmental girders.

4.4.7 Effect of PBL spacing

In Series-V, the specimens PBL-1 and PBL-SD25 were combined with PBL16 in order to discuss the effect of PBL spacing. **Figure 4-22** plots the load and relative displacement relationship of all specimens. **Figure 4-23** shows the crack patterns of all specimens. In **Fig. 4-22**, all specimens exhibited linear relationship until the separation crack

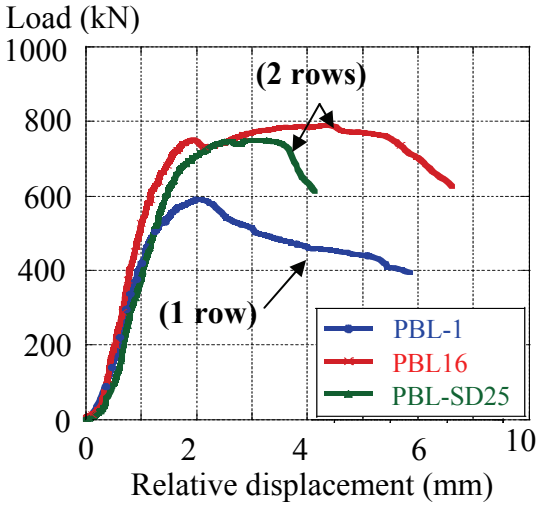

Figure 4-22 Load-relative displacement in Series-V

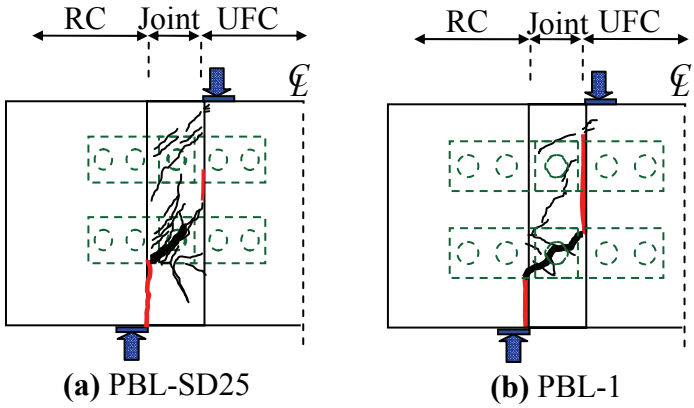

(a) PBL-SD25 **(b)** PBL-1

Figure 4-23 Crack patterns of Series-II

occurred at 398.6, 580.4 and 572.8 kN in PBL-1, PBL16 and PBL-SD25, respectively. After that, the load reached to peak at the load of 590.8, 750.2 and 789.4 kN in PBL-1, PBL-SD25 and PBL16, respectively. It can be said that the difference in the shear capacities of two PBL with cast-in-place UFC was insignificant although the ratio of the PBL spacing to the hole diameter of PBL (*S/D*) increased from 1.5 to 2.5. It can also be observed that the differences in crack pattern of all specimens were very slight. However, the spacing of PBL seems to affect the post-peak behavior of PBL with cast-in-place UFC even if the effect on shear capacity was slight.

4.5 Resistance Mechanism of PBL with Cast-in-place UFC Connection

The high shear resistance can be achieved by using the PBL with cast-in-place UFC, due to the high strength of UFC and high shear resistance of PBL. **Figure 4-24(a)** illustrates

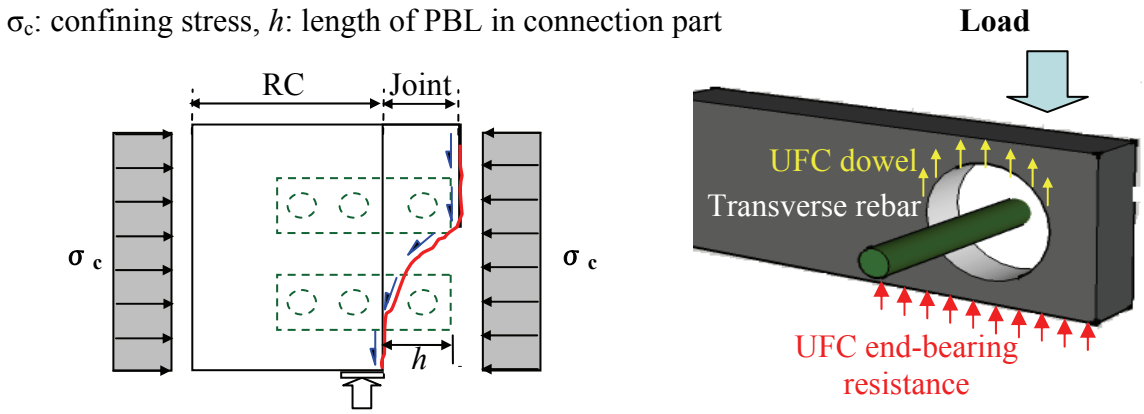

(a) Resistance mechanism of connection **(b)** Contribution of PBL

Fig. 4-24 Shear resistance mechanism of PBL with cast-in-place UFC connection

the mechanical resistance characteristics of a PBL with cast-in-place UFC connection and all of the contributions in PBL are explained in **Fig. 4-24(b)**.

It should be mentioned that the effect of normal stress due to the maximum bending moment corresponding to the peak load on PBL with cast-in-place connection was calculated and checked. By calculating the stress at the location of PBL due to the maximum moment, the result indicated that the stress at the location of PBL was very small especially comparing with yielding strength of PBL which less than 5 percentage. Therefore, it can be said that the influence of normal stress is slight and can be omitted.

As all results discussed above, the contribution on shear resistance characteristics of PBL with cast-in-place UFC connection can be derived from four factors as follows; first, the end-bearing resistance between PBL and UFC. This can be expressed as, the end-bearing resistance forces from the contacting area between PBL and cast-in-place UFC increase with the increase in end-bearing resistance from the thickness of PBL. The experimental investigation indicated that the crushing of cast-in-place UFC under the PBL was not observed due to the high compressive strength of cast-in-place UFC used in the connection part. Consequently, the shear capacity can be significantly increased. In addition, the strain of PBL was still in elastic region and the increment tendency from the induced prestressing forces could not be observed as the results of strain of PBL at the peak load as shown in **Table 4-6**. This is inferred that the end-bearing resisting force was still in elastic manner.

Second contribution is the resistance of UFC dowel in the hole of PBL. The UFC

Table 4-6 The measured strains of PBL and transverse rebar at the peak load in Series-IV

Specimen	Peak load (kN)	The average strain of lower PBL on the failure side ($x10^{-6}$)	The strain of transverse rebar inside the of lower PBL ($x10^{-6}$)
PBL16	789.4	354	331
PBL-P5	1440.8	419	382
PBL-P10	1633.0	450	58
PBL-P15	2147.0	157	174

dowel action is a shear mechanism attributed to the cast-in-place UFC formed through the holes of PBL which it occurs when the two faces of PBL attempt to move apart from each other which cutting across the formed cast-in-place UFC. The two faces of PBL transfer the shear stresses to the cast-in-place UFC in the PBL holes. From the experimental result in Series-II, the obvious increment tendency of the shear capacity with the increase in hole diameter of PBL due to the dowel effect of the UFC in the hole of PBL was observed.

The shear resistance of transverse rebar is considered as the third contribution. The shear resistance of transverse rebar originates from the dowel action of transverse rebar between two faces of PBLs. The strain values of transverse rebar at the peak load in Series-IV is summarized in **Table 4-6**. It is presented that the obvious increment tendency from the induced prestressing forces could not be found. Apparently, all of transverse rebar's strains were still in elastic state even at the peak load. Hence, it can be referred as the resistance of transverse rebar is related to the elastic modulus of steel. As similar way of the end-bearing action, the contribution of shear resistance of transverse rebar and the dowel action of cast-in-place UFC contributed to the shear resistance. Therefore, the yielding of transverse rebar in the hole of PBL cannot be observed.

The last significant contribution comes from the prestressing stresses on connection part. The shear capacity is significantly increased by inducing the prestressing forces on the cross section area of the connection part. This can be described as the closure of the separation cracks between connection part and the other part which resulting from the confining forces on the connection. Therefore, the loads can be carried by the friction force between the connection and the other.

There is a scattering of the strains of PBL and transverse rebar at the peak load in

Series-IV as presented in **Table 4-6**. This result can be implied that the influence of prestressing force on the contribution of end-bearing resistance and shear resistance of transverse rebar could not be found. In the case of the dowel action of cast-in-place UFC in the PBL holes, because the direction of prestressing force is parallel to the cross section plane of cast-in-place UFC, the influence of prestressing force on UFC dowel action was supposed to be slight.

Hence, as considering of the force acting at the PBL with cast-in-place UFC connection discussed above, it can be indicated that the shear force is resisted by the summation of end-bearing resistance of cast-in-place UFC, dowel action of UFC in the hole of PBL, shear resistance of transverse rebar and the prestressing forces on the connection. Therefore, the development of predictive equation was mechanically modeled as the summation of all contribution which will be explained in next section. It should be also noted that as the effect of PBL spacing is neglected in the model as it is less significant

4.6 Investigation on Shear Capacity of PBL with Cast-in-place UFC Connection

4.6.1 Comparison with the existing shear capacity equation of PBL

The shear capacity of PBL for steel girder and RC slab at rib hole (V_{ud}) can be calculated in two conditions according to JSCE standard specifications for hybrid structures (JSCE, 2009). In case of the PBL hole contains a transverse rebar, Eq. (4-4) is used. As this formula was originally proposed for application to normal strength concrete and steel girder, the applicable range is set as shown in Eq. (4-5). In the case of the hole of PBL without a transverse rebar, the shear capacity can be computed by using Eq. (4-6) and the applicable range for this equation is presented in Eq. (4-7).

$$V_{ud} = 1.45 \times ((d^2 - \phi_{st}^2) \times f_c^{'} + \phi_{st}^2 \times f_{st}) - 26.1 \times 10^3 \quad (4\text{-}4)$$

$$51.0 \times 10^3 < (d^2 - \phi_{st}^2) \times f_c^{'} + \phi_{st}^2 \times f_{st} < 488.0 \times 10^3 \quad (4\text{-}5)$$

$$V_{ud} = 3.38 d^2 (\frac{t}{d})^{0.5} \times f_c^{'} - 39.0 \times 10^3 \quad (4\text{-}6)$$

$$22.0\times10^3 < d^2(\frac{t}{d})^{0.5}\times f_c^{'} < 194.0\times10^3 \quad (4\text{-}7)$$

where, V_{ud} is shear capacity (N), d is diameter of the PBL hole (mm), $Ø_{st}$ is diameter of transverse rebar (mm), $f_c^{'}$ is compressive strength of concrete (MPa) and f_{st} is tensile strength of transverse rebar (MPa), t is thickness of PBL (mm)

In this calculation, the equations were applied beyond their application range in order to clarify the applicability of the existing equation to PBL connection with cast-in-place UFC connection. The experimental results of nine shear capacities of PBL connection in this study and two specimens from Tanaka et al. (Tanaka et al., 2006) were compared with those obtained by the JSCE equation. It should be mentioned that no transverse rebar was provided inside the holes of PBL in Tanaka-1 and Tanaka-2 specimens. Moreover, PBL used in Tanaka-2 specimen has only two holes.

Table 4-7 summarizes the calculation results of shear capacity by Eqs. (4-4) and (4-6) and the results of experimentally observed. The average of experimental value by calculation value (V_{exp}/V_{ud}) equals to 0.47. The results indicate that Eqs. (4-4) and (4-6) overestimate the experimental results. The two main reasons can be explained as first the effect of end-bearing resistance which corresponds to the thickness of PBL is not taken into account in these equations. Second, the applicable range is originated for the normal strength concrete where coarse aggregate is contained. However, the cast-in-place UFC was used in this experiment. Although UFC contains no coarse aggregate comparing with normal concrete, cast-in-place UFC has much greater compressive strength which around 100 MPa and also the existence of steel fibers. Therefore, this equation was applied beyond their limitation and reflected in the significant increase in the shear resistance of PBL with cast-in-place UFC. Therefore, the equation should be modified in order to use for PBL joint with cast-in-place UFC.

Table 4-7 Experimentally observed and calculation results

Name	t (mm)	h (mm)	d (mm)	$Ø_{st}$ (mm)	A_s (mm^2)	E_s (GPa)	f'_{c_UFC} (MPa)	E_{UFC} (GPa)	σ'_c (MPa)	V_{exp} (kN)	V_{ud} (kN)	V_{exp} /V_{ud}	V_{PBL} (kN)	V_{exp} /V_{PBL}
PBL9	9	92.5	40	9.53	71.3	201	102.5	42.4	-	382.9	968.6	0.40	301.5	1.27
PBL16	16	92.5	40	9.53	71.3	201	123.8	46.3	-	394.7	968.6	0.44	406.0	0.97
PBL22	22	92.5	40	9.53	71.3	201	107.5	43.5	-	429.1	968.6	0.41	450.1	0.95
PBL-D30	16	90.0	30	9.53	71.3	201	112.4	44.8	-	350.9	701.8	0.62	320.1	1.10
PBL-D50	16	95.0	50	9.53	71.3	201	107.9	43.8	-	417.5	835.0	0.28	475.9	0.88
PBL-r13	16	92.5	40	12.7	126.7	201	110.2	44.7	-	440.2	1068.7	0.41	435.1	1.01
PBL-r16	16	92.5	40	15.9	198.6	201	107.5	43.0	-	454.0	1194.8	0.46	484.1	0.94
PBL-P5	16	92.5	40	9.53	71.3	201	108.5	44.8	5	720.4	-	-	612.6	1.18
PBL-P10	16	92.5	40	9.53	71.3	201	107.4	43.3	10	816.5	-	-	856.4	0.95
PBL-P15	16	92.5	40	9.53	71.3	201	113.5	45.0	15	1073.5	-	-	-	-
PBL-1	16	92.5	40	9.53	71.3	201	109.4	45.1	-	295.4	484.3	0.51	326.5	0.90
PBL-SD25	16	92.5	40	9.53	71.3	201	104.6	42.8	-	375.1	968.6	0.39	392.0	0.96
Tanaka-1	25	120.0	70	-	-	-	114.0	44.8	-	880.0	1282.8	0.69	846.2	1.04
Tanaka-2	22	120.0	50	-	-	-	114.0	44.8	-	709.0	1200.0	0.59	567.9	1.25

t: thickness of PBL, h : length of PBL in connection part, d : the hole diameter of PBL, $Ø_{st}$: diameter of transverse rebar, A_s : area of transverse rebar, E_s : elastic modulus of transverse rebar, f'_{c_UFC} : compressive strength of cast-in-place UFC, E_{UFC} : elastic modulus of cast-in-place UFC, σ'_c: prestressing stress on connection part, V_{exp} : shear capacity from experiment, V_{ud} : shear capacity calculated from JSCE equation, V_{PBL} : shear capacity calculated from proposed equation

4.6.2 Proposed shear capacity equation

Since the equation which applicable to PBL with cast-in-place UFC is distrusted, the shear capacity equation was proposed based on four contribution terms in order to rationally evaluate the shear capacity of PBL with cast-in-place UFC connection. The regression model is shown in Eq. (4-8).

$$V_{PBL} = \sum_{i=1}^{n_{PBL}} [\alpha_1 (h_i t_i E_{UFC}) + \sum_{j=1}^{n_{hole}} \left\{ \alpha_2 A_{sj} E_{sj} + \alpha_3 \frac{\pi}{4} (d_j{}^2 - \phi_{stj}{}^2) \sqrt{f'_{c\_UFC}} \right\}] + \alpha_4 (A_c \sigma'_c) \quad (4\text{-}8)$$

where, V_{PBL} is the shear capacity of PBL with cast-in-place UFC connection (N), n_{PBL} is the number of PBLs, n_{hole} is number of holes provided on a PBL, t_i is the thickness of PBL i in the connection part (mm), h_i is the length of PBL i in connection part (mm), A_{sj} is the area of transverse rebar in the PBL hole j (mm^2), E_{sj} is the elastic modulus of transverse rebar (GPa), d_j is the diameter of the hole of PBL j (mm), $Ø_{st}$ is the diameter of transverse rebar in the PBL hole j (mm), E_{UFC} is the elastic modulus of cast-in-place UFC (GPa), A_c is the prestressing area (mm^2), σ'_c is the prestressing stress (MPa).

The four contributions of regression model for predicting shear capacity of PBL with cast-in-place UFC are based on the resisting mechanism of each PBL and the prestressing forces on the cross section area of connection as explained in section **4.5**. The first term corresponds to the end-bearing resistance of concrete which is not considered in JSCE equation. Elastic modulus of cast-in-place UFC (E_{UFC}) was selected in order to represent the contribution of end-bearing resistance since the crushing at the end-bearing of cast-in-place UFC was not observed as discussed in section **4.4.3**. The contribution of transverse rebar is represented in the second term where the elastic modulus of transverse rebar (E_s) is used. UFC dowel is considered in the third term. Based on the experimental results, it was also shown that the square root of compressive strength of UFC agreed well with the shear capacity. Moreover, from the study done by Oguejiofor and Hosain (1997), the function of square root of compressive strength of concrete was suggested as the expression of dowel action of concrete inside the PBL. Therefore, the contribution of UFC dowel is originated by the function of cross section area of cast-in-place UFC and square root of compressive strength of cast-in-place UFC in this study. The last term is accounted for the contribution of prestressing forces which is assumed to be the linear relationship between shear capacity and prestressing stress as shown in **Fig. 4-21**.

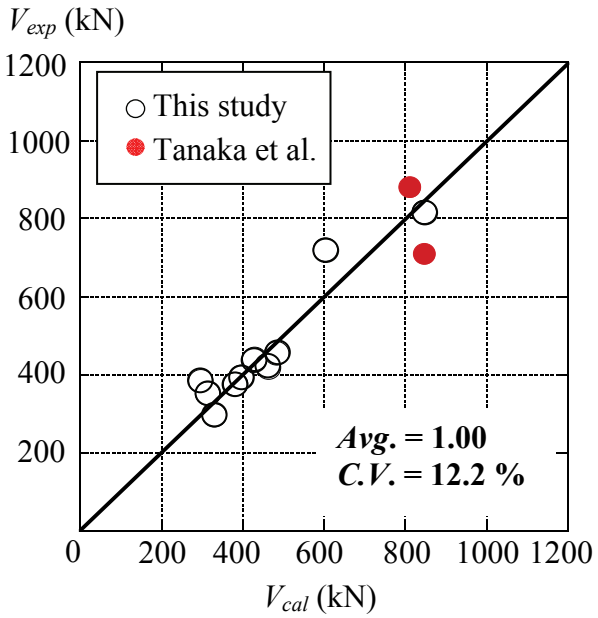

Figure 4-25 Accuracy of proposed equation

According to shear resisting mechanism explained before, the shear capacity is assumed to be a combination of resisting components of PBL which are end-bearing resistance of PBL, shear resistance of transverse rebar, UFC dowel and shear frictional resistance along the failure plane due to the induced prestressing force on the connection area. The regression analysis was used to derive the shear capacity equation. By using the least-squares procedure, α_1, α_2, α_3 and α_4 were examined. The coefficient of determination (R^2) was 0.9926. Based on the regression analyses of experimental results, the shear capacity equation of PBL with cast-in-place UFC connection can be expressed as shown in Eq. (4-9).

$$V_{PBL} = \sum_{i=1}^{n_{PBL}} [0.80(h_i t_i E_{UFC}) + \sum_{j=1}^{n_{hole}} \left\{0.95 A_{sj} E_{sj} + 2.8 \times \frac{\pi}{4}(d_j^{\,2} - \phi_{stj}^{\,2})\sqrt{f'_{c\_UFC}}\right\}] + 0.67(A_c \sigma'_c) \qquad (4\text{-}9)$$

4.6.3 Result of the calculation

Table 4-7 summarizes the results of calculation obtained by Eq. (4-9) and experimentally observed. **Figure 4-25** illustrates the accuracy of the proposed equation against the experimental values. The two experimental results from Tanaka et al. (2006) were also compared with the proposed equation. The average (*Avg.*) and the coefficient of variation (*C.V.*) of the ratio of the experimental and calculated value (V_{exp}/V_{cal}) for total 13 specimens are 1.00 and 12.2%, respectively. In the case of 11 specimens without prestressing force, the

values of *avg.* and *C.V.* are 1.02 and 12.9%, respectively. Even though the numbers of tested specimens is limited in order to derive the widely applicable range equation, it is found that good agreement between experimental results and calculated results was observed. In case of the calculation results of Tanaka-1 and Tanaka-2 specimens, it is also indicated that the proposed equation is able to give reasonable results even if the transverse rebar is not provided in the specimen and regardless of location of the hole of PBL. Moreover, the significant contribution of prestressing forces on the connection part can be accounted for in this equation. Thus, the proposed equation can be used to evaluate the shear capacity of PBL with cast-in-place UFC connection. However, the empirical equation used to estimate the shear capacity of PBL with cast-in-place UFC connection is suggested to be prudently used within the limit of the investigated parameters and the safety factor is needed in order to provide reliable and safety design.

It is also recommended to carry out further experimental investigation of PBL with cast-in-place UFC connection. The predicting shear capacity equation should be further developed which based on the relationship of the contribution. Additional parameters such as size and arrangement of PBL shall be considered in order to include rational reduction factors.

4.7 Summary of Chapter 4

1) The Perfobond strip (PBL) with cast-in-place UFC connection was proposed for the connection for UFC-PC hybrid girder in this study. By comparing shear capacity of the proposed PBL with cast-in-place UFC and shear capacity of UFC segment, it is indicated that the sufficient performance in transferring shear forces between each UFC and concrete segments is secured.

2) With the increase in thickness and the hole diameter of PBL, the shear capacity of PBL with cast-in-place UFC slightly increased. This is because the end-bearing and dowel effect of PBL increased with the increase in thickness and hole diameter of PBL. Moreover, the shear capacity of PBL with cast-in-place UFC connection increased by 11 and 15% when the diameter of transverse rebar increased from 10 to 13 and 16 mm, respectively, due to the increase of shear resistance of transverse rebar. However, the difference in the shear capacity of PBL with cast-in-place UFC connection with different specing to diameter ratio (*S/D*) was very slight.

3) By inducing the prestressing force on the cross section of PBL with cast-in-place UFC connection, the shear capacity was significantly increased. This is because the friction force drastically increases when the prestressing forces are induced on the connection. Consequently, the separation crack width greatly reduces.

4) Shear resisting mechanism of PBL with cast-in- place UFC connection was investigated. The contribution on shear resistance characteristics comes from, first, end-bearing resistance of UFC. Second is the dowel action of UFC in the hole of PBL together with shear resistance of transverse rebar in third term. The last contribution comes from the prestressing stress on the connection part.

5) The equation for predicting the shear capacity of PBL with cast-in-place UFC connections was proposed. The proposed equation was found to be capable to accurately predict the shear capacity of PBL with cast-in-place UFC connections with and without prestressing forces.

CHAPTER 5

Effect of bending moment on shear behavior of PBL joint connection

5.1 Introduction

In chapter 4, PBL with cast-in-place UFC connection was proposed as one of the connection methods for UFC-PC hybrid structures. Push-out test of PBL with cast-in-place UFC connection was conducted in order to investigate the shear behavior of connection. The shear resistance mechanism of PBL with cast-in-place UFC connection was investigated. The contribution on shear resistance characteristics comes from end-bearing resistance of UFC, the dowel action of UFC in the hole of PBL, shear resistance of transverse rebar and the prestressing stress on the connection. However, the effect of bending moment and location of connection has not been investigated yet.

The proper location of connection should be located where the shear force is dominant than the bending moment. However, in real construction, the effect of location and bending moment on the shear behavior of PBL with cast-in-place UFC connection supposes to be varied and should be investigated. The aim of this chapter is to investigate the effect of location and bending moment on the shear behavior of the PBL with cast-in-place UFC connection. The loading tests of the UFC-PC hybrid girders were carried out. The experimental parameter was the location of the connection. Three specimens with different locations of the connection were prepared. The effect of bending moment on shear behavior of PBL with cast-in-place UFC connection is examined based on the results of shear capacities, force and displacement relationship and shear resistance mechanism.

5.2 Experimental Program

5.2.1 Experimental cases

Three specimens with different location of the connection along the shear span were prepared in order to investigate the effect of bending moment on the shear behavior of the

Table 5-1 Experimental cases

No.	Name	t (mm)	D (mm)	$Ø_{st}$ (mm)	L_j (mm)
1	PBL16	16	40	10	85
2	PBL-M1				100
3	PBL-M2				150
4	PBL-M3				200

t: the thickness of PBL, D: the diameter of PBL hole, $Ø_{st}$: the diameter of transverse rebar, L_j: the distance between supporting point to the center of connection

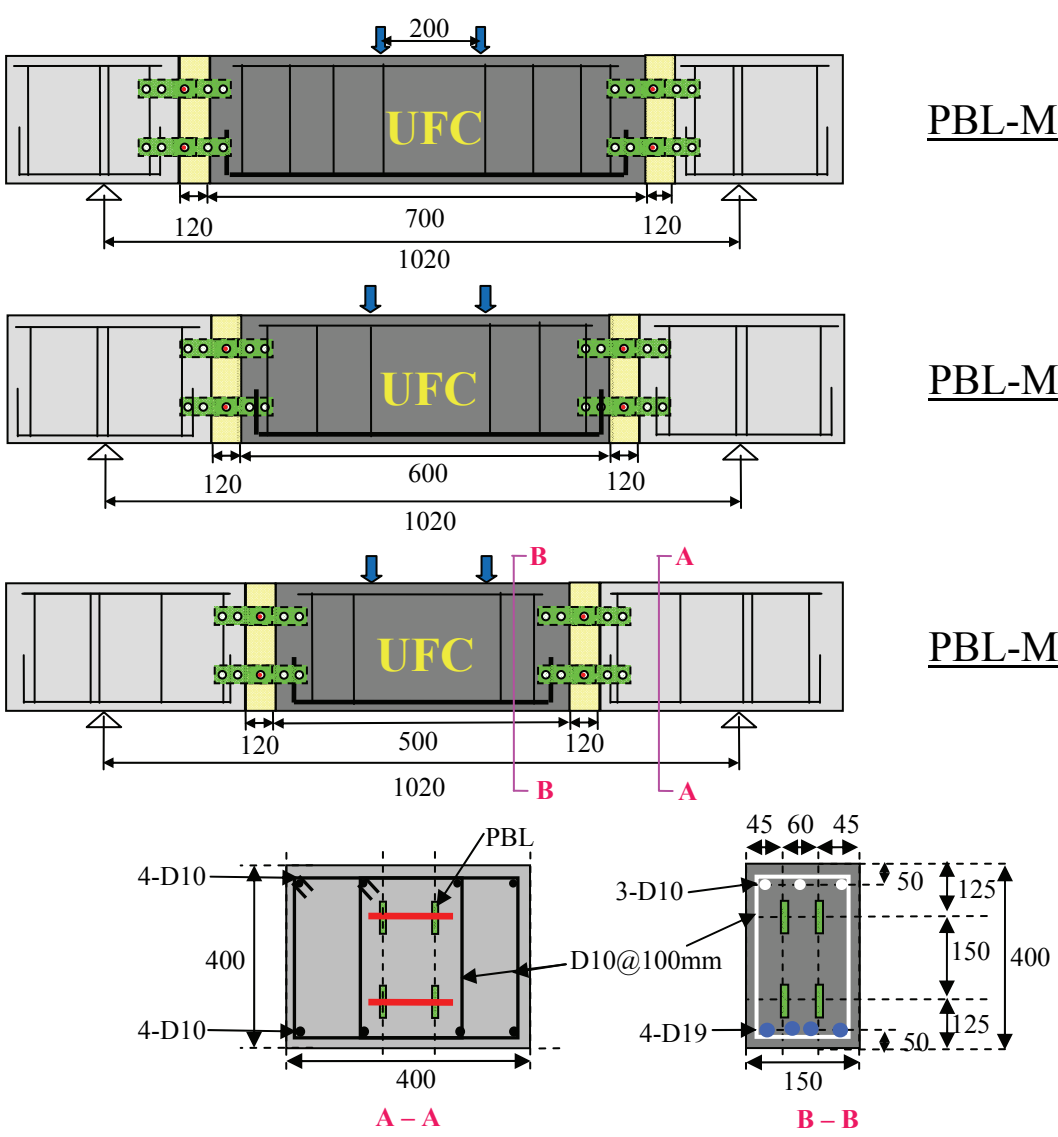

Figure 5-1 Details of specimens

connection. Four-point bending test were conducted. **Table 5-1** summarizes the test variation, the location of the center line of connection from the support and the specimen name. The

locations of the connection were 100, 150 and 200 mm from the supporting point. **Figure 5-1** illustrates the details of specimen, arrangement of reinforcement and cross section of all specimens. The specimen consisted of three parts, which were UFC precast segment located at the middle part and two RC parts located at both sides of the specimen. PBLs were embedded in each part. Each part of the specimen was joined with two connections between RC and UFC parts. The configuration and arrangement of PBL on the part was the same as PBL16 specimen in chapter 4 as shown in **Fig. 4-4**. **Figure 4-5** shows the detail dimension of PBLs used in this experiment. Total span lengths of the specimens were the same but the location of connections were different. Therefore, the length of both RC and UFC segments were varied as shown in **Fig. 5-1**.

In all specimens, three of steel reinforcements with 19.1 mm nominal diameter were provided in the tension side of UFC segment. Moreover, steel reinforcements with 9.53 mm nominal diameter were used as the longitudinal reinforcements for RC parts and stirrups for UFC and RC parts as shown in **Fig. 5-1**. It should be noted that there was no reinforcement provided inside UFC segment for the specimen in push out test experiment (chapter 4).

5.2.2 Materials

The self-compacting concrete was used in this experiment. **Table 5-2** summarizes the details of mix proportion. The designed compressive strength of concrete was 70 MPa at 7-day age. The materials used in the concrete mixes were high-early strength cement, fine aggregates, coarse aggregates, viscosity improver and superplasticizer, which was high-performance air entrained (AE) water reducing agent.

Table 5-3 shows the mix proportion of UFC. The UFC segment was fabricated in advance before the connection with RC segments. After casting, the segment underwent the steam curing following the JSCE recommendation (JSCE, 2004). The designed compressive strength of UFC segment was 180 MPa. In case of cast-in-place UFC, the designed compressive strength was 100 MPa with normal curing for 7 days. The steel reinforcements with 9.53 mm nominal diameter were used for RC part and as transverse rebar inside the hole of PBL. The steel reinforcements with 19.1 mm nominal diameter, the yield strength: f_y=395 MPa and the ultimate strength: f_u=520 MPa were used as the tension reinforcement for the UFC segment. The characteristics of the reinforcement used in this study are shown in **Table 5-4**.

Table 5-2 Mix proportion of concrete

G_{max}	Water cement ratio	Fine aggregate ratio	Unit weight (kg/m^3)					
(mm)	(%)	(%)	*W*	*C*	*S*	*G*	*SP*	*V*
15	30	45	165	550	831	792	*W*×1.1%	*C*×0.15%

where, G_{max} : maximum size of coarse aggregate
W : water
C : high early strength cement, density = 3.14 g/cm^3
S : fine aggregate, density = 2.59 g/cm^3, F.M. = 2.42
G : coarse aggregate, density = 2.68 g/cm^3, F.M. = 6.82
SP : superplasticizer
V : viscosity improver

Table 5-3 Mix proportion of UFC

Flow (mm)	Unit quantity(kg/m^3)			Admixture (kg/m^3)
	Water	Premix binder	Steel fiber	
260±20	180	2254	157	22

Table 5-4 Details of PBL and steel reinforcements

	Nominal diameter (mm)	Grade	Yield strength (MPa)	Tensile strength (MPa)
PBL	-	SS400	345	450
D10	9.53	SD345	390	505
D19	19.1	SD345	395	520

PBL with 16 mm in thickness was used in this experiment. **Table 5-4** lists the characteristics of PBL.

5.2.3 Fabrication of the specimens

As shown in **Fig. 5-1**, the specimen consisted of three parts; the middle part was precast UFC segment and two precast concrete segments located at both ends of the specimen. Both precast concrete and UFC segment which PBL were embedded had been fabricated in

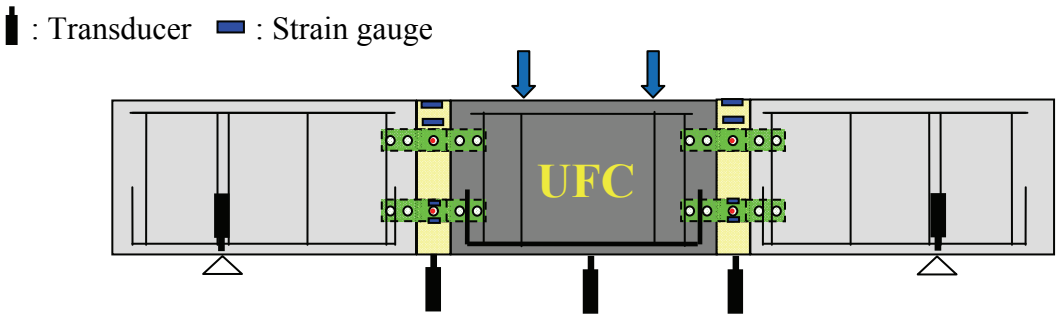

Figure 5-2 Measurement items

advance, then, connecting together by using cast-in-place UFC. In all specimens, the same fabrication process of connection as explained in session **4.3.2** was used (See session **4.3.2**, **Figs. 4-6** and **4-7**).

5.2.4 Loading method and measurement items

The specimens were subjected to a four-point bending test with the load applied on the UFC segment as shown in **Fig. 5-1**. The supporting points were located on the RC segment part placed on the roller supports. Total span lengths of the specimens were the same but the location of connections were different. Teflon sheets and grease were inserted between the specimen and supports. At the loading points on the top surface of the specimen, steel plates with 50 mm width, steel rollers and a load distribution beam were placed.

Figure 5-2 illustrates the location of measurement items used in the experiment. The applied load was measured during the loading test. Displacements at the middle of connection part and supporting point were measured by using transducers. Strain gauges were used for measuring the strain of PBL strips plate. Moreover, the strains of the transverse rebars were measured at the middle point of rebars by using strain gauges. The opening widths between RC segment and connection part were measured by using transducers with interval of 100 mm along vertical direction of the specimens. In the same way, the opening widths between connection part and UFC segment were measured by using π-gauges and transducers with interval of 100 mm along the vertical direction of the specimen. In addition, strain of cast-in-place UFC on the upper part were measured by using concrete gauges.

Table 5-5 Mechanical properties of concrete and UFC, and the result of loading tests

Name	Mechanical properties of concrete		Mechanical properties of cast-in-place UFC		Mechanical properties of precast UFC		Result of loading test
	f'_c (MPa)	f_t (MPa)	f'_{c_UFC} (MPa)	f_{t_UFC} (MPa)	$f'_{c\_UFC\_PC}$ (MPa)	$f_{t\_UFC\_PC}$ (MPa)	V_u (kN)
PBL16	84.3	3.3	123.8	11.2	185.4	13.6	394.7
PBL-M1	75.4	2.7	135.4	10.8	199.7	12.5	462.1
PBL-M2	70.8	2.8	108.4	10.3			352.2
PBL-M3	70.4	2.8	108.4	10.3			336.4

f'_c: compressive strength of concrete, f_t: tensile strength of concrete, f'_{c_UFC}: compressive strength of cast-in-place UFC, f_{t_UFC}: tensile strength of cast-in-place UFC, $f'_{c\_UFC\_PC}$: compressive strength of UFC segment, $f_{t\_UFC\_PC}$: tensile strength of UFC segment, V_u: shear capacity of connection

5.3 Experimental Results and Discussions

5.3.1 Shear capacities

Table 5-5 summarizes the mechanical properties of concrete and UFC, and the result of loading tests. It can be seen that by increasing the distance of PBL with cast-in-place UFC connection from the supporting point, the shear capacity decreased.

5.3.2 Shear force-displacement relationships, failure modes and crack patterns

The relationship between shear force and the relative displacement is plotted in **Fig. 5-3**. **Figure 5-4** shows the observed crack patterns at the peak loads of all specimens. It is obvious that only one critical crack was remarkable in each specimen.

In all specimens, the shear failures at the connections were observed. The failure behavior was found to be similar with push out test specimens and can be explain as follow. First, the specimens exhibited linear behavior from the initial up to the first separation crack at the interface between concrete and cast-in-place UFC. After the first separation crack occurred, the load still linearly increased up to the propagation of the main diagonal crack occurred on a connection part. The main diagonal crack continuously initiated from the first separation crack. Afterwards, the main crack propagated to the interface between precast RC and cast-in-place UFC. Additionally, the appearance of the diagonal crack reduced the inclination of force-

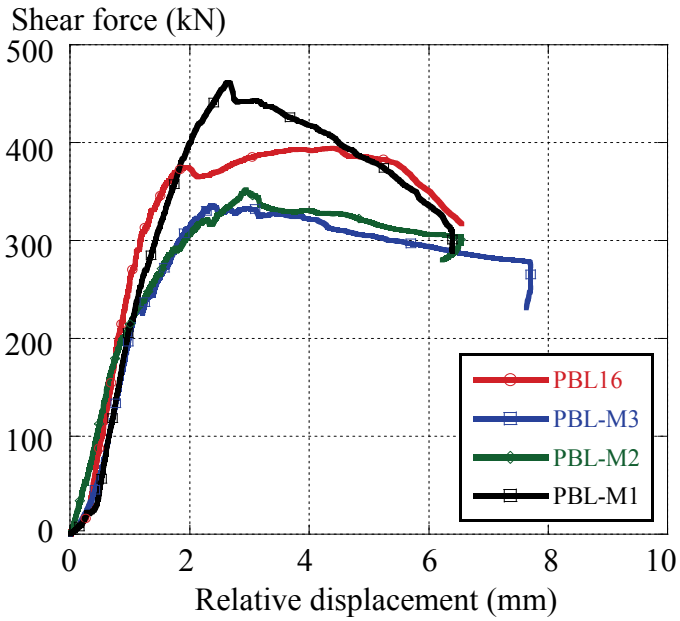

Figure 5-3 Shear force and relative displacement relationships

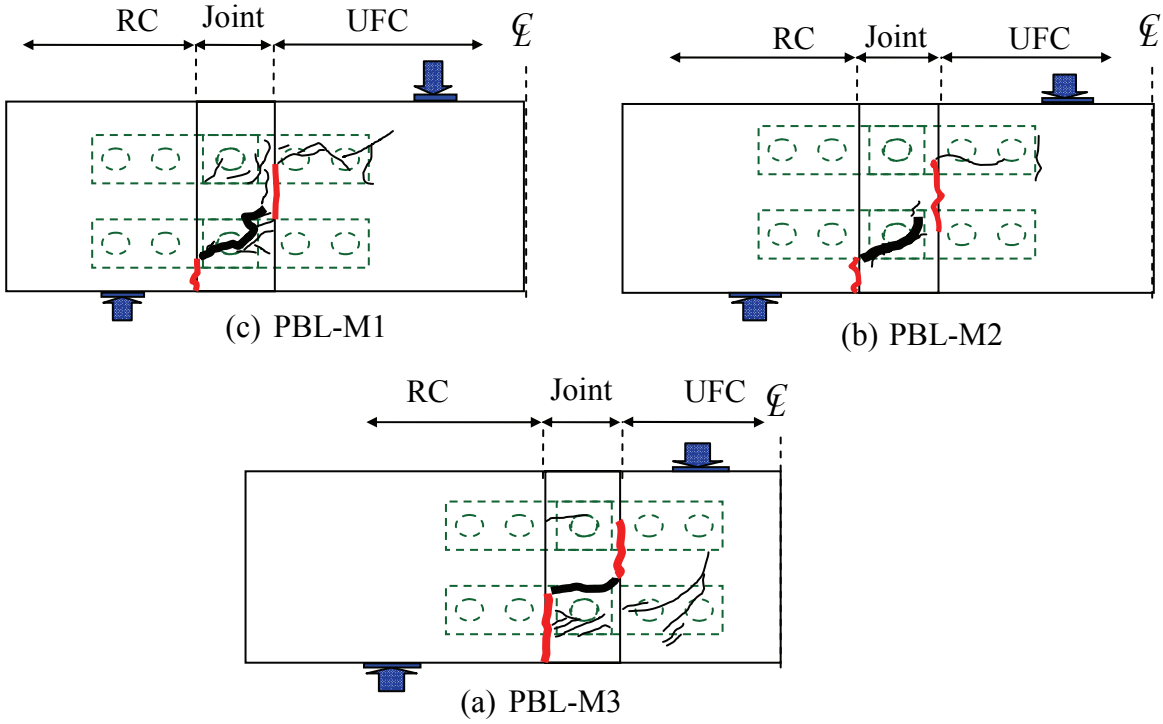

Figure 5-4 Crack patterns

relative displacement relationship of the specimens. After this stage, the rate of load increment became slow and the load and relative displacement behaved nonlinearly. Near the peak, the separation crack between precast and cast-in-place UFC propagated, the load reached the peak and dropped as the separation crack between precast and cast-in-place UFC propagated and widened. Similar failure pattern of shear failure was observed in all specimens.

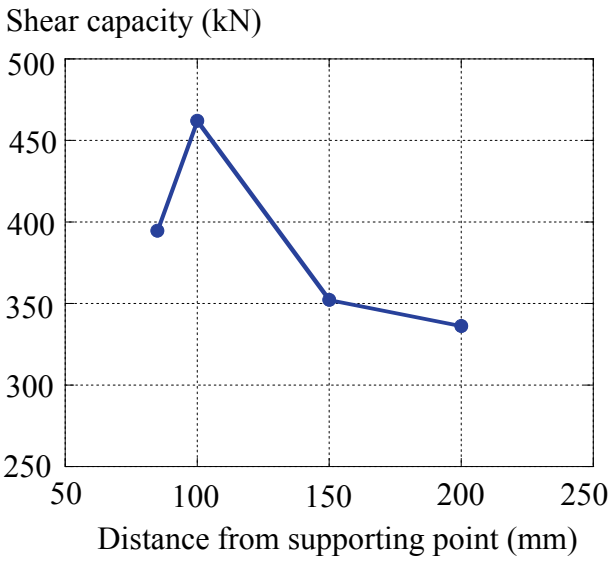

Figure 5-5 Shear capacity and relative displacement relationships

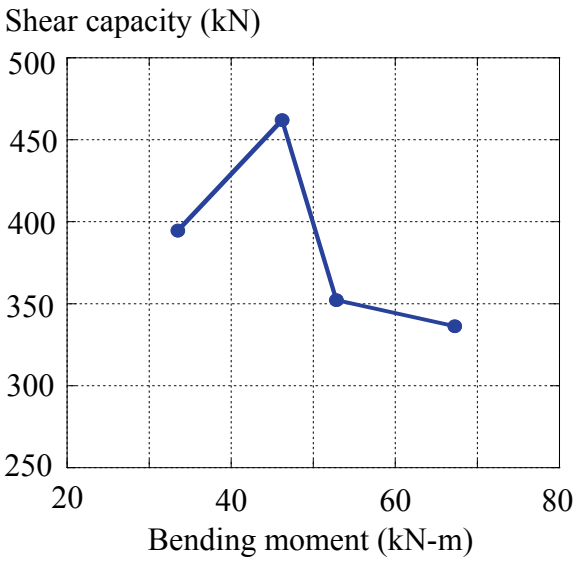

Figure 5-6 Shear capacity and relative displacement relationships

5.3.3 Effect of the bending moment on shear capacity of PBL connection

The effect of bending moment is discussed based on the experimental results of PBL-M1, PBL-M2, PBL-M3 and PBL16 specimens in which the bending moment on the connection was varied. **Figure 5-5** plots the relationship between shear capacity and distance from the supporting point to the center of the connection. The shear capacity and bending moment relationship of all specimens are illustrated in **Fig. 5-6**. From **Figs. 5-5** and **5-6**, there is the clear tendency of the decrement of shear capacity as the increase of bending moment on the PBL connection. The shear resistance mechanism of PBL with cast-in-place UFC had discussed in previous chapter, the shear resistances of connection come from the fictional resistance of cast-in-place UFC and shear contributions of PBL. As the bending moment at the connection part increases, the frictional resistance of cast-in-place UFC supposes to decrease. It should be also noted that there was no yielding of PBL or crushing of cast-in-place UFC in the experiment. This is inferred that the influence of bending moment on the shear contributions of PBL was slight. In the other word, the bending moment is affected on only frictional resistance of cast-in-place UFC.

5.4 Summary of Chapter 5

The effect of bending moment on the shear behavior of PBL with cast-in-place UFC connection was investigated. Although within the limited of the experimental data but the experimental results indicated that shear capacity of PBL with cast-in-place UFC connection decreases as the increase of bending moment at the location of PBL with cast-in-place UFC connection. This can be explained as the decrease of frictional resistance of cast-in-place UFC when the bending moment at the PBL with cast-in-place UFC increases. Moreover, similar shear failure behavior of PBL with cast-in-place UFC connection was also observed.

However, with limited number of experimental data, it is recommended to investigate further experiment considering range of bending moment together with additional parameters such as size and arrangement of PBL.

CHAPTER 6

Conclusions and recommendations

6.1 General Conclusions

The concept of UFC-PC hybrid structure is introduced and proposed in this study. The UFC-PC hybrid structure consists of PC segment at both ends and UFC segment at the middle of span. This proposal lies in the development of new competitive structural system that offers improvement in usability, aesthetics and durability, while minimizing the volume of materials by making full use of every single part of UFC. Hence, the final goal of this study is to develop the UFC-PC hybrid structure. In order to achieve this goal, the study on the utilization of UFC for each part of the structure and verification of its performance were carried out. First, the application of UFC as the permanent formwork for the precast concrete part was studied with the shear keys interface and screws and bolts system introduced. An experiment was performed in order to investigate the shear behavior of RC beams using UFC U-shaped permanent formwork. It was evident that the shear capacity of RC beams using UFC U-shaped permanent formwork significantly increased to more than twice that of normal RC beams. Second, the shear performance of the joint connection between UFC and PC segments was studied. The Perfobond strip (PBL) with cast-in-place UFC joint connection was proposed and its shear performance was examined. An experimental study using push-out test was conducted. The efficient force transferring between two segments was confirmed. Furthermore, shear capacity equation of PBL with cast-in-place UFC connection was developed. The findings on the utilization of UFC in this study provide the understanding and offer the basic knowledge for the development of competitive UFC-PC hybrid structural system. Based on all of the experimental results, the conclusions of the studies on the utilization of UFC for UFC-PC hybrid structures can be drawn as follows.

a) Shear behavior of RC beams using UFC U-shaped permanent formwork

The construction method using UFC U-shaped permanent formwork was introduced to be used with the PC segment. By using the UFC U-shaped permanent formwork, the shear capacity of RC beams can be increased to more than twice comparing with normal RC beams.

The bond characteristic between interfaces of RC and UFC permanent formwork is found to be important in improving the load carrying capacity and deformation performance. By using the proposed shear keys interface and screws and bolts system, the sufficient compatibility between UFC permanent formwork and RC can be formed. Since a UFC permanent formwork prevents widening of diagonal crack inside RC by shear keys and screws and bolts, the shear capacity drastically increases.

The thickness of UFC permanent formwork and shear span to effective depth ratio (*a/d*) were found to have a significant effect on the shear behavior of RC beams using UFC permanent formwork. With an increase in the thickness of UFC permanent formwork, the shear capacity of RC beams using UFC permanent formwork increases. Failure mode of RC beams using UFC permanent formwork changes depending on the shear span to effective depth ratio. Moreover, by providing the stirrups, the shear capacity of RC beams using UFC permanent formwork increases as both UFC permanent formwork and stirrups prevent the widening of the diagonal crack.

Significant reduction of the weight of beams by 68 to 82 percent compared with the ordinary RC beams can be achieved by using the UFC permanent formwork in this study. The significant reduction of the self weight of the structure results in the high performance on the seismic resistance. Besides, the shear carried by UFC permanent formwork in RC beams failed in the diagonal tension was investigated by using the stress obtained from the tension softening curve. The cracking propagation behavior especially crack width at the peak load is the essential parameter in order to predict the shear stresses along the diagonal crack line. The diagonal model using together with tension softening curve was proven to be the reasonable method to predict the shear carried by UFC permanent formwork. In case of RC beams using UFC permanent formwork failed in shear compression, shear carried by UFC permanent formwork found to be in the function of compression stress along the strut line. The compressive stress-strain relationship is one of the methods to calculate the compression forces acted on the UFC permanent formwork. In general, the use of UFC permanent formwork found to be not only increases the durability performance but also significantly enhance the shear performance of the structures.

b) Shear behavior of PBL with cast-in-place UFC connection

The connection system is one of the important requirements in developing UFC-PC hybrid structures. In this study, the PBL with cast-in-place UFC connection was proposed as the connection for UFC-PC hybrid structures. Its performance was examined by the push-out experiment. By comparing the shear capacity of PBL with cast-in-place UFC connection obtained from the experiment with the shear capacity of UFC segment, it is found that the efficient performance on shear force transferring between UFC and concrete segments can be achieved.

The influences of thickness of PBL, diameter of PBL hole, diameter of transverse rebar, prestressing forces induced on the connection and spacing of PBLs to diameter of PBL hole ratio were considered in the experiment. The results revealed that the shear capacity of PBL with cast-in-place UFC connection slightly increase with increase in thickness of PBL and hole diameter of PBL. This is due to the increase of end-bearing resistance between contracting area of PBL and cast-in-place UFC and dowel action of PBL formes inside PBL hole. Moreover, the shear capacity of PBL with cast-in-place UFC increases when the diameter of transverse rebar increases as a result of increase in shear resistance of transverse rebar. However, the difference in the shear capacity of connection with different spacing of PBLs to diameter of PBL hole ratio is slight. Additionally, by inducing the prestressing force on the cross section of connection, the shear capacity significantly increases due to the increase of friction force between interfaces of connection.

Shear resistance mechanism of PBL with cast-in-place UFC connection was investigated. The contribution of shear resistance characteristics comes from end-bearing resistance of UFC, the dowel action of PBL formed, together with shear resistance of transverse rebar in PBL hole and prestressing stress on the connection as the last contribution.

As a result, the equation for predicting the shear capacity of PBL with cast-in-place UFC connection was proposed based on the experimentally observed shear resistance mechanism. The equation was validated with 13 specimens in this study and 2 specimen from the other researcher and found to capable to accurately predict the shear capacity of PBL with cast-in-place UFC connection with and without prestressing forces.

In addition, the effect of bending moment on the shear behavior of PBL with cast-in-place UFC connection was discussed. The results showed that the shear capacity gradually

decrease as the increase of the bending moment occurred at the location of the connection. This can be explained as the decrease of frictional resistance of cast-in-place UFC when the bending moment at the PBL with cast-in-place UFC increases. Moreover, similar shear failure behavior of PBL with cast-in-place UFC connection was also observed.

6.2 Recommendations for the Further Study

Since the presented study has engaged with the individual parts of the whole UFC-PC hybrid structure, in order to precisely implementing the practical design and construct of this type of structure, the experiments on the all entire UFC-PC hybrid girders is recommended to conduct.

Besides, for the UFC permanent formwork, the current study showed the significant improvement in shear performance for RC beams. The method to investigate the shear carried by UFC permanent formwork was proposed based on the crack opening width at the peak load of UFC. However, it is difficult to find the certain crack width value in the practical design and also the larger size of real structure compare with this study is common. Therefore, it is recommended to conduct further experiment in order to introduce rational reduction factor of the tensile strength based on tension softening curve in real design.

The equation for predicting the shear capacity of PBL with cast-in-place UFC connection was proposed based on the experimental results whose the applicable range was certified in the limited range of the experimental parameters considered in this study. In the practical design, the scale of the structure is much larger. The further study should be performed in order to extend the applicable range of the equation.

REFERENCES

Abe, T., Kida, T., Niimi, A., Takano, M. and Tanaka, S. (2009): Shear Strength and Theorical Punching Shear Capacity Formulas for the Composite Surface of RC Slab using UFC Permanent Form, *Journal of Structural Engineering*, JSCE, Vol. 55A, pp. 1478-1487. (in Japanese)

Association Francaise de Genie Civil (AFGC) (2013): Ultra High Performance Fibre-Reinforced Concrete Recommendations, Revised edition, June 2013

Behloul, M., Lee, K. C. and Etienne, D. (2004): Seonyu Ductal Footbridge, *fib Symposium 2004*.

Benjamin, A. G. (2013): UHPC in U.S. Highway Infrastructure: Experience and Outlook, *Proceedings of RILEM-fib-AFGC International Symposium on Ultra-High Performance Fibre-Reinforced Concrete*, pp. 361-369.

Blais, P. Y. and Couture, M. (1999): Precast, Prestressed Pedestrain Bridge – World's First Reactive Powder Concrete Structure, *PCI Journal*, Vol. 44, No. 5, pp. 60-71.

Hajar, Z., Simon, A., Thibaux, T. and Wyniecki, P. (2004): Construction of an Ultra-High-Performance Fiber-Reinforced Concrete Thin-shell Structure over Millau Viaduct Toll Gates, *fib Symposium 2004*.

Hong, S. G. and Kang, S. H. (2013): Formwork Development using UHPFRC, *Proceeding of the RILEM-fib-AFGC International Symposium on Ultra-High Perfomance Fibre-Reinforced Concrete (UHPFRC 2013)*, pp. 197-206.

Hosotani, M., Musha, H., Kasakura, K., Inahara, H., Watanabe, N., Sakamoto, J., Ohkuma, H. and Ohtake, A. (2008): UFC Application and the Feature of PC Bridge in Japan, Proceedings of the 8th International Symposium on Utilization of High-Strength and High-Performance Concrete, Vol. 2, pp. 1233-1240.

Ikeda, H., Nakamura, K., Nakasu, M. and Ikeda, S. (2002): Construction of the Superstructures of Kiso and Ibi River Bridges, *Proceedings of the first fib Congress 2002,* Session 1, pp. 51-60.

Japan Society of Civil Engineers (JSCE) (2004): Recommendations for Design and Construction of Ultra High Strength Fiber Reinforced Concrete Structures (Draft)*, Concrete Library 113*. (in Japanese)

Japan Society of Civil Engineers (JSCE) (2006): Recommendations for Design and Construction of Ultra High Strength Fiber Reinforced Concrete Structures (Draft)*, JSCE Guidelines for Concrete No.9.*

Japan Society of Civil Engineers (JSCE) (2009): *Standard Specifications for Hybrid Structures-2009*. (in Japanese)

Kakei, T., Kawaguchi, T., Niwa, J. and Hyodo, H. (2003): Fracture Properties of Ultra High Strength Steel Fiber Reinforced Cementitious Composites, *Proceedings of Cement and Concrete*, Vol. 57, pp. 230-231. (in Japanese)

Kayser, R. J. and Nowak, S. A. (1989): Reliability of Corroded Steel Girder Bridges, *Journal of Structural Safety*, Vol. 6, pp.53-63.

Kurita, A. and Ohyama, O. (2003): Recent Steel-Concrete Hybrid Bridges in Japan, *International Journal of Steel Structures*, KSSC, pp. 271-279.

Leonhardt, F., Andra, W., Andra, H. P. and Harre, W. (1987): Neues, vorteilhaftes Verbundmitted Fur Stahlverbund-Trabwerke mit hoher Dauerfestigkeit, *Beton und Stahlbetondau*, pp. 325-331.

Makita, T. and Bruhwiler, E. (2013): Fatigue Behavior of Composite R-UHPFRC-RC Structure Members, *Proceeding of the RILEM-fib-AFGC International Symposium on Ultra-High Perfomance Fibre-Reinforced Concrete (UHPFRC 2013)*, pp. 167-176.

Mazzacane, P., Riciotti, R., Teply, F., Tollini, E. and Corvez, D. (2013): MUCEM: The Builder's Perspective, *Proceeding of the RILEM-fib-AFGC International Symposium on Ultra-High Perfomance Fibre-Reinforced Concrete (UHPFRC 2013)*, pp. 3-16.

Mutsuyoshi, H., Nguyen, D. H. and Kasuga, A. (2010): Recent Technology of Prestressed Concrete Bridges in Japan, *Proceedings of IABSE-JSCE Conference on Advances in Bridge Engineering-II*, pp. 46-55.

Murata, H. (2007): Mechanical Properties of Composite PC structures Using UFC Web, Doctoral thesis, Department of Civil Engineering, Tokyo Institute of Technology, Japan.

Murata, H., Niwa, J., Tanaka, Y. and Katagiri, M. (2007): Study on Composite PC Structures using Prestressed UFC Truss Members, *Journal of Japan Society of Civil Engineers (JSCE),* Ser. E2 (Materials and Concrete Structures), Vol. 63, No.1, p. 92-102. (in Japanese)

Musha, H., Watanabe, N., Inahara, H. and Ohshima, K. (2009): Feature and Application of UFC (Ductal) Structure: From the Pedestrian Bridge of the Span 50m to the Airport Runway Slab of 192,000 m^2, *Taisei Technology Center report*, No.42.

Musha, H., Ohkuma, H. and Kitamura, T. (2013a): Innovative UFC Structures in Japan, *Proceedings of RILEM-fib-AFGC International Symposium on Ultra-High Performance Fibre-Reinforced Concrete (UHPFRC 2013)*, pp. 17-26.

Musha, H., Kono, K., Kawaguchi, T. and Kobayashi, T. (2013b): Sustainable UFC Structures in Japan and its Durability Performance, *Proceedings of Third International Conference on Sustainable Construction Materials and Technologies (SCMT3)*, e278.

Nakamura, H. and Higai, T. (1999): Compressive Fracture Energy and Fracture Zone Length of Concrete, *JCI-C51E Seminar on Post-Peak Behavior of RC Structures Subjected to Seismic Loads*, Vol. 2, pp. 259-272.

Nakasu, M., Ito, M., Yanaka, M. and Maeda, H. (2000): Design and Construction of the Connection for Kisogawa and Ibigawa Bridges, *Journal of Prestressed Concrete*, Vol. 42, No. 1, pp. 37-45. (in Japanese)

Niwa, J. (1983): Equation for Shear Strength of Reinforced Concrete Deep Beams Based on FEM Analysis, *Proceeding of the Japan Concrete Institute 2nd Colloquium on Shear Analysis of RC Structures*, pp. 119-128. (in Japanese)

Niwa, J., Yamada, K., Yokozawa, K. and Okamura, H. (1987): Revaluation of the Equation for Shear Strength of Reinforced Concrete Beams without Web Reinforcement, Concrete Library of JSCE No. 9, pp. 65-84.

Oguejiofor, E. C. and Hosain, M. U. (1997): Numerical Analysis of Push-out Specimens with Perfobond Rib Connectors, *Journal of Computers and Structures*, Vol. 62, No. 4, pp. 617-624.

Perry, V. and Royce, M. (2007): Innovative Field-Cast UHPC Joints for Precast Bridge Decks (Side-by-Side Deck Bulb-Tees), Village of Lyons, NY – Design, Protoyping Testing and Construction, 2007 Concrete Bridge Conference, USA.

Resplendino, J. and Toutlemonde, F. (2013): The UHPFRC Revolution in Structural Design and Construction, *Proceedings of RILEM-fib-AFGC International Symposium on Ultra-High Performance Fibre-Reinforced Concrete (UHPFRC 2013)*, pp. 791-804.

Richard, P. and Cheyrezy, M. (1995): Composition of Reactive Powder Concretes, *Journal of Cement and Concrete Research,* Vol. 25, No. 7, pp. 1501-1511.

Shibata, K., Watanabe, K., Niwa, J. and Kawaguchi, T. (2009): Shear Strengthening Effect of UFC Panels on RC Beams, *Proceedings of Japan Concrete Institute*, Vol. 31, No. 2, pp. 1633-1638. (in Japanese)

Shirai, K., Matsuda, K. and Tanaka, S. (2008): Durability of UFC Formwork Left In-Place and Its Application, *Proceedings of 8th International Symposium on Utilization of High-Strength and High-Performance Concrete*, pp. 870-875.

Tanaka, Y., Musya, H., Ootake, A., Shimoyama, Y. and Kaneko, O. (2002): Design and Construction of Sakata-Mirai Footbridge using Reactive Powder Concrete, *Proceedings of the first fib Congress 2002*.

Tanaka, Y., Musha, H., Fukuura, N. and Ooshima, K. (2006): Design of Perfobond Strip Applied for Reactive Powder Concrete Bridge, *Proceedings of the 2nd fib Congress 2006*, Session 5, pp. 1-11.

Thorenfeldt, E., Tomaszewicz, A. and Jensen, J. J. (1987): Mechanical Properties of High-Strength Concrete and Application in Design, *Proceedings of the Symposium on Utilization of High-Strength Concrete*, Tapir, Trondheim, pp. 149-159.

Wringley, R. G. (2001): Permanent Formwork in Construction (CIRIA C558), *CIRIA/Concrete Society*, pp. 13-16.

Yoshioka, T. (2005): The Lastest Technologies of Prestressed Concrete Bridges in Japan, *Proceedings of the JSCE-VIFCEA Joint Seminar on Concrete Engineering in Vietnam*, pp. 72-86.

APPENDIX

Pictures of the specimens after the loading tests

1.1 Shear Behavior of RC Beams using UFC U-shaped Permanent Formwork

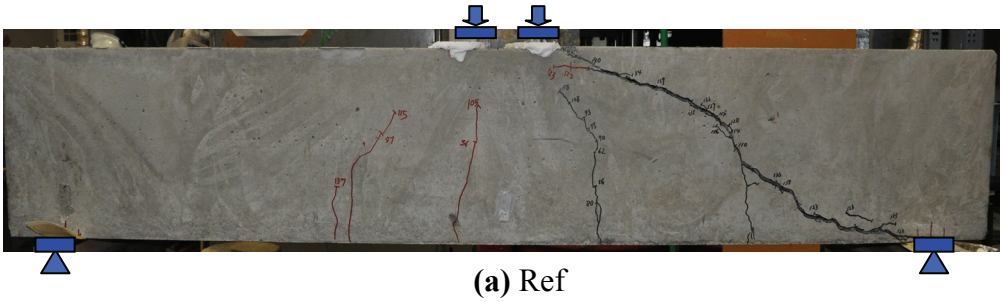

(a) Ref

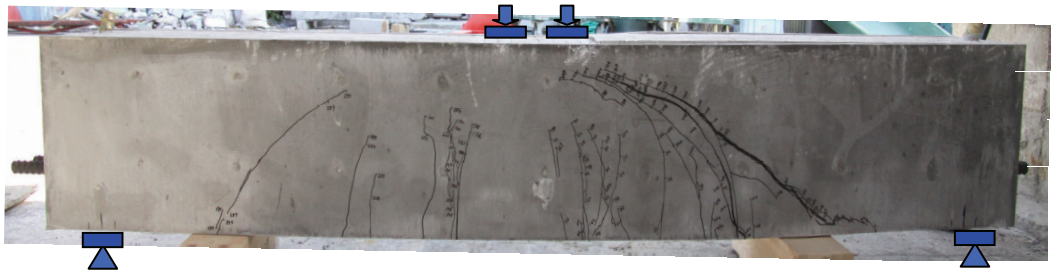

(b-1) UFC20-S (UFC)

(b-2) UFC20-S (RC)

Figure A-1 Specimens in Series-I (1)

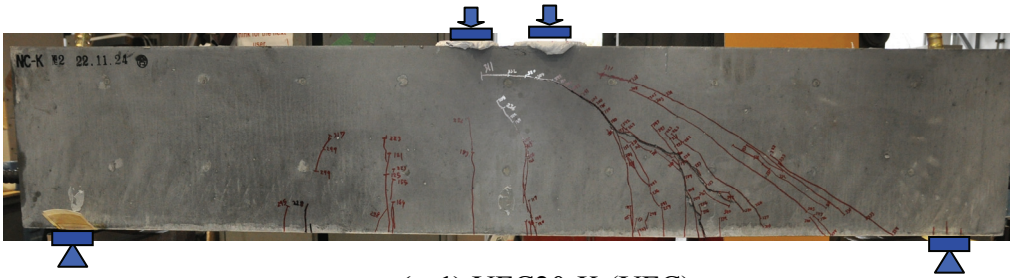

(a-1) UFC20-K (UFC)

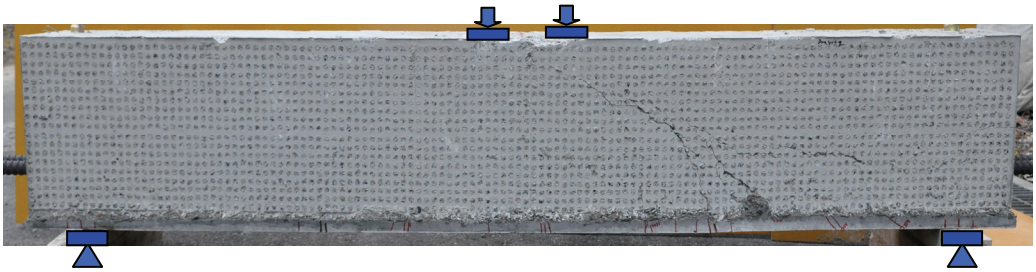

(a-2) UFC20-K (RC)

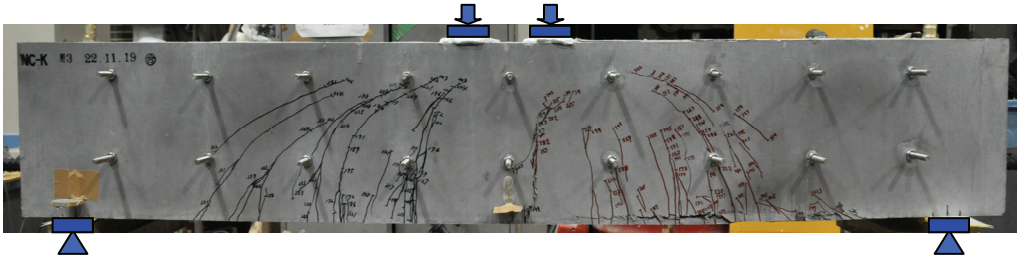

(b-1) UFC20-SB (UFC)

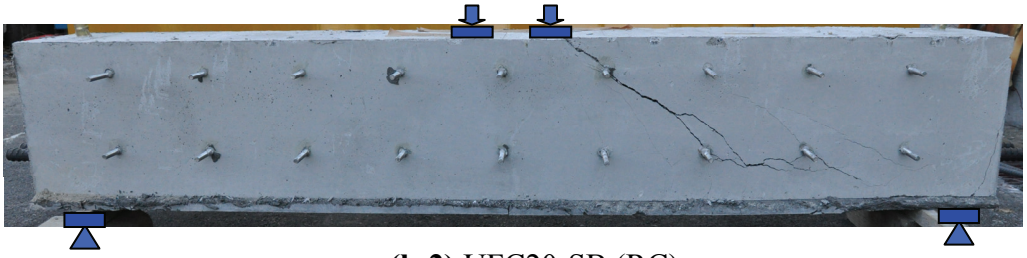

(b-2) UFC20-SB (RC)

Figure A-2 Specimens in Series-I (2)

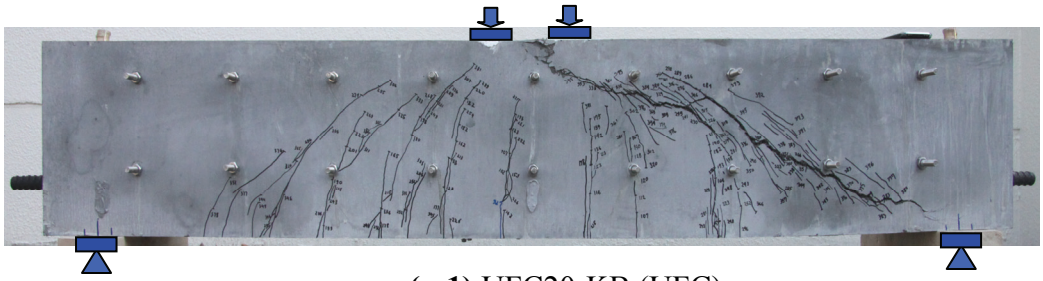

(a-1) UFC20-KB (UFC)

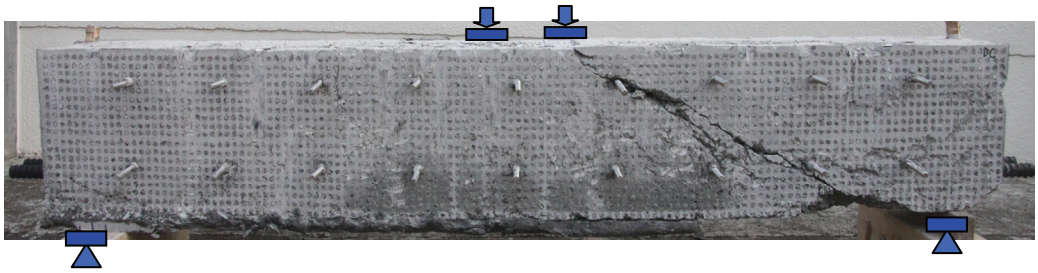

(a-2) UFC20-KB (RC)

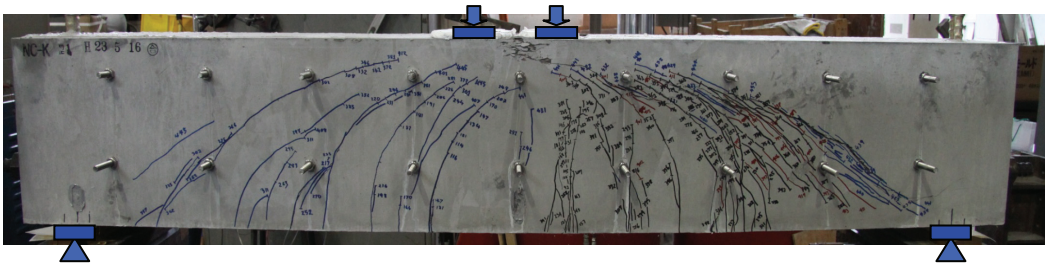

(b-1) UFC30-KB (UFC)

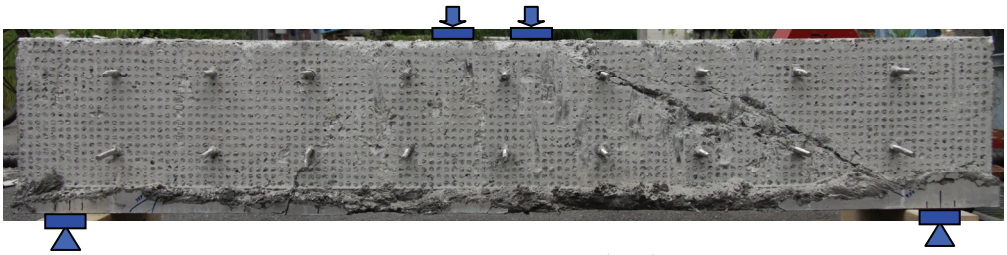

(b-2) UFC30-KB (RC)

Figure A-3 Specimens in Series-I and II

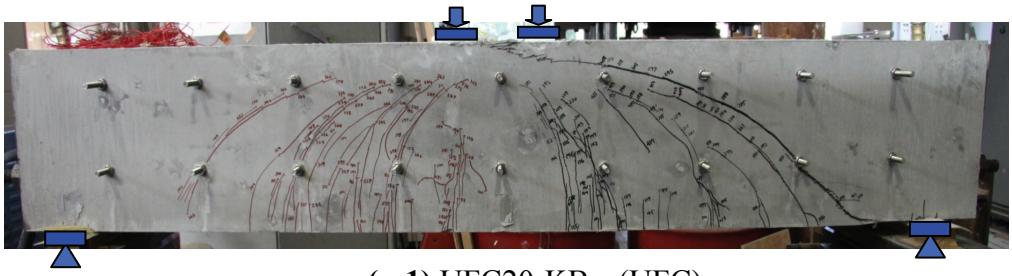

(a-1) UFC20-KB-r (UFC)

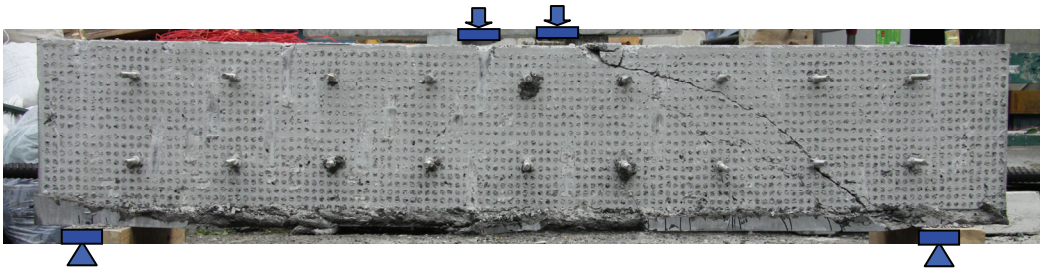

(a-2) UFC20-KB-r (RC)

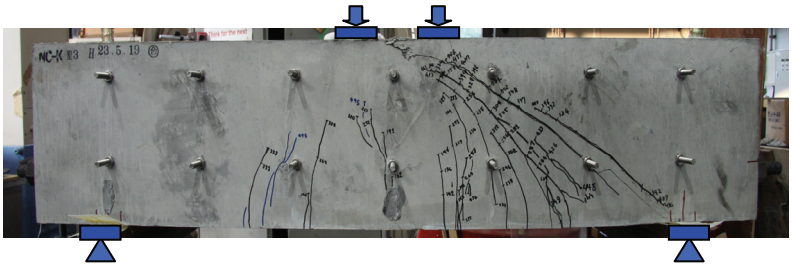

(b-1) UFC20-KB-ad21 (UFC)

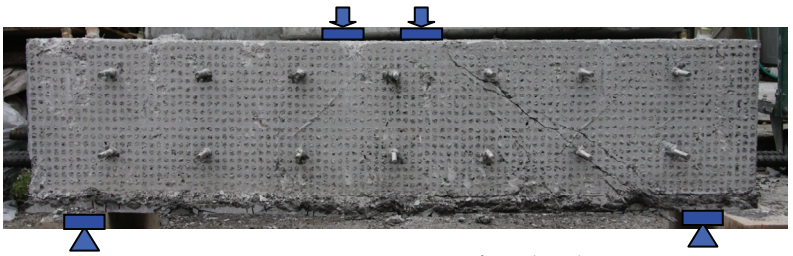

(b-2) UFC20-KB-ad21 (RC)

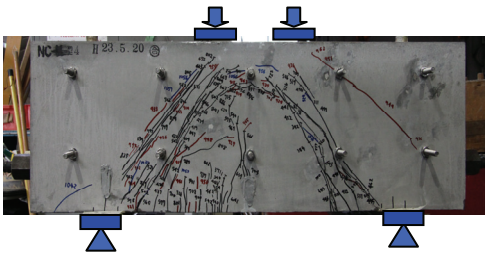

(c-1) UFC20-KB-ad1 (UFC)

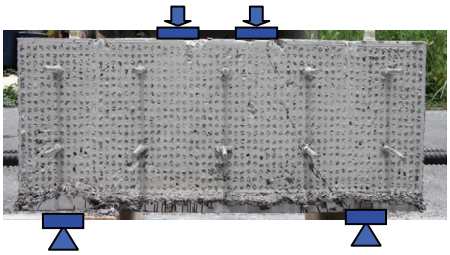

(c-2) UFC20-KB-ad1 (RC)

Figure A-4 Specimens in Series-III and IV

1.2 Shear Behavior of PBL Joint Connection for UFC-PC Hybrid Girder

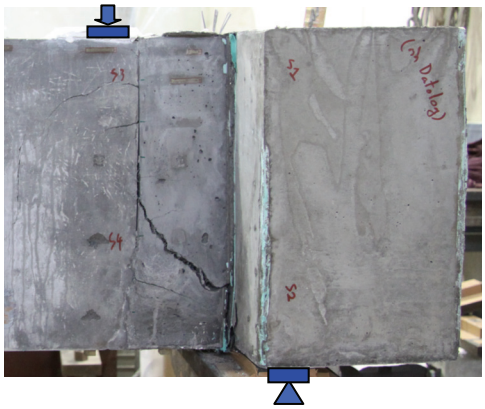

(a) PBL9

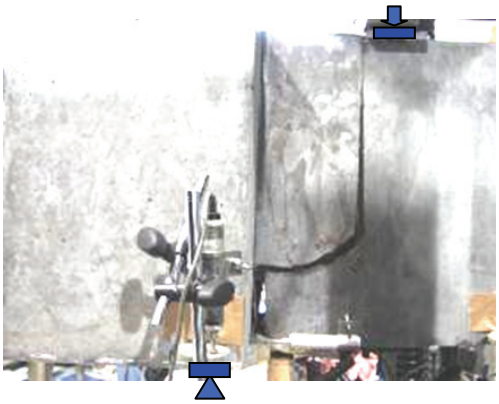

(b) PBL16

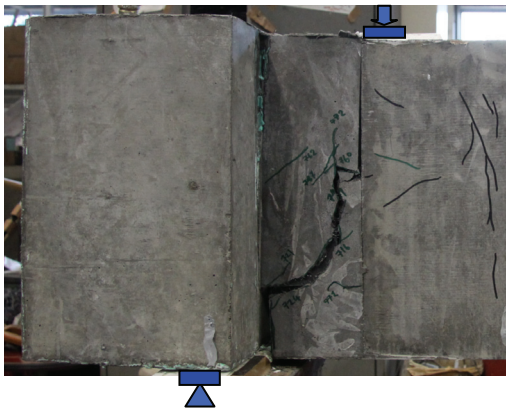

(c) PBL22

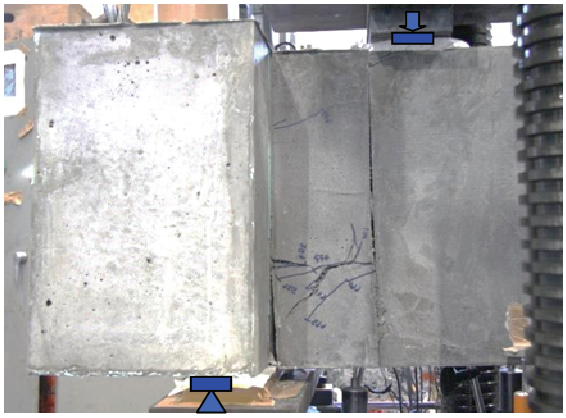

(d) PBL-D30

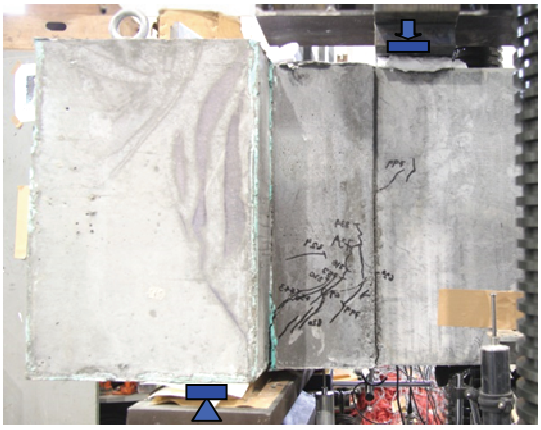

(e) PBL-D50

Figure A-5 Specimens in Series-I and II

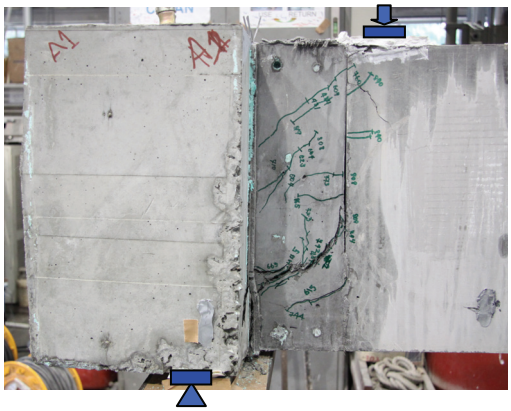

(a) PBL-r13

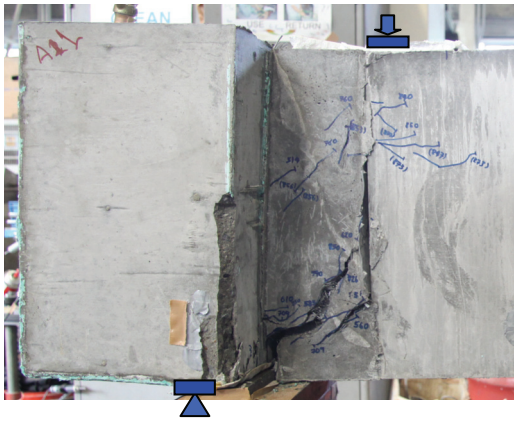

(b) PBL-r16

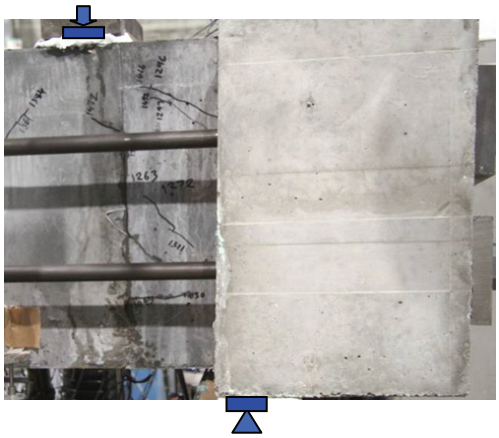

(c) PBL-P5

(d) PBL-P10

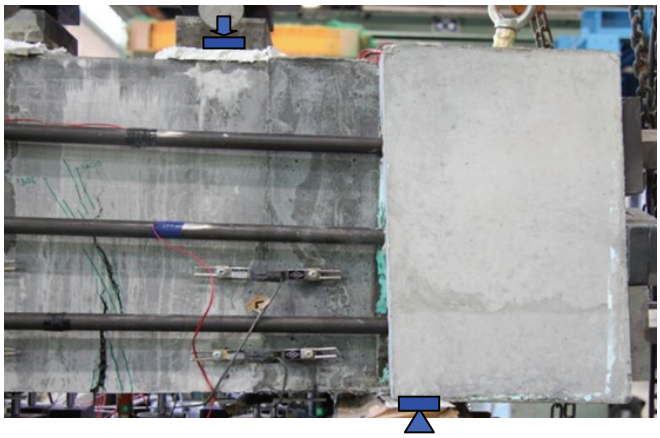

(e) PBL-P15

Figure A-6 Specimens in Series-III and IV

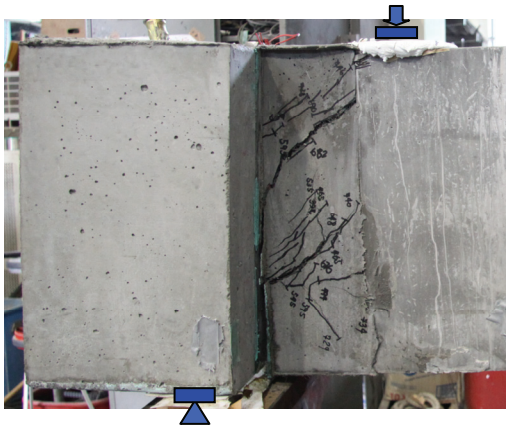

(a) PBL-SD25

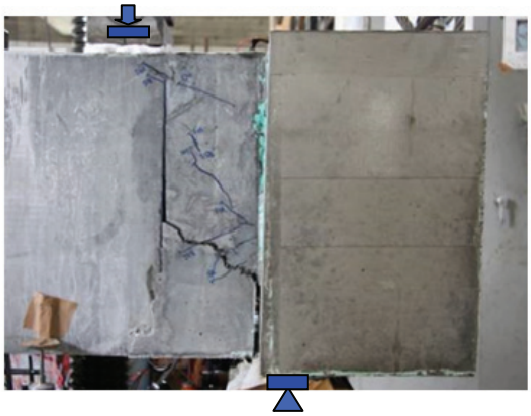

(b) PBL-SD1

Figure A-7 Specimens in Series-V

1.3 Effect of Bending Moment on Shear Behavior of PBL Connection

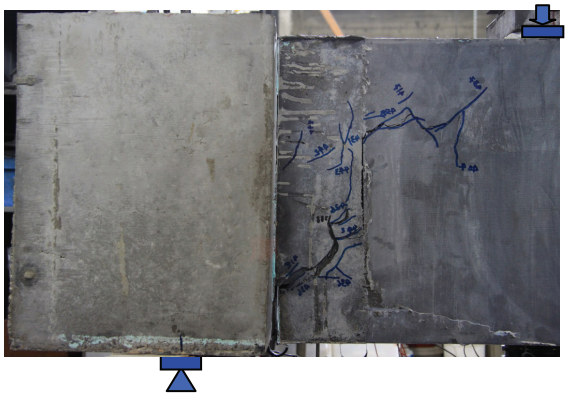

(a) PBL-M1

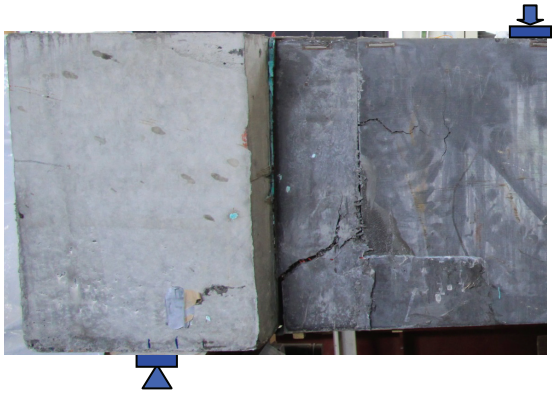

(b) PBL-M2

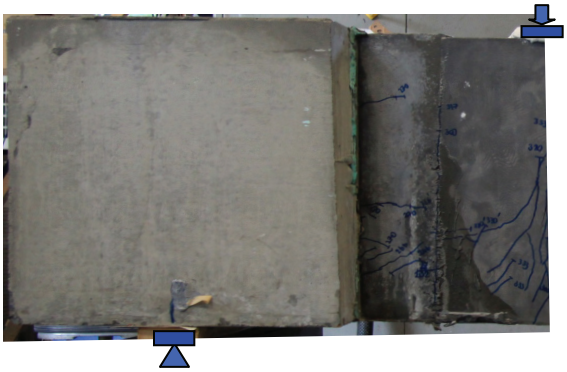

(c) PBL-M3

Figure A-8 Specimens in chapter 5